DIPLOMARBEIT

Simulation of critical current density for different geometries

Ausgeführt am Institut für
Festkörperphysik
der Technischen Universität Wien

unter der Anleitung von

Ao.Univ.Prof. Dipl.-Ing. Dr.techn. Michael REISSNER

durch

Sebastian Schiffer

Josef-Österreicher-Gasse 17/10, 1230 Wien

January 2015 _____

Declaration

I hereby declare and confirm that this thesis is entirely the result of my own original work. Where other sources of information have been used, they have been indicated as such and properly acknowledged. I further declare that this or similar work has not been submitted for credit elsewhere.

Vienna, January 11, 2015

Sebastian Schiffer

Acknowledgment

I want to thank my advisor Prof. Reissner for his support, his feedback, and the great amount of time he invested proofreading this thesis.

I also want to thank my sister, who corrected this thesis, as well as my parents and girlfriend for their steady help and encouragement.

Abstract

Critical current densities of superconducting materials can either be measured by direct current measurements, or indirectly by magnetic flux measurements. The disadvantage of the direct method is the much higher resistance of the measurement contacts in comparison to the superconductors resistance. The indirect method on the other hand measures the magnetic moment. In order to calculate the current density, the geometry of the superconductor needs to be known. Additionally, demagnetizing effects modify the magnetic field in the sample. The purpose of this thesis is to investigate the demagnetizing effects on the critical current densities in type-II superconductors. The insights from this thesis are meant to help calculating the demagnetizing effects, especially of magnesium diboride multifilament superconductors, in the future.

Regarding the theoretical calculations, formulas for the magnetic moment were derived in great detail for several geometries, including cylinders, cuboids, hollow cylinders and elliptic cylinders. Furthermore, the demagnetization factors for a cylinder and an infinite long bar have been computed. Also, a new formula to calculate the current density of the magnetic moment of cuboids and cylinders was proposed.

Niobium cylinders and cuboids of several lengths were measured by magnetic flux measurements in order to compare the critical current densities and the magnetization values with the theoretical calculations.

Depending on the regarded geometry, two formulas relating current density to magnetic moment are usually used. The first formula is used to calculate the magnetic moment of geometries where one of two dimensions perpendicular to the applied magnetic field, is much longer than the other one. The second formula is used for geometries where both of the dimensions located perpendicular to the magnetic field are almost equally long. In this thesis, these two formulas are compared and the differences between them are discussed.

Contents

1. Introduction

Superconductors have been discovered for over 100 years. They have been object to many experiments, due to their interesting behaviour, especially if put into a magnetic field. The magnetization of superconductors is dependent on their geometric shape and the current flowing through it. The relation between magnetization and critical current density can be calculated easily with two formulas which are dependent on the geometry of the superconductor. The first formula is used for geometries where one of the dimensions which are perpendicular to the applied field is much longer than the other one. The second formula is used for geometries where both sides perpendicular to the magnetic field are almost equally long.

Additionally, the magnetic quantities vary in different geometric properties due to demagnetizing effects. These demagnetizing factors have been studied since the 19^{th} century. Poisson, Thomson and Maxwell contributed to this topic [1]. For a long time spheres and ellipsoids were the only geometries for superconductors with analytic demagnetization factors until 1960. At this time T. T. Taylor [2, 3] calculated the factor for cylinders parallel and perpendicular to a magnetic field. For infinite long bars perpendicular to a magnetic field D. X. Chen et al. [4] calculated an analytic expression for the demagnetizing factor for various values of the susceptibility.
In other geometries, there exist no analytic expressions for superconductors. This field of research has been relying heavily on numerical approaches. The most recent numerical calculations for square bars and various susceptibilities on demagnetizing factors are by D. X. Chen et al. [5]. For type-II superconducting cylinders in axial direction Alvaro Sanchez and Carles Navau [6] did numerical calculations.
Although not used in this thesis, there have been some articles describing approaches with variational principles for calculating demagnetization factors. Here the method using magnetization point poles was applied [7, 8, 9].

The necessary theory of superconductors and their magnetic properties is presented in the second chapter of this thesis. Also, the differences between the two formulas relating magnetic moment and critical current density to each other, are presented. Next, the influence of the demagnetization effects are discussed. The last section of the chapter contains some information about magnetic flux measurements.

In the third chapter of this thesis the methods used for the numerical calculations of the demagnetizing factors for a cylinder with its main axis parallel and perpendicular to the magnetic field, for a long bar with its long side perpendicular to the magnetic field and for a general cuboid in the magnetic field are presented.

In the fourth chapter theoretical calculations of the formulas connecting critical current densities and magnetic moment to each other are described for various geometries in great detail. Also, the results of the numerical calculations of the demagnetizing factors for the cylinder and long bar are given. In the last section, the results of the measurements are given. These contain the evaluation of the magnetic susceptibility from the virgin magnetic curves of the samples and the calculation of the magnetization and the critical current density. The results of the magnetization and the critical current density are compared with the ones where the demagnetizing effects have been taken into account.

The last chapter is a short conclusion about the results of this thesis.

The full program code used for numerical calculations can be found in appendix A. The magnetic hysteresis curves measured are found in appendix B. Appendix C contains the virgin magnetic moment curves while appendix D and E contain the magnetization and the critical current density as a function of the internal and applied magnetic field.

A CD is attached which contains a digital copy of this thesis, all measured data, the program code of appendix A, and the compiled programs.

2. General Concepts

2.1. Superconductors

2.1.1. Type I superconductors

Type I superconductors were first discovered by H. Kamerlingh Onnes in 1911. He measured zero resistivity in several metals, when he cooled them down below a certain temperature. Meissner and Ochsenfeld observed perfect diamagnetism of superconductors in 1933. Appropriate theories to describe this effect emerged in the sixties [10].

The superconducting state is defined by the material having no electric resistivity in theory *and* being perfectly diamagnetic. Experiments have proven that there is no decrease in current in a closed superconducting circuit over years [10], which is equivalent to having zero resistivity for practical purposes. Fig. 2.1 shows the relation between the magnetic field and the magnetization in a type-I superconductor.

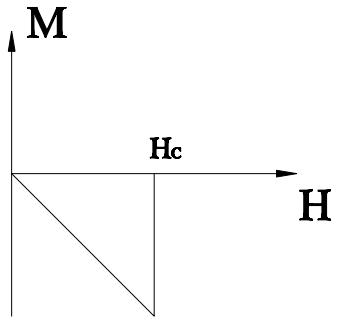

Figure 2.1.: The superconductor is perfectly diamagnetic until the applied field reaches a certain strength H_C. The material becomes immediately normal conducting at this point.

The London equations provide the theoretical background to describe the behaviour

$$\vec{E} = \frac{\partial}{\partial t}\left(\Lambda \cdot \vec{j}\right) \tag{2.1}$$

$$\vec{B} = \vec{\nabla} \times \left(\Lambda \cdot \vec{j}\right) \tag{2.2}$$

which relates the electric field E and the magnetic induction B to the current density j. The so called London length Λ is a material dependent factor.

2.1.2. Type-II superconductors

Type II superconductors do not show this perfect transition between conductivity and superconductivity as presented in Fig. 2.2. Instead they show a mixed state, the so called Shubnikov phase. Then the superconductor is no longer perfectly shielded. The magnetic field can penetrate the material.

The material enters the Shubnikov phase at the applied critical field H_{C1}. At this point, vortices appear near the surface of the superconductor. The vortices are moving inwards if the applied magnetic field is increased and new vortices appear near the surface. With increasing field, the density of vortices increases, until they are so dense, that the normal conducting regions overlap and superconductivity disappears. This field is called upper critical field H_{C2}.

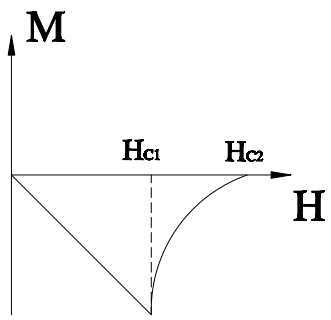

Figure 2.2.: The superconductor is perfectly diamagnetic until the applied field reaches a certain strength H_{C1}. At this point the material is penetrated by the field until the vortices fill up the whole material. This is the case when he field reaches H_{C2}, at which the material becomes normal conducting.

2.1.3. The Bean model

In Beans critical state model [11] the current density j, inside a type-II superconductor is assumed to be a constant and independent of the internal magnetic field H_i. The internal field decreases linearly inside the sample. This behavior is due to Ampère's law which relates j and H_i in the following way:

$$\vec{\nabla} \times \vec{H}_i = \vec{j} \tag{2.3}$$

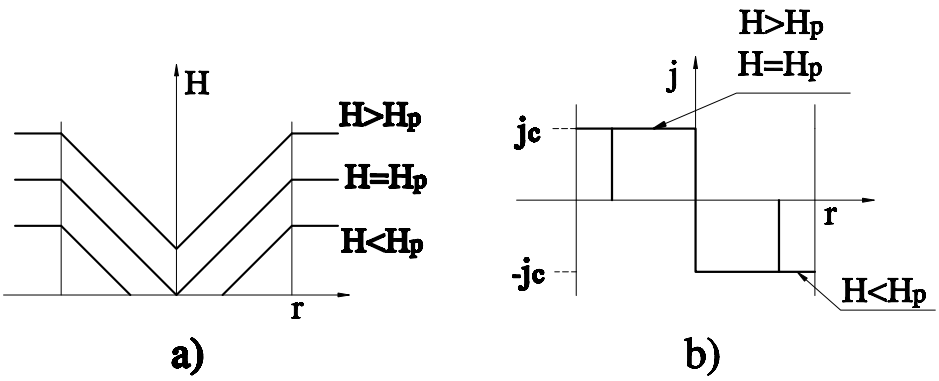

Figure 2.3.: The field penetrates the surface and decreases within the sample. The field moves inward, as the field is increased as seen in Fig. a). The critical current density is constant. It moves towards the inside of the sample as the field is increased. From the point on where the field has reached H_p, there is no change in the critical current density as seen in Fig. b).

This leads to a magnetic field dependent penetration depth. As the magnetic field increases, the magnetization does too, until a certain field H_p is reached. The magnetization stays constant if the field is increased any further. The effects for the field inside the sample and the current density as the field increases can be seen in Fig. 2.3. If the field is removed, the electromagnetic force due to Ampères law, has the effect that the field decreases at the surface.

2.2. Magnetic moment

The derivation of the magnetic moment can be found in full length in the book "*Electromagnetism*" by Pollack and Stump [12].

2.2.1. Two formulas

If the critical current density is known, one can calculate the magnetic moment of a body, where one of the two sides perpendicular to the applied field is much longer than the other one, by the relation:

$$\mathrm{d}\vec{m}_s = F\ \mathrm{d}\vec{I} \tag{2.4}$$

F is the area that is enclosed by the electric current $I = j \cdot A$ and the surface vector of F is perpendicular to current I. The surface vector of the area A is parallel to the current and current density j. If the sides perpendicular to the magnetic field

are rather equally long, one uses the relation

$$\vec{m}_p = \frac{1}{2} \int_V \vec{r} \times \vec{j}\,(\vec{r})\ \mathrm{d}V \tag{2.5}$$

In this section, these two formulas are compared and, if applied correctly, both formulas give the correct results for the magnetic moment. Two examples are illustrated in the following.

Square bar with side L parallel to a magnetic field

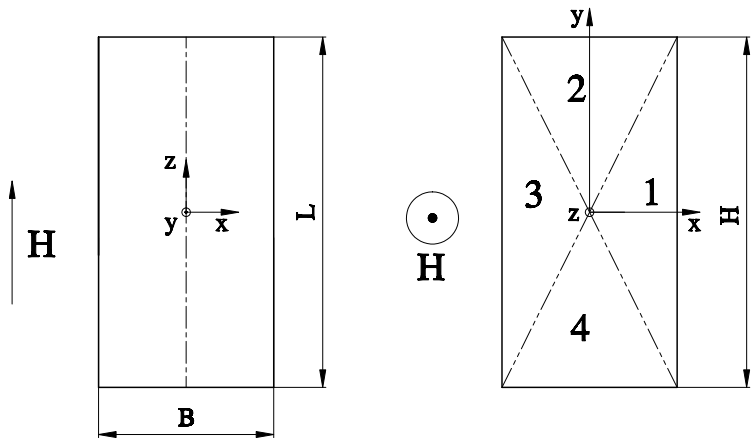

Figure 2.4.: Square bar with its length L parallel to the applied field. The numbers 1 and 3 indicate the areas where the current flows parallel to the height H. In the areas 2 and 4 the current flows parallel to the width B.

As derived from chapter 4, the magnetic moment of a cuboid with length L, width B and height H for the magnetic field applied parallel to H (Fig. 2.4) is according to formula (2.5),

$$\vec{m}_p = \frac{1}{6} jLB^3\ \vec{e}_z \tag{2.6}$$

Using formula (2.4) the magnetic moment calculates to,

$$\vec{m}_s = \vec{e}_z \int_0^L \int_0^{\frac{B}{2}} \underbrace{4\frac{2x \cdot x}{2}}_{F}\ \underbrace{j\ \mathrm{d}x\mathrm{d}z}_{\mathrm{d}I} = 4jL \left[\frac{x^3}{3}\right]_0^{\frac{B}{2}} \vec{e}_z = jL\frac{B^3}{6}\ \vec{e}_z \tag{2.7}$$

Both formulas give the same expression.

Rectangular bar with side L perpendicular to a magnetic field

Assuming that one side, in this case L, perpendicular to the magnetic field is much longer than the other side perpendicular to the magnetic field (Fig. 2.5), the formula

$$\vec{m}_s = \frac{1}{4} j L H B^2 \, \vec{e}_y \tag{2.8}$$

is used, which is also derived from chapter 4. Calculated with formula (2.5) the

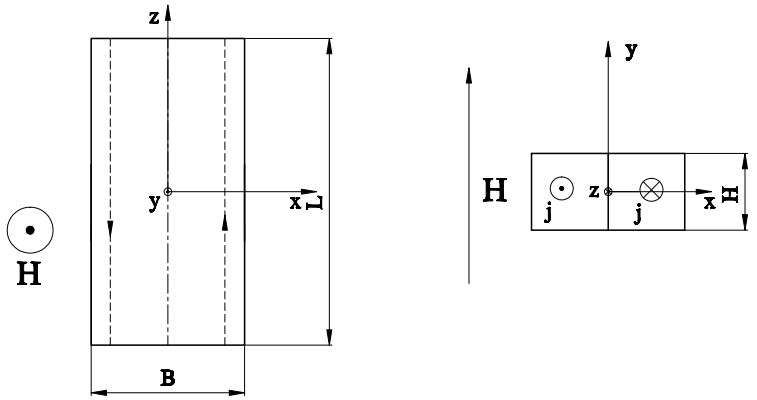

Figure 2.5.: Square bar with its length L perpendicular to the applied field. If the length L is much longer than the width B, it can be assumed that the current density flows through the surface perpendicular to L.

magnetic moment gives

$$\vec{m}_p = \frac{2}{2} \int_0^L \int_0^H \int_0^{\frac{B}{2}} jx \; \mathrm{d}x\mathrm{d}z\mathrm{d}y = \left[2\frac{jLHx^2}{2} \right]_0^{\frac{B}{2}} = \frac{jLHB^2}{4} \, \vec{e}_y \tag{2.9}$$

A factor of two is necessary, to reach the correct result. In order to explain this factor, we compare the two formulas (2.5) and (2.4)

$$\vec{m}_p = \frac{1}{2} \int_V \vec{r} \times \vec{j} \; \mathrm{d}V \tag{2.10}$$

$$\mathrm{d}\vec{m}_p = \frac{1}{2} \vec{r} \times \vec{j} \; \mathrm{d}V = \frac{1}{2} \vec{r} \times \underbrace{\vec{j}\mathrm{d}A}_{\mathrm{d}\vec{I}} \mathrm{d}z = \frac{1}{2} \vec{r} \times \vec{e}_y \; \mathrm{d}z\mathrm{d}I \tag{2.11}$$

$$\Rightarrow \mathrm{d}\vec{m}_p = \underbrace{\frac{1}{2} Lx}_{F} \; \mathrm{d}I \; \vec{e}_y \tag{2.12}$$

It can be seen that for the two formulas to be equivalent, the area F in $\mathrm{d}m_p$ has to be associated with $\frac{1}{2}Lx$, whereas in formula (2.4) $F = Lx$. This results from the

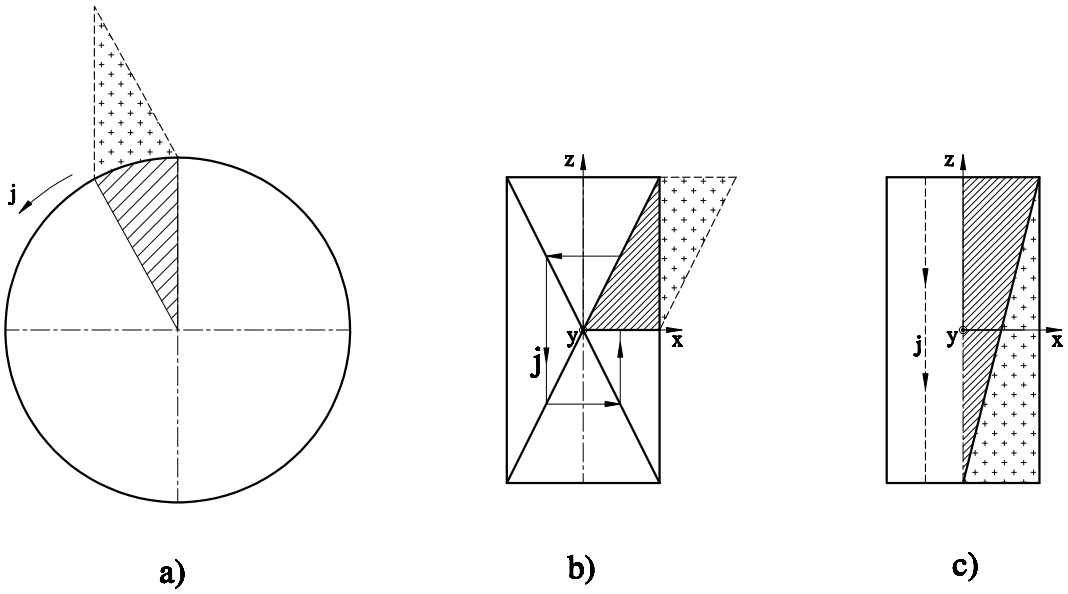

Figure 2.6.: The factor of one half in formula (2.5) is necessary for closed integration paths because the cross product of $r \times j$ gives the dashed area *and* the dotted area for F. The correct value would be half of F, as can be seen in picture a) and b). If the integration path is open the cross product would give the correct area F, but the factor of one half subtracts the dotted area in picture c).

fact that the formula (2.5) adds up infinitesimal triangles, which is necessary if the integration path is closed. One can see in Fig. 2.6 that if the area F is calculated by a cross product as in formula (2.5), the factor $\frac{1}{2}$ is necessary in order to gain the correct result. If the integration path is open, the area F needs to be rectangular and therefore the factor $\frac{1}{2}$ is not needed. So the formula (2.5) has to be multiplied by a factor of two, as it was done in derivation (2.9).

The main difference between the formulas is that in the case of formula (2.4) it is assumed that the current closes *only* at the edges. This assumption is only valid if one of the two sides perpendicular to the magnetic field is much longer than the other one.

2.2.2. Parallel axis theorem

There is a useful formula for calculating complex geometries which are perpendicular to the magnetic field. It is assumed that the dimension perpendicular to the field is much longer than the other dimensions, therefore equation (2.4) is used. Additionally, it is assumed that the cross section does not change along the length. The length of

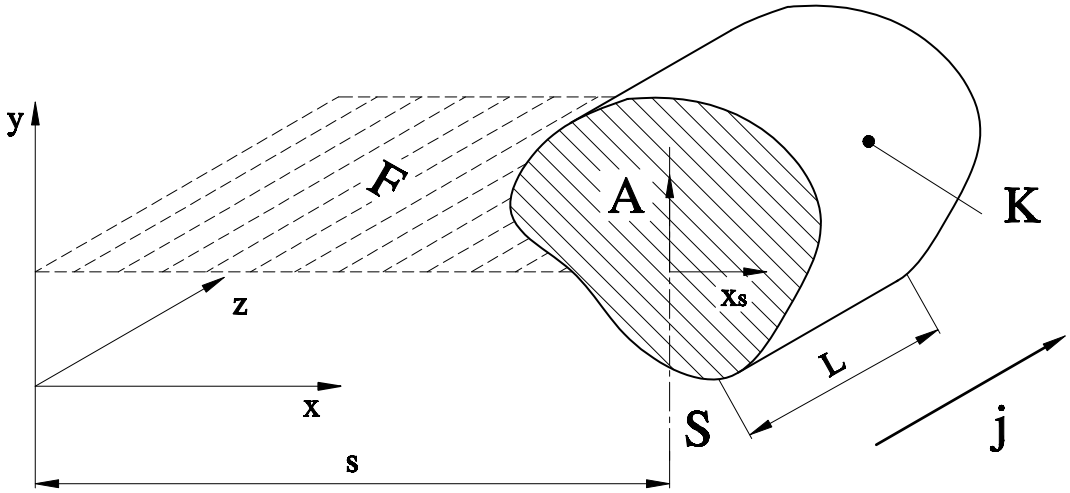

Figure 2.7.: The magnetic moment of the body K is evaluated with respect to the location of the origin. Every dimension in $x-$direction can be written as $x = s + x_s$, where s is the location of the center of mass in $x-$direction of the body K.

the sample is L with the cross section area being A. The idea is that the center of mass projected on the $x-$axis (s) does not change over the length of the sample. If a new coordination system is imagined at the center of mass, with the coordinate x_s, every dimension in $x-$direction can be written as $x = s + x_s$ (Fig. 2.7). Since s remains constant the magnetic moment with respect to the origin can easily be evaluated by knowing the volume V and s. This leads to the following relation

$$\mathrm{d}\vec{m}_K = \mathrm{d}\vec{I}\, F = \underbrace{Lx}_{F} \cdot \underbrace{j\ \mathrm{d}x\mathrm{d}y\ \vec{e}_y}_{\mathrm{d}\vec{I}} = L(x_S + s) j\ \mathrm{d}x\mathrm{d}y\ \vec{e}_y$$

$$m_K = jL\vec{e}_y \left[\int_A (x_S + s)\ \mathrm{d}A \right] = jL \underbrace{\vec{e}_y \int_A x_S\ \mathrm{d}A}_{0} + jLs\ \vec{e}_y \int_A \mathrm{d}A = jsLA\ \vec{e}_y$$

$$\Rightarrow \vec{m}_K = jsV\ \vec{e}_y$$

As an example the magnetic moment of a rectangular bar is calculated using the parallel axis theorem. A bar with length L and width B perpendicular to the applied magnetic field is considered. The height H is parallel to the field. The half of the

cuboid that is in the positive $x-$region is cut into two prisms with a triangular cross section as shown in Fig. 2.8. The magnetic moment of the lower prism is denoted m_1 and the magnetic moment of the upper prism is denoted m_2. To calculate these magnetic moments, only the volumes and the centers of mass have to be evaluated for both prisms, which can be done without integration.

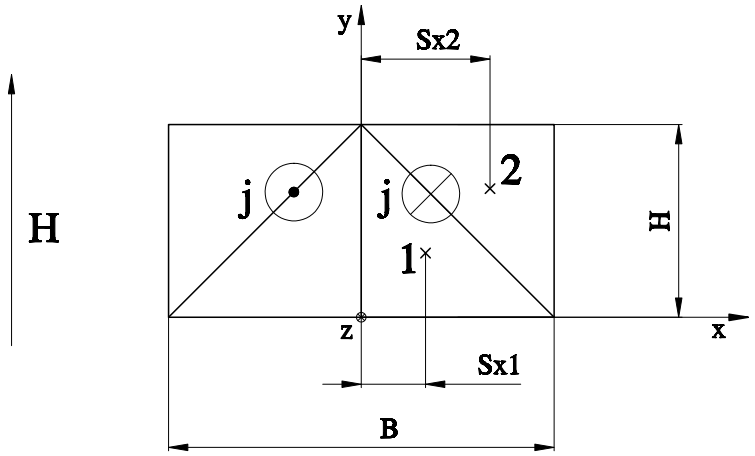

Figure 2.8.: Cross section of the profile calculated with the parallel axis theorem. S_{x1} and S_{x2} are the centers of mass for section (1) and (2).

$$\vec{m}_1 = 2jL\frac{\frac{B}{2}\cdot H}{2}\frac{B}{6}\,\vec{e}_y = \frac{jLB^2H}{12}\,\vec{e}_y$$
$$\vec{m}_2 = 2jL\vec{e}_y\frac{\frac{B}{2}\cdot H}{2}\frac{2B}{6} = \frac{2jLB^2H}{12}\,\vec{e}_y$$
$$\vec{m} = \vec{m}_1 + \vec{m}_2 = \frac{jLB^2H}{4}\,\vec{e}_y$$

This is the same solution as derived earlier. (Compare to equation (2.9)).

2.3. Demagnetizing effects

2.3.1. Magnetostatics

Exposing a magnetic material to a magnetic field, causes the material to become magnetized. The relation between applied field, magnetic induction and magnetization is given by

$$\vec{B} = \mu_0(\vec{H} + \vec{M}) \tag{2.13}$$

where μ_0 is the magnetic permeability of free space. Ampère's law states that

$$\vec{\nabla} \times \vec{H} = \vec{j} \tag{2.14}$$

where $\vec{j}$ is the current density. Inserted into equation (2.13) one gets

$$\vec{\nabla} \times \vec{B} = \mu_0 \left(\vec{j}_f + \vec{j}_m \right) \tag{2.15}$$

where $\vec{j}_f$ the free or applied current and $\vec{j}_m$ is the current which flows through the material due to the applied magnetic field.

2.3.2. Magnetic scalar potential

In analogy to electrostatics, a magnetic scalar potential is introduced in this subsection. If there is no free current applied to the sample, equation (2.14) changes to

$$\vec{\nabla} \times \vec{H} = 0 \tag{2.16}$$

The volume and surface magnetic pole densities for two materials (1) and (2), which are connected by the surface, are defined as

$$\rho_M = -\vec{\nabla} \cdot \vec{M} \qquad \sigma_M = \left(\vec{M}_1 - \vec{M}_2 \right) \cdot \vec{e}_n \tag{2.17}$$

where $\vec{M}_1$ and $\vec{M}_2$ are the magnetization vectors of medium (1) and (2). $\vec{e}_n$ is the surface unit vector pointing outwards of material (1). If medium (2) is vacuum the surface pole density simplifies to

$$\sigma_M = \vec{M}_1 \cdot \vec{e}_n \tag{2.18}$$

These potentials will later be used in chapter 3 for numerical calculations.

2.3.3. Demagnetizing effects

The geometry of the sample plays a vital role influencing the magnetic field. A magnetic field can be produced by currents or by magnetic poles [13]. The demagnetizing field H_d is caused by the magnetic poles. Therefore the magnetic field inside the sample is

$$\vec{H}_i = \vec{H}_a + \vec{H}_d \tag{2.19}$$

where H_a is the applied magnetic field. The demagnetizing field points in the opposite direction as the applied field for $\chi > 0$ and points in the same direction for $\chi < 0$.

2.3.4. Demagnetizing factor

If the vector of the applied field and the magnetization vector are parallel, the vector notation is not necessary. For the rest of the section only the scalar values parallel to the field are considered. To account for the magnetizing effects the demagnetizing factor is introduced by

$$H_d = -N \cdot M \tag{2.20}$$

This factor relates magnetization to the demagnetizing field. Inserted into equation (2.19) one obtains with $B = \mu_0 H$

$$H_i = \frac{B_a}{\mu_0} - N \cdot M \tag{2.21}$$

This formula will be important in chapter 4, since the applied field and the magnetic moment are measured. The measured moment relates to H_i and not to H_a and therefore H_a needs to be corrected [14].

2.3.5. Magnetic susceptibility

The material dependent factor χ relates the magnetic field to the magnetization. In this thesis, it is assumed that the material is homogeneous and therefore χ is constant. This is generally not true for all materials.
The susceptibility measured is not the true susceptibility due to demagnetizing effects. Like for the magnetic moment m and the magnetization M, χ also relates to H_i and not H_a. Since the susceptibility χ_m calculated by

$$\chi_\mathrm{m} = \frac{M}{H_a} \tag{2.22}$$

does not use the correct field, H_a needs to be exchanged by H_i (equation (2.21)), which gives the following relation between the measured susceptibility χ_m and the real susceptibility χ

$$\chi_\mathrm{m} = \frac{M}{H_i + N \cdot M} = \frac{\frac{M}{H_i}}{1 + N \cdot \frac{M}{H_i}} = \frac{\chi}{1 + N \cdot \chi} \tag{2.23}$$

2.4. Approach to a realistic current density in type-II superconductors

In this section a more realistic current density inside a cuboid shaped superconductor will be derived. This is a two dimensional approach. The starting point are the Maxwell equations with no electrical field

$$\vec{\nabla} \times \vec{B} = \mu_0 \left(\vec{j}_f + \vec{j}_m \right) \tag{2.24}$$

$$\vec{B} = \mu_0 \left(\vec{H} + \vec{M} \right) \tag{2.25}$$

$$\Rightarrow \vec{\nabla} \times \vec{H} + \vec{\nabla} \times \vec{M} = \vec{j}_f + \vec{j_m} \tag{2.26}$$

Since there is no applied current, $\vec{j}_f = 0$. This together with formula (2.5) leads to the following equations

$$\vec{\nabla} \times \vec{M} = \vec{j}_m \tag{2.27}$$

$$\vec{M} = \frac{\mathrm{d}\vec{m}}{\mathrm{d}V} \tag{2.28}$$

$$\vec{m} = \frac{1}{2} \int_V \vec{r} \times \vec{j}_m \, \mathrm{d}V \tag{2.29}$$

If it is assumed that the field applied to the sample is pointing in $z-$direction and that no current is flowing in direction of the applied field, one obtains from equation (2.27)

$$\begin{pmatrix} \partial_x \\ \partial_y \\ \partial_z \end{pmatrix} \times \begin{pmatrix} 0 \\ 0 \\ M_z \end{pmatrix} = \begin{pmatrix} f(x,y) \\ g(x,y) \\ 0 \end{pmatrix} \tag{2.30}$$

f and g are the x and y component of the current density and only functions of the x and y coordinates. Evaluating this equation leads to

$$\left.\begin{aligned} \partial_y \cdot M_z &= f(x,y) \\ \partial_x \cdot M_z &= -g(x,y) \end{aligned}\right\} \rightarrow \partial_x f(x,y) = -\partial_y g(x,y) \tag{2.31}$$

This relation will be used later. Next equations (2.28) and (2.29) are combined to

$$\vec{M} = \frac{1}{2} \left(\vec{r} \times \vec{j}_m \right) \tag{2.32}$$

and inserted into equation (2.27):

$$\vec{\nabla} \times \left(\vec{r} \times \vec{j}_m \right) = -2\vec{j}_m \tag{2.33}$$

This is a differential equation of first order. In order to simplify this expression the cross products are rewritten to

$$\vec{r} \left(\vec{\nabla} \cdot \vec{j}_m \right) + \left(\vec{j}_m \cdot \vec{\nabla} \right) \vec{r} - \vec{j}_m \left(\vec{\nabla} \cdot \vec{r} \right) - \left(\vec{r} \cdot \vec{\nabla} \right) \vec{j}_m = -2\vec{j}_m \tag{2.34}$$

$$\vec{r} \cdot \left(\partial_x f(x,y) + \partial_y g(x,y) \right) + \vec{j}_m - 3\vec{j}_m - (x\partial_x + y\partial_y + z\partial_z)\vec{j}_m = -2\vec{j}_m \tag{2.35}$$

The insertion of equation (2.31) gives the final partial differential equations of first order (PDEs)

$$x \cdot \partial_x f(x,y) + y \cdot \partial_y f(x,y) = 0 \tag{2.36}$$

$$x \cdot \partial_x g(x,y) + y \cdot \partial_y g(x,y) = 0 \tag{2.37}$$

$$\partial_x f(x,y) + \partial_y g(x,y) = 0 \tag{2.38}$$

The last equation is equal to equation (2.31) which is not surprising since this condition was demanded to derive the PDEs. The next step is to make an Ansatz to solve these PDEs. The following Ansatz was found to satisfy the PDEs:

$$f(x,y) = \frac{-y^k}{(x^m + y^m)^l} \qquad g(x,y) = \frac{x^k}{(x^m + y^m)^l} \tag{2.39}$$

There are three unknown parameters k, l and m, which have to be determined by inserting the Ansatz into the PDE. Inserting into (2.38) gives

$$\frac{m \cdot l \cdot x^{m-1} \cdot y^k}{(x^m + y^m)^{l+1}} - \frac{m \cdot l \cdot x^k \cdot y^{m-1}}{(x^m + y^m)^{l+1}} = 0 \tag{2.40}$$

This expression can only be true for all x and y if $k = m - 1$. The second condition can be obtained by inserting the Ansatz in either equation (2.36) or equation (2.37)

$$\frac{m \cdot l \cdot x^m \cdot y^{m-1}}{(x^m + y^m)^{l+1}} + \frac{m \cdot l \cdot y^m \cdot y^{m-1}}{(x^m + y^m)^{l+1}} - \frac{(m-1) \cdot y^{m-1}}{(x^m + y^m)^l} = 0 \tag{2.41}$$

$$\frac{m \cdot l \cdot y^{m-1} \cdot (x^m + y^m)}{(x^m + y^m)^{l+1}} - \frac{(m-1) \cdot y^{m-1}}{(x^m + y^m)^l} = 0 \tag{2.42}$$

$$(m \cdot l) - (m-1) = 0 \tag{2.43}$$

This leads to the condition of $l = 1 - \frac{1}{m}$. There is no condition to determine m. Therefore it has to be chosen to fit the measurements. $m = 2$ was found to be the best value. The functions f and g become with this value for m and the obtained values for k and l:

$$f(x,y) = \frac{-y}{\sqrt{x^2 + y^2}} \qquad g(x,y) = \frac{x}{\sqrt{x^2 + y^2}} \tag{2.44}$$

2.4.1. Cuboid

Based on the solution above, the current density induced by an external magnetic field can be described using symmetry arguments for a cuboid with its cross section perpendicular to the applied field (Fig. 2.9) as

$$j_x = -\frac{j}{2}\left(\frac{y-b}{\sqrt{(x-a)^2 + (y-b)^2}} + \frac{y+b}{\sqrt{(x-a)^2 + (y+b)^2}} + \right.$$
$$\left. + \frac{y-b}{\sqrt{(x+a)^2 + (y-b)^2}} + \frac{y+b}{\sqrt{(x+a)^2 + (y+b)^2}}\right) \tag{2.45}$$

$$j_y = +\frac{j}{2}\left(\frac{x-a}{\sqrt{(x-a)^2 + (y-b)^2}} + \frac{x-a}{\sqrt{(x-a)^2 + (y+b)^2}} + \right.$$
$$\left. + \frac{x+a}{\sqrt{(x+a)^2 + (y-b)^2}} + \frac{x+a}{\sqrt{(x+a)^2 + (y+b)^2}}\right) \tag{2.46}$$

with half length a and half width b. This current distribution is more of an approx-

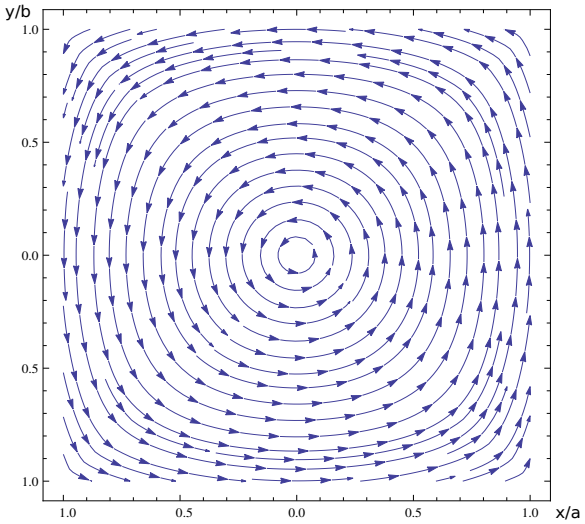

Figure 2.9.: New current distribution for a cuboid of length 2 and width 2. The applied magnetic field is perpendicular to the sheet.

imation than an exact solution, since the current leaves and enters the sample at the border. One could argue that surface currents could compensate this effect, but further analysis of this model needs to be done.
However, if this current distribution is inserted into formula (2.29) and integrated over the length of $2a$ the width of $2b$ and the height of H one obtains

$$
\begin{aligned}
m(j,a,b,H) &= \frac{jH}{6}\cdot \\
&\left\{ 12a^2b + 12ab^2 - 8ab\sqrt{a^2+b^2} + 4b^3 \ln\left[\frac{\left(\sqrt{a^2+4b^2}+a\right)\left(\sqrt{a^2+4b^2}-a\right)}{4b\left(\sqrt{a^2+b^2}+a\right)} \right] + \right. \\
&\quad + 3a^2b \ln\left[\frac{b^2}{\left(\sqrt{a^2+b^2}-a\right)\left(\sqrt{a^2+b^2}+a\right)} \right] + \\
&\quad \left. + a^3 \ln\left[\frac{\left(\sqrt{a^2+b^2}-b\right)^3\left(\sqrt{4a^2+b^2}+b\right)^7\left(\sqrt{4a^2+b^2}-b\right)^7}{4^7a^{16}\left(\sqrt{a^2+b^2}+b\right)} \right] \right\}
\end{aligned}
\tag{2.47}
$$

If we compare this expression to the formula of the magnetic moment of a cuboid (2.48) and to the formula of an infinite long cuboid with its longest side perpendicular to the magnetic field (2.49) and plot the ratio of m to m_p and m_s as the function of length to width ratio (L/B), it can be seen from graph (2.10) that the magnetization

is in perfect agreement for large values of L/B. The formulas for m_p and m_s are derived in section 4.

$$\vec{m}_p = \frac{jH}{12}\left(L^2B + B^2L\right)\vec{e}_z \tag{2.48}$$

$$\vec{m}_s = \frac{jH}{4}B^2L\,\vec{e}_z \tag{2.49}$$

Also the formula takes correctly into account the values for square shaped cross

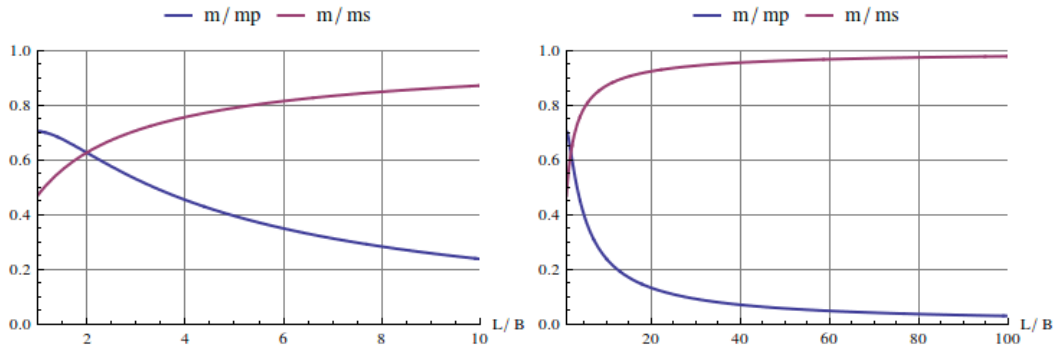

Figure 2.10.: The magnetic moment calculated by the adjusted current density m and the magnetic moment of a cuboid with a square like cross section perpendicular to the magnetic field m_p do not match for low length to width ratios L/B (left picture). The formula for m adjusts m_p. On the other hand is the magnetic moment calculated by the adjusted current density m and the magnetic moment calculated with the formula for an infinitly long cuboid with its longest side perpendicular to the magnetic field m_s in perfect agreement for large L/B ratios (right picture).

sections perpendicular to the magnetic field.

2.4.2. Cylinder

For a cylinder with its main axis perpendicular to the magnetic field, the current distribution of the previous subsection can be applied. The only change is that b is a function of the radius. An analytic expression for the magnetic moment can not be determined, but the values can be obtained by numerical integration. The magnetic moment can be compared to the magnetic moment of a cylinder with its main axis perpendicular to the magnetic field m_p and to the magnetic moment of an infinitly cylinder with its main axis perpendicular to the magnetic field m_s. Both formulas

are derived in detail in chapter 4. (Compare to equations (4.5) and (4.7)).

$$\vec{m}_p = \frac{jLR^2\pi}{32}\,(3L + 4R)\,\vec{e}_z \tag{2.50}$$

$$\vec{m}_s = \frac{4}{3}jLR^3\,\vec{e}_z \tag{2.51}$$

As for the cuboid perpendicular to the magnetic field the respective formula for the

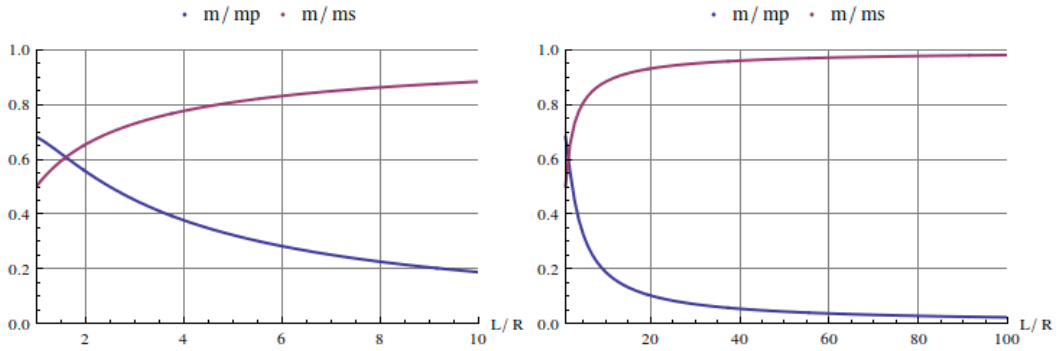

Figure 2.11.: The magnetic moment calculated by the adjusted current density m and the magnetic moment of a cylinder with a square like cross section perpendicular to the magnetic field m_p do not match for low length to radius ratios L/R (left picture). The formula for m adjusts m_p. On the other hand the magnetic moment calculated by the adjusted current density m and the magnetic moment calculated with the formula for an infinitly long cylinder with its main axis perpendicular to the magnetic field m_s is in perfect agreement for large L/R ratios (right picture).

corresponding magnetic moment of a cylinder adjusts the value of m_p for low length to radius ratios L/R as seen in Fig. 2.11. For higher L/R ratios the adjusted formula agrees with the theoretical values of m_s, especially as L goes towards infinity.

2.5. Vibrating Sample Magnetometer

For the magnetic measurements the vibrating sample magnetometer option of the Physical Properties Measurements System (PPMS) of Quantum Design with a 9 T superconducting coil was used (Fig. 2.12). The sample (4) is attached to a non magnetic rod (2). This rod vibrates in direction of its axis. The frequency during the experiments of this thesis was 40 Hz. The amplitude was 2 mm. A superconducting solenoid (5) provides a homogeneous magnetic field. The vibrating sample induces an alternating magnetic field in the measurement coil system (3). The voltage measured is proportional to the magnetic moment of the sample [13]. The rate at that the field changed during measurements was $1.1 \cdot 10^{-4}$ T per second at a temperature of 5 K.

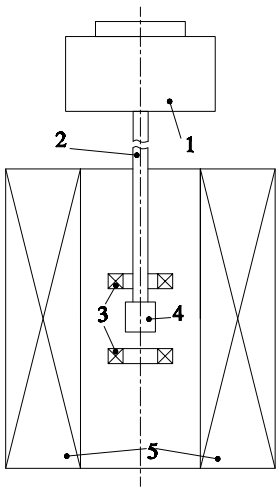

Figure 2.12.: Schematic picture of a VSM measurement device.

The material was niobium, which was chosen because it is an element and a type-II superconductor with high critical temperature. Cylinder samples, hollow cylinder samples as well as cuboid shaped samples were measured with their longest side L parallel and perpendicular to the magnetic field.

3. Implementation of the program code for calculating demagnetizing factors

In this chapter, the implementation of the program code, in order to calculate the demagnetizing factor numerically, is discussed for the case of a cylinder with its main axis parallel and perpendicular to the magnetic field as well as of a rectangular infinite long bar with its main axis perpendicular to the magnetic field. The last implementation of a general cuboid could not be finished since there was not enough time to do so in this thesis.
In order to solve the linear systems of equations which will be presented in this chapter, a lower upper (LU) decomposition routine [15] from the LAPACK [16] package was used. The code was written mainly in FORTRAN only the cylinders were implemented in MATHEMATICA too. There were special functions needed, particularly the hypergeometric and gamma function. For these, the code written by Zhang and Jin [17] was used.

3.1. Cylinder with its main axis parallel to the magnetic field

The mathematical background and idea for the calculation presented here can be found in *"Electric Polarizability of a Short Right Circular Conducting Cylinder"* from T. T. Taylor [2] who analytically calculated the demagnetizing factor in 1960. Originally Taylor calculated the electric polarizability of a short fully conducting cylinder parallel and perpendicular to an electric field. It is later shown that the transverse *electric* polarizability α_{tt} can be used to calculate the longitudal *magnetic* polarizability β_{ll}. Fully conducting means that $\chi = -1$.
As a first step he constructed a generalized system of orthogonal polynomials in order to express the charge density at the side and on the top of the cylinder. Since this whole derivation is too long and only important as theoretical background but not for practical calculations it is not rewritten in this thesis, but can be found in the article.

Finally, an expansion of the in the interior generated potential was obtained. The

coefficients of this expansion have the following form

$$\left[s_b Y_0^{s_b} + \sum_{m=0}^{N_s-1} s_m Y_0^{s_m} + w_b Y_0^{l_b} + \sum_{m=0}^{N_l-1} w_m Y_0^{l_m} \right] = 1 \tag{3.1}$$

$$\sum_{p=1}^{\infty} \left[s_b Y_p^{s_b} + \sum_{m=0}^{N_s-1} s_m Y_p^{s_m} + w_b Y_p^{l_b} + \sum_{m=0}^{N_l-1} w_m Y_p^{l_m} \right] = 0 \tag{3.2}$$

$$\sum_{m=0}^{N_s-1} s_m - \left(\frac{b}{a}\right)^{\nu} \sum_{m=0}^{N_l-1} w_m = 0 \tag{3.3}$$

where the Y_0 and Y_p are matrix coefficients, defined by equations (3.5) and (3.6) below. This linear set of equations is solved in order to obtain the coefficients s_b, s_m, w_b and w_m. In order to satisfy the interior potential the expression has to be 1 for $p = 0$ and 0 for as many p as possible. Although this may be true theoretically, it was found, that for numerical calculations most accurate results were gained only for a specific amount of equations [18]. The last equation assures that the side and end densities match each other at the edges.

The set of equations has to be solved for s_b, s_m, w_p and w_m. The minimum value for p, in order to be able to solve the linear system of equations, is defined by N_s and N_l as

$$p_{min} = N_s + N_l \tag{3.4}$$

which is two less than the total number of equations. The coefficients $Y_p^{s_m}$ and $Y_p^{l_m}$ are defined as

$$\begin{aligned} Y_p^{s_m} =& \frac{(-1)^{p+m} 2^{2p-\nu} \Gamma\left(m+p+\frac{3}{2}\right) \Gamma\left(m+p+\frac{1}{2}\right)}{\Gamma\left(\frac{1}{2}\right) \Gamma\left(2p+3\right) \Gamma\left(2m+\frac{3}{2}+\nu\right)} \left(\frac{a^2}{bc}\right) \left(\frac{b}{c}\right)^{2m+2} \cdot \\ & \cdot {}_2F_1\left(m+p+\frac{3}{2}, m-p+1+\nu; 2m+\frac{3}{2}+\nu; \frac{b^2}{c^2}\right) \end{aligned} \tag{3.5}$$

$$\begin{aligned} Y_p^{l_m} =& \frac{(-1)^{m} 2^{2p-\nu} \Gamma\left(m+p+\frac{3}{2}\right) \Gamma\left(m+p+2\right)}{\Gamma\left(\frac{1}{2}\right) \Gamma\left(2p+3\right) \Gamma\left(2m+3+\nu\right)} \left(\frac{a}{c}\right) \left(\frac{a}{c}\right)^{2m+2} \cdot \\ & \cdot {}_2F_1\left(m+p+\frac{3}{2}, m-p+1+\nu; 2m+3+\nu; \frac{a^2}{c^2}\right) \end{aligned} \tag{3.6}$$

The coefficients $Y_p^{s_b}$ and $Y_p^{l_b}$ are obtained from equations (3.6) and (3.5) by setting ν and m to zero. The coefficients $Y_0^{s_m}$ and $Y_0^{l_m}$ are obtained from formula (3.5) and (3.6) by setting m to zero and ν to $-\frac{1}{3}$. For $Y_0^{s_b}$ and $Y_0^{l_b}$ ν, m and p have to be zero. The value of ν is $-\frac{1}{3}$ for equation (3.3), $Y_p^{s_m}$ and $Y_p^{l_m}$. The function $\Gamma(x)$ represents the gamma function and ${}_2F_1(a, b; c; z)$ is the hypergeometric function. a is the radius, b is half the length of the cylinder and $c = \sqrt{a^2 + b^2}$.

After having obtained s_b, s_m, w_b and w_m by solving the linear set of equations, the electric polarizability can be calculated as

$$a_{tt} = \frac{\alpha_{tt}}{V\epsilon_0} = \left[s_b + \frac{\Gamma\left(\frac{1}{2}\right)}{2^{\frac{2}{3}}\Gamma\left(\frac{7}{6}\right)} s_0 \right] + \frac{a}{b}\left[\frac{1}{4} w_b + \frac{1}{2^{\frac{2}{3}}\Gamma\left(\frac{8}{3}\right)} w_0 \right] \tag{3.7}$$

The magnetic polarizability can be calculated from this result, with V the volume of the cylinder [3].

$$\frac{\mu_0 \beta_{ll}}{V} = -\frac{1}{2}\frac{\alpha_{tt}}{\epsilon_0 V} = -\frac{1}{2} a_{tt} \tag{3.8}$$

With this polarizability it is possible to calculate the demagnetizing factor of the cylinder. The relationship between longitudinal magnetic polarizability β_{ll} and demagnetization factor N_{mz} is

$$\frac{\mu_0 \beta_{ll}}{V} = \frac{1}{N_{mz} - 1} \tag{3.9}$$

according to [19]. The expression for N_{mz} calculates to

$$N_{mz} = 1 - \frac{2}{a_{tt}} \tag{3.10}$$

The full program code can be found in appendix A.1, along with a short description of how it is working.

3.2. Cylinder with its main axis perpendicular to the magnetic field

This time the article *"Magnetic Polarizability of a Short Right Circular Conducting Cylinder"* by T. T. Taylor [3] is used to implement the code in FORTRAN. As for the cylinder with its main axis parallel to the magnetic field, in this calculation also $\chi = -1$ is necessary. The procedure is similar to the one explained in the previous section. To obtain the perpendicular magnetic polarizability β_{tt} another system of orthogonal polynomials is introduced with the correct asymptotic behaviour near the edges. After building the expansion for the internal potential the following system of equations is obtained

$$\left[f_b Z_0^{s_b} + \sum_{m=0}^{N_s-1} f_m Z_0^{s_m} + f_b Z_0^{l_b} + \sum_{m=0}^{N_l-1} g_m Z_0^{l_m} \right] = 1 \tag{3.11}$$

$$\sum_{p=1}^{\infty} \left[f_b Z_p^{s_b} + \sum_{m=0}^{N_s-1} f_m Z_p^{s_m} + f_b Z_p^{l_b} + \sum_{m=0}^{N_l-1} g_m Z_p^{l_m} \right] = 0 \tag{3.12}$$

$$\sum_{m=0}^{N_s-1} f_m - \left(\frac{b}{a}\right)^{\nu'} \sum_{m=0}^{N_l-1} g_m = 0 \tag{3.13}$$

where Z_0 and Z_p are matrix coefficients defined by equations (3.15) and (3.16) below. The linear system of equations is solved in order to obtain the coefficients f_b, f_m and g_m Analog to the parallel cylinder the second equation needs to be zero for as many p as possible. As in the previous section the last equation is a boundary condition and there is a specific number for p_{min} to obtain most accurate results. Note that f_b appears twice and that there is no g_b. Therefore one equation less is needed and the minimum number for p is:

$$p_{min} = N_s + N_l - 1 \tag{3.14}$$

The coefficients $Z_p^{s_m}$ and $Z_p^{l_m}$ are defined as

$$\begin{aligned} Z_p^{s_m} =& \frac{(-1)^{p+m} 2^{2p+1-\nu'} \Gamma\left(m+p+\frac{3}{2}\right) \Gamma\left(m+p+\frac{1}{2}\right)}{\Gamma\left(\frac{1}{2}\right) \Gamma\left(2p+3\right) \Gamma\left(2m+\frac{3}{2}+\nu'\right)} \left(\frac{a^2}{bc}\right) \left(\frac{b}{c}\right)^{2m+2} \cdot \\ & \cdot \left[\left(m+p+\frac{1}{2}\right) {}_2F_1\left(m+p+\frac{3}{2}, m-p+\nu'; 2m+\frac{3}{2}+\nu'; \frac{b^2}{c^2}\right) + \right. \\ & \left. + \frac{1}{2} {}_2F_1\left(m+p+\frac{3}{2}, m-p+1+\nu'; 2m+\frac{3}{2}+\nu'; \frac{b^2}{c^2}\right) \right] \end{aligned} \tag{3.15}$$

$$\begin{aligned} Z_p^{l_m} =& \frac{(-1)^{m} 2^{2p+1-\nu'} \Gamma\left(m+p+\frac{5}{2}\right) \Gamma\left(m+p+2\right)}{\Gamma\left(\frac{1}{2}\right) \Gamma\left(2p+3\right) \Gamma\left(2m+3+\nu'\right)} \left(\frac{b}{c}\right) \left(\frac{a}{c}\right)^{2m+4} \cdot \\ & \cdot {}_2F_1\left(m+p+\frac{5}{2}, m-p+1+\nu'; 2m+3+\nu'; \frac{a^2}{c^2}\right) \end{aligned} \tag{3.16}$$

The function $\Gamma(x)$ represents the gamma function and ${}_2F_1(a, b; c; z)$ is the hypergeometric function. a is the radius, b is half the length of the cylinder and $c = \sqrt{a^2 + b^2}$. The value of ν is $\frac{2}{3}$ for equation (3.3), $Z_p^{s_m}$ and $Z_p^{l_m}$. The coefficients $Z_0^{s_m}$ and $Z_0^{l_m}$ are obtained, from $Z_p^{s_m}$ and $Z_p^{l_m}$, by setting p to zero. The values of p, m and ν are zero, for the coefficients $Z_p^{s_m}$ and $Z_p^{l_m}$, to obtain $Z_0^{s_b}$ and $Z_0^{l_b}$. For $Z_p^{s_b}$ and $Z_p^{l_b}$ the value of ν and m is zero.

After having obtained f_b, f_m and g_m by solving the linear set of equations, the magnetic polarizability can be calculated as

$$\frac{\mu_0 \beta_{tt}}{V} = -\left[f_b + \frac{\Gamma\left(\frac{1}{2}\right)}{2^{\frac{5}{3}} \Gamma\left(\frac{13}{6}\right)} f_0 \right] \tag{3.17}$$

where V is the volume of the cylinder. The relationship between N_{mx} and β_{tt} is directly calculatable due to

$$b_{tt} = \frac{\mu_0 \beta_{tt}}{V} = \frac{1}{N_{mx} - 1} \tag{3.18}$$

After rearranging this expression, the final result for the perpendicular demagnetizing factor is obtained

$$N_{mx} = 1 + \frac{1}{b_{tt}} \tag{3.19}$$

The full program code can be found in the appendix A.2, along with a short description of how it is working.

3.3. Infinite bar with its longest side perpendicular to the magnetic field

Even though there exist analytical calculations for demagnetization factors for bars of infinite length with their longest side perpendicular to the magnetic field [4], a program is implemented for two reasons: First, the analytical calculations are only true for $\chi = -1, 0$ and ∞ and second, the program should help to implement the much more complex program for a finite cuboid, which will be discussed in the next section. For the program the method given by D. X. Chen et al. [20] and described in the following, was used.

A scalar potential for the magnetic field H is assumed. This potential V fulfills the following relations

$$-\vec{\nabla} V = \vec{H} \tag{3.20}$$

$$\vec{\nabla}^2 V = 0 \tag{3.21}$$

For a rectangular cross section, according to Gauss law, the surface pole density σ is related to V by

$$\mu_0 \frac{\partial}{\partial x} \left[V_1(a, y) - V_2(a, y) \right] = \sigma(a, y) \tag{3.22}$$

$$\mu_0 \frac{\partial}{\partial y} \left[V_1(x, b) - V_2(x, b) \right] = \sigma(x, b) \tag{3.23}$$

where V_1 and V_2 are the potentials in the sample and in free space respectively. The magnetization can also be expressed in terms of the surface pole density by

$$M^x_{vol} = \frac{1}{\mu_0 ab} \left[\int_0^b a\sigma(a, y)\, \mathrm{d}y + \int_0^a x\sigma(x, b)\, \mathrm{d}x \right] \tag{3.24}$$

The easiest way to calculate the demagnetizing factor is by evaluating M inside the volume by

$$N_m = \frac{H_a}{M_{vol}} - \frac{1}{\chi} \tag{3.25}$$

In order to discretise the integral (3.24) the surface has to be divided in small quadratic cells with length Δx or Δy. The discretization is made in the following way

$$x(i) = i\,\Delta x \qquad \text{with} \quad \Delta x = \frac{a}{0.5 + n_x} \tag{3.26}$$

$$y(j) = \frac{2j-1}{2}\,\Delta y \quad \text{with} \quad \Delta y = \frac{b}{n_y} \tag{3.27}$$

where n_x and n_y are the number of cells in the positive $x-$, $y-$quadrant. There is no $z-$coordinate since it is assumed that the bar is infinitly long in that direction. Therefore the magnetization does not change along the $z-$axis. The indices for the surface area sections of the bar as seen in Fig. 3.1 are

$$i : x > 0, y = b \qquad -i : x < 0, y = b \tag{3.28}$$

$$i_- : x > 0, y = -b \qquad -i_- : x < 0, y = -b \tag{3.29}$$

$$j : x = a, y > 0 \qquad -j : x = a, y < 0 \tag{3.30}$$

$$j_- : x = -a, y > 0 \qquad -j_- : x = -a, y < 0 \tag{3.31}$$

This notation secures that the whole surface of the bar is mapped. With this division

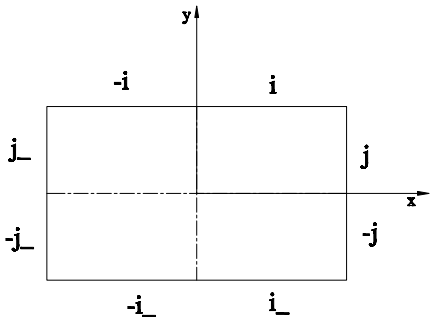

Figure 3.1.: In this figure the indices for the different surface area sections of a bar infinitly long along the $z-$axis, are shown.

the magnetization of the body, M_{vol}, becomes

$$M_{vol} = \frac{1}{\mu_0 ab}\left[\sum_{i'=1}^{n_x}\Delta x_{i'}\left(\frac{1}{2}\sigma^{i'}\Delta x_{i'} + \sum_{i=1}^{i'-1}\sigma^{i'}\Delta x_i + \sum_{j=1}^{n_y}\sigma^j\Delta y_j\right) + \frac{1}{2}M_{mid}\,b\Delta x_0\right] \tag{3.32}$$

where M_{mid} is the magnetization of the mid plane at $x = 0$. It is defined as

$$M_{mid} = \frac{1}{\mu_0 b}\left[\sum_{i=1}^{n_x}\sigma^i\Delta x_i + \sum_{j=1}^{n_y}\sigma^j\Delta x_j\right] \tag{3.33}$$

where σ^i are the surface pole density elements with the center point at $x(i)$. In order to derive σ^i a system of linear equations has to be solved. To be solvable there have to be $n_x + n_y$ equations for all $\sigma(x(i), y(j))$. The surface pole density $\sigma(x(i), y(j))$ interacts with the field produced by all surface pole densities $\sum \sigma(x(i'), y(j'))$

$$\frac{\sigma^j}{\chi} + \sum_{i'=1}^{n_x} \left(N_x^{j,i'} + N_x^{j,i'_-} - N_x^{j,-i'} - N_x^{j,-i'_-} \right) \sigma^{i'} + \\ + \sum_{j'=1}^{n_y} \left(N_x^{j,j'} + N_x^{j,-j'} - N_x^{j,j'_-} - N_x^{j,-j'_-} \right) \sigma^{j'} = \mu_0 H_a \tag{3.34}$$

$$\frac{\sigma^i}{\chi} + \sum_{i'=1}^{n_x} \left(N_y^{i,i'} + N_y^{i,i'_-} - N_y^{i,-i'} - N_y^{i,-i'_-} \right) \sigma^{i'} + \\ + \sum_{j'=1}^{n_y} \left(N_y^{i,j'} + N_y^{i,-j'} - N_y^{i,j'_-} - N_y^{i,-j'_-} \right) \sigma^{j'} = 0 \tag{3.35}$$

This holds true since $\sigma^i/\chi = \mu_0 M$ and $N_a^b \sigma^c = -\mu_0 H$. The indices of the N_x and N_y indicate the location of the surface pole densities. The algebraic sign in front of the N_x and N_y determines the direction of the field through this surface element. The magnetic field is applied in $x-$direction. The last pieces to write out the linear system of equations are the functions N_x and N_y. To evaluate them the starting point is an infinite straight wire. The field produced by it is equal to

$$\vec{H}(x, y) = \frac{x\vec{e}_x + y\vec{e}_y}{2\pi \left(x^2 + y^2\right)} \tag{3.36}$$

In order to evaluate the fields of the bar an integration over the $x-$ and $y-$coordinate is necessary

$$\vec{H}(x, y) = \frac{\sigma}{2\pi\mu_0} \int_{-t}^{t} \frac{(x - x')\,\vec{e}_x + y\vec{e}_y}{(x - x')^2 + y^2}\, \mathrm{d}x' \tag{3.37}$$

$$\vec{H}(x, y) = \frac{\sigma}{2\pi\mu_0} \int_{-t}^{t} \frac{x\vec{e}_x + (y - y')\,\vec{e}_y}{x^2 + (y - y')^2}\, \mathrm{d}y' \tag{3.38}$$

After the integration the field of an infinite long surface sheet with width $2t$ is the result

$$H_x(x,y) = \frac{\sigma}{4\pi\mu_0} G_x(x,y;t) = \frac{\sigma}{4\pi\mu_0} G_y(-y,x;t) \tag{3.39}$$

$$H_y(x,y) = \frac{\sigma}{4\pi\mu_0} G_y(x,y;t) = -\frac{\sigma}{4\pi\mu_0} G_x(-y,x;t) \tag{3.40}$$

$$G_x(u,v;t) = \ln\left[\frac{(u+t)^2+v^2}{(u-t)^2+v^2}\right] \tag{3.41}$$

$$G_y(u,v;t) = 2\left[\arctan\left(\frac{u+t}{v}\right) - \arctan\left(\frac{u-t}{v}\right)\right] \tag{3.42}$$

This ultimately leads to

$$\vec{N}^{i,\pm i'_\pm} = -\frac{1}{4\pi}\vec{G}\left(x_i \mp x_{i'}, b \mp b; \frac{\Delta x_{i'}}{2}\right) \tag{3.43}$$

$$\vec{N}^{j,\pm i'_\pm} = -\frac{1}{4\pi}\vec{G}\left(a \mp x_{i'}, y_j \mp b; \frac{\Delta x_{i'}}{2}\right) \tag{3.44}$$

$$\vec{N}^{i,\pm j'_\pm} = -\frac{1}{4\pi}\vec{G}\left(-b \mp y_{j'}, x_i \mp a; \frac{\Delta y_{j'}}{2}\right) \times \vec{e}_z \tag{3.45}$$

$$\vec{N}^{j,\pm j'_\pm} = -\frac{1}{4\pi}\vec{G}\left(-y_j \mp y_{j'}, a \mp a; \frac{\Delta y_{j'}}{2}\right) \times \vec{e}_z \tag{3.46}$$

The main program code can be found in the appendix A.3, along with a short description of how it is working.

3.4. Square bar with its longest side perpendicular to the magnetic field

This method is similar to the program in the previous section. It was implemented using "*Demagnetizing Factors for Square Bars*" [5]. It should be noted that this program could not be finished due to the limited amount of time available for this thesis. However the method and implementation is presented here.

The idea of calculating the demagnetizing factor is to cut the surface into tiles. Every tile has his own surface pole density and produces its own field. The formula to obtain the field of one tile is

$$\vec{H}(x,y,z) = \frac{1}{4\pi\mu_0} \int_{-t_z}^{t_z}\int_{-t_y}^{t_y}\int_{-t_x}^{t_x} \frac{\sigma(\vec{r}')\,(\vec{r}-\vec{r}')}{|\vec{r}-\vec{r}'|^3}\,\mathrm{d}x'\mathrm{d}y'\mathrm{d}z' \tag{3.47}$$

where $2t_x$, $2t_y$, $2t_z$ are the dimensions of the tiles. The field was averaged over one tile in [5]. In this thesis this was not followed since the program did not return the

correct results even for the non averaged approach. The indices for the different surface area sections are defined as

$$\begin{aligned} ij:\ x>0,\ y>0,\ z=c \qquad & -ij:\ x<0,\ y>0,\ z=c \\ i-j:\ x>0,\ y<0,\ z=c \qquad & -i-j:\ x<0,\ y<0,\ z=c \qquad (3.48) \\ (ij)_-:\ x>0,\ y>0,\ z=-c \qquad & (-ij)_-:\ x<0,\ y>0,\ z=-c \\ (i-j)_-:\ x>0,\ y<0,\ z=-c \qquad & (-i-j)_-:\ x<0,\ y<0,\ z=-c \qquad (3.49) \end{aligned}$$

$$\begin{aligned} ik:\ x>0,\ z>0,\ y=b \qquad & -ik:\ x<0,\ z>0,\ y=b \\ i-k:\ x>0,\ z<0,\ y=b \qquad & -i-k:\ x<0,\ z<0,\ y=b \qquad (3.50) \\ (ik)_-:\ x>0,\ z>0,\ y=-b \qquad & (-ik)_-:\ x<0,\ z>0,\ y=-b \\ (i-k)_-:\ x>0,\ z<0,\ y=-b \qquad & (-i-k)_-:\ x<0,\ z<0,\ y=-b \qquad (3.51) \end{aligned}$$

$$\begin{aligned} jk:\ y>0,\ z>0,\ x=a \qquad & -jk:\ y<0,\ z>0,\ x=a \\ j-k:\ y>0,\ z<0,\ x=a \qquad & -j-k:\ y<0,\ z<0,\ x=a \qquad (3.52) \\ (jk)_-:\ y>0,\ z>0,\ x=-a \qquad & (-jk)_-:\ y<0,\ z>0,\ x=-a \\ (j-k)_-:\ y>0,\ z<0,\ x=-a \qquad & (-j-k)_-:\ y<0,\ z<0,\ x=-a \qquad (3.53) \end{aligned}$$

In Fig. 3.2 the indexed surface areas of the cuboid can be seen. This notation secures that the whole surface of the bar is mapped. The back side is indexed analog, of the form $(l,m)_-$, as seen in formulas (3.48) to (3.53). The main equations to obtain the

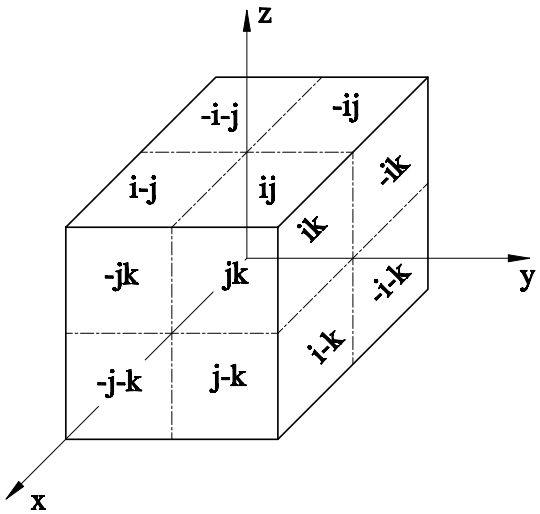

Figure 3.2.: In this figure the indices for the different surface area sections of a square bar are shown. The areas indexed of the form $(l,m)_-$ are not shown, but they lie on the surfaces at the back of the cuboid.

σ^i have the following form for a field pointing in $z-$direction.

$$\begin{aligned}\frac{\sigma^{jk}}{\chi} + \sum_{j',k'}^{n_1} \Big(& N_x^{jk,j'k'} - N_x^{jk,j'-k'} + N_x^{jk,-j'k'} - N_x^{jk,-j'-k'} + \\ & + N_x^{jk,(j'k')-} - N_x^{jk,(j'-k')-} + N_x^{jk,(-j'k')-} - N_x^{jk,(-j'-k')-} \Big) \sigma^{j'k'} + \\ + \sum_{i',k'}^{n_2} \Big(& N_x^{jk,i'k'} - N_x^{jk,i'-k'} + N_x^{jk,-i'k'} - N_x^{jk,-i'-k'} + \\ & + N_x^{jk,(i'k')-} - N_x^{jk,(i'-k')-} + N_x^{jk,(-i'k')-} - N_x^{jk,(-i'-k')-} \Big) \sigma^{i'k'} + \\ + \sum_{i',j'}^{n_3} \Big(& N_x^{jk,i'j'} + N_x^{jk,i'-j'} + N_x^{jk,-i'j'} + N_x^{jk,-i'-j'} + \\ & - N_x^{jk,(i'j')-} - N_x^{jk,(i'-j')-} - N_x^{jk,(-i'j')-} - N_x^{jk,(-i'-j')-} \Big) \sigma^{i'j'} = 0 \end{aligned} \tag{3.54}$$

$$\begin{aligned}\frac{\sigma^{ik}}{\chi} + \sum_{j',k'}^{n_1} \Big(& N_y^{ik,j'k'} - N_y^{ik,j'-k'} + N_y^{ik,-j'k'} - N_y^{ik,-j'-k'} + \\ & + N_y^{ik,(j'k')-} - N_y^{ik,(j'-k')-} + N_y^{ik,(-j'k')-} - N_y^{ik,(-j'-k')-} \Big) \sigma^{j'k'} + \\ + \sum_{i',k'}^{n_2} \Big(& N_y^{ik,i'k'} - N_y^{ik,i'-k'} + N_y^{ik,-i'k'} - N_y^{ik,-i'-k'} + \\ & + N_y^{ik,(i'k')-} - N_y^{ik,(i'-k')-} + N_y^{ik,(-i'k')-} - N_y^{ik,(-i'-k')-} \Big) \sigma^{i'k'} + \\ + \sum_{i',j'}^{n_3} \Big(& N_y^{ik,i'j'} + N_y^{ik,i'-j'} + N_y^{ik,-i'j'} + N_y^{ik,-i'-j'} + \\ & - N_y^{ik,(i'j')-} - N_y^{ik,(i'-j')-} - N_y^{ik,(-i'j')-} - N_y^{ik,(-i'-j')-} \Big) \sigma^{i'j'} = 0 \end{aligned} \tag{3.55}$$

$$\begin{aligned}
&\frac{\sigma^{ij}}{\chi} + \sum_{j',k'}^{n_1} \Big(N_z^{ij,j'k'} - N_z^{ij,j'-k'} + N_z^{ij,-j'k'} - N_z^{ij,-j'-k'} + \\
&\qquad + N_z^{ij,(j'k')-} - N_z^{ij,(j'-k')-} + N_z^{ij,(-j'k')-} - N_z^{ij,(-j'-k')-} \Big) \sigma^{j'k'} + \\
&+ \sum_{i',k'}^{n_2} \Big(N_z^{ij,i'k'} - N_z^{ij,i'-k'} + N_z^{ij,-i'k'} - N_z^{ij,-i'-k'} + \\
&\qquad + N_z^{ij,(i'k')-} - N_z^{ij,(i'-k')-} + N_z^{ij,(-i'k')-} - N_z^{ij,(-i'-k')-} \Big) \sigma^{i'k'} + \\
&+ \sum_{i',j'}^{n_3} \Big(N_z^{ij,i'j'} + N_z^{ij,i'-j'} + N_z^{ij,-i'j'} + N_z^{ij,-i'-j'} + \\
&\qquad - N_z^{ij,(i'j')-} - N_z^{ij,(i'-j')-} - N_z^{ij,(-i'j')-} - N_z^{ij,(-i'-j')-} \Big) \sigma^{i'j'} = \mu_0 H_a
\end{aligned} \tag{3.56}$$

It is obvious that there have to be $n_p = n_1 + n_2 + n_3$ equations in order to solve this system of equations. The surface in the positive $x-$, $y-$ and $z-$direction was divided in n_p elements. The coordinate for each direction is

$$x(i) = (2i-1)\Delta x \qquad \text{with} \quad \Delta x = \frac{a}{2n_x} \tag{3.57}$$

$$y(j) = (2j-1)\Delta y \qquad \text{with} \quad \Delta y = \frac{b}{2n_y} \tag{3.58}$$

$$z(k) = (2k)\Delta z \qquad \text{with} \quad \Delta z = \frac{c}{1+2n_z} \tag{3.59}$$

The functions N can be calculated with the following relations

$$N_x^{jk,\pm j'\pm k'_\pm} = \frac{1}{4\pi} F_2(y_j \mp y_{j'}, z_k \mp z_{k'}, a \mp a, \Delta y, \Delta z) \tag{3.60}$$

$$N_x^{jk,\pm i'\pm k'_\pm} = \frac{1}{4\pi} F_1(a \mp x_{i'}, z_k \mp z_{k'}, y_j \mp b, \Delta x, \Delta z) \tag{3.61}$$

$$N_x^{jk,\pm i'\pm j'_\pm} = \frac{1}{4\pi} F_1(a \mp x_{i'}, y_j \mp y_{j'}, z_k \mp c, \Delta x, \Delta y) \tag{3.62}$$

$$N_y^{ik,\pm j'\pm k'_\pm} = \frac{1}{4\pi} F_1(b \mp y_{j'}, z_k \mp z_{k'}, x_i \mp a, \Delta y, \Delta z) \tag{3.63}$$

$$N_y^{ik,\pm i'\pm k'_\pm} = \frac{1}{4\pi} F_2(x_i \mp x_{i'}, z_k \mp z_{k'}, b \mp b, \Delta x, \Delta z) \tag{3.64}$$

$$N_y^{ik,\pm i'\pm j'_\pm} = \frac{1}{4\pi} F_1(b \mp y_{j'}, x_i \mp x_{i'}, z_k \mp c, \Delta y, \Delta x) \tag{3.65}$$

$$N_z^{ij,\pm j'\pm k'_\pm} = \frac{1}{4\pi} F_1(c \mp z_{k'}, y_j \mp y_{j'}, x_i \mp a, \Delta z, \Delta y) \tag{3.66}$$

$$N_z^{ij,\pm i'\pm k'_\pm} = \frac{1}{4\pi} F_1(c \mp z_{k'}, x_i \mp x_{i'}, y_j \mp b, \Delta z, \Delta x) \tag{3.67}$$

$$N_z^{ij,\pm i'\pm j'_\pm} = \frac{1}{4\pi} F_2(x_i \mp x_{i'}, y_j \mp y_{j'}, c \mp c, \Delta x, \Delta y) \tag{3.68}$$

$$\begin{aligned} F_1(u,v,w;t,d) =& f_1(u+t,v-d,w) - f_1(u+t,v+d,w) + \\ &+ f_1(u-t,v+d,w) - f_1(u-t,v-d,w) \end{aligned} \tag{3.69}$$

$$\begin{aligned} F_2(u,v,w;t,d) =& f_2(t-u,d-v,w) + f_2(t+u,d-v,w) + \\ &+ f_2(t-u,v+d,w) + f_2(u+t,v+d,w) \end{aligned} \tag{3.70}$$

$$f_1(u',v',w') = \operatorname{arcsinh}\left(\frac{v'}{\sqrt{u'^2+w'^2}}\right) \tag{3.71}$$

$$f_2(u',v',w') = \arctan\left(\frac{u'v'}{w'\sqrt{u'^2+v'^2+w'^2}}\right) \tag{3.72}$$

The numbers n_x, n_y and n_z are the numbers of elements for each direction. They are related to n_p as $n_1 = n_y \cdot n_z$, $n_2 = n_x \cdot n_z$ and $n_3 = n_x \cdot n_y$.
Once the σ are known the volume magnetization can be calculated.

$$M_{vol} = \frac{1}{\mu_0 abc}\left(\sum_{j,k}^{n_1} z(k)\sigma^{jk}\Delta y\Delta z + \sum_{i,k}^{n_2} z(k)\sigma^{ik}\Delta x\Delta z + \sum_{i,j}^{n_3} c\,\sigma^{ij}\Delta x\Delta y\right) \tag{3.73}$$

This formula is similar to (3.24) given in the last section. After obtaining M_{vol} the demagnetizing factor can be calculated by

$$N_m = \frac{H_a}{M_{vol}} - \frac{1}{\chi} \tag{3.74}$$

The computer program was written in FORTRAN. The main parts of the program can be found in appendix A.4, along with a short description of how it is working. Unfortunately the program does not return correct values for the demagnetization factor. There was not enough time to determine, why the program is not working the way it should be. The correction of the code is left for future works.

4. Results

In the first part of this chapter, the theoretical calculations regarding the relation between magnetic moment and critical current density are performed for various geometries. The second part of the chapter deals with the results from the numerical calculations of the demagnetizing factor. The last part contains the evaluation of measurement data.

4.1. Formulas for magnetic moment

The relations between magnetic moment and current density are derived in the following sections for various geometries.

4.1.1. Cylinder

Magnetic field parallel to the main axis

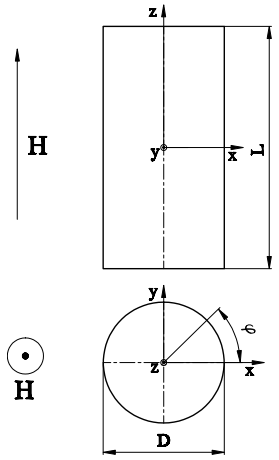

Figure 4.1.: A cylinder with its main axis parallel to the magnetic field. The critical current density flows in the $xy-$plane perpendicular to the length L of the cylinder.

The cylinder with its main axis parallel to the magnetic field, as seen in Fig. 4.1,

is calculated by following formula

$$\vec{m} = \frac{1}{2} \int_V \vec{r} \times \vec{j}(\vec{r}) \mathrm{d}V \tag{4.1}$$

$$\begin{aligned} m &= \frac{1}{2} \int_0^R \int_0^{2\pi} \int_{-\frac{L}{2}}^{\frac{L}{2}} \begin{pmatrix} r \cdot \cos(\varphi) \\ r \cdot \sin(\varphi) \\ z \end{pmatrix} \times \begin{pmatrix} -j \cdot \sin(\varphi) \\ j \cdot \cos(\varphi) \\ 0 \end{pmatrix} \cdot r \cdot \mathrm{d}r\mathrm{d}\varphi\mathrm{d}z \\ &= \frac{j}{2} \int_0^R \int_0^{2\pi} \int_{-\frac{L}{2}}^{\frac{L}{2}} \begin{pmatrix} -z \cdot r \cdot \cos(\varphi) \\ -z \cdot r \cdot \sin(\varphi) \\ r^2 \end{pmatrix} \mathrm{d}r\mathrm{d}\varphi\mathrm{d}z = \frac{j\pi}{1} \int_0^R \int_{-\frac{L}{2}}^{\frac{L}{2}} \begin{pmatrix} 0 \\ 0 \\ r^2 \end{pmatrix} \mathrm{d}r\mathrm{d}z \\ &= \frac{j\pi R^3}{3} \int_{-\frac{L}{2}}^{\frac{L}{2}} \begin{pmatrix} 0 \\ 0 \\ 1 \end{pmatrix} \mathrm{d}z \end{aligned}$$

$$\vec{m} = \frac{j\pi L R^3}{3} \, \vec{e}_z \tag{4.2}$$

Magnetic field perpendicular to main axis

This geometry is a bit more difficult than the cylinder with its main axis parallel to the magnetic field. It has to be divided into two different parts in order to get the full result for the magnetic moment. Formula (2.5) is applied, because it is assumed that the diameter $2R$ and the height H of the cylinder are almost equal in length. The First section I, as seen in Fig. 4.2, is calculated:

$$\begin{aligned} \vec{m}_1 &= \frac{1}{2} 2 \int_{y=-R}^{R} \int_{z=0}^{\sqrt{\frac{H^2}{4} - \frac{H^2}{4R^2} y^2}} \int_{x=\frac{-2R}{H} z}^{R} \begin{pmatrix} x \\ y \\ z \end{pmatrix} \times \begin{pmatrix} 0 \\ 0 \\ j \end{pmatrix} \mathrm{d}x\mathrm{d}z\mathrm{d}y = \\ &= j \, \vec{e}_y \int_{y=-R}^{R} \int_{z=0}^{\sqrt{\frac{H^2}{4} - \frac{H^2}{4R^2} y^2}} \int_{x=\frac{-2R}{H} z}^{R} x \, \mathrm{d}x\mathrm{d}y\mathrm{d}z = \\ &= j \, \vec{e}_y \int_{y=-R}^{R} \int_{z=0}^{\sqrt{\frac{H^2}{4} - \frac{H^2}{4R^2} y^2}} R^2 - \frac{4R^2}{H^2} z^2 \, \mathrm{d}z\mathrm{d}y = \\ &= j \, \vec{e}_y \int_{y=-R}^{R} R^2 \sqrt{\frac{H^2}{4} - \frac{H^2}{4R^2} y^2} - \frac{4R^2}{3H^2} \left(\frac{H^2}{4} - \frac{H^2}{4R^2} y^2 \right)^{\frac{3}{2}} \, \mathrm{d}y \end{aligned}$$

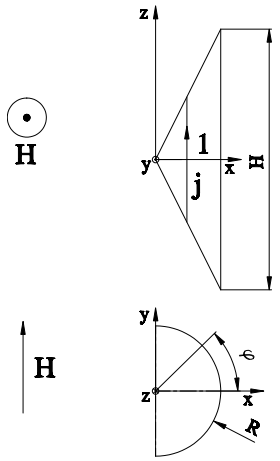

Figure 4.2.: A cylinder with its main axis perpendicular to the magnetic field. The critical current density flows in the $xz-$plane. In order to calculate the magnetic moment, the geometry has to be divided into two sections. In section I, the critical current density flows parallel to the height H of the cylinder.

$y = R\sin(\varphi) \Rightarrow \mathrm{d}y = R\cos(\varphi)\mathrm{d}\varphi$ is substituted to obtain

$$\vec{m}_1 = j\ \vec{e}_y \int_{\frac{-\pi}{2}}^{\frac{\pi}{2}} \frac{H}{2} R^3 \cos(\varphi) - \frac{4R^2}{3H^2}\frac{H^3}{8} R\cos(\varphi)^4\ \mathrm{d}\varphi =$$

$$= j\left[\frac{HR^3\pi}{4} - \frac{4R^2}{H^2}\left(\frac{H}{2}\right)^3 \frac{3R\pi}{8}\right]\vec{e}_y = \frac{jHR^3\pi}{4}\left(1 - \frac{3}{4}\right)\vec{e}_y$$

$$\vec{m}_1 = \frac{jHR^3\pi}{16}\ \vec{e}_y \tag{4.3}$$

After obtaining the result for the magnetic moment in section I, section II, as seen in Fig. 4.3, is calculated.

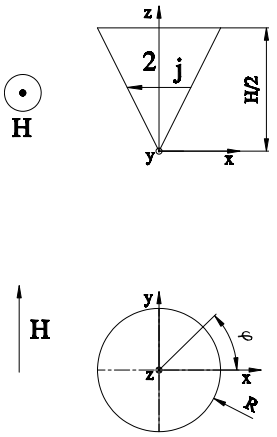

Figure 4.3.: A cylinder with its main axis perpendicular to the magnetic field. The critical current density of section II flows in the $xz-$plane perpendicular to the height H of the cylinder.

$$\vec{m}_2 = \frac{1}{2}2 \int_{y=-R}^{R} \int_{x=0}^{\sqrt{R^2-y^2}} \int_{z=\frac{H}{2R}x}^{\frac{H}{2}} \begin{pmatrix} x \\ y \\ z \end{pmatrix} \times \begin{pmatrix} -j \\ 0 \\ 0 \end{pmatrix} \mathrm{d}z\mathrm{d}x\mathrm{d}y =$$

$$= j\ \vec{e}_y \int_{y=-R}^{R} \int_{x=0}^{\sqrt{R^2-y^2}} \int_{z=\frac{H}{2R}x}^{\frac{H}{2}} z\ \mathrm{d}z\mathrm{d}x\mathrm{d}y =$$

$$= j\ \vec{e}_y \int_{y=-R}^{R} \int_{x=0}^{\sqrt{R^2-y^2}} \frac{H^2}{8} - \frac{H^2}{8R^2}x^2\ \mathrm{d}x\mathrm{d}y =$$

$$= j\ \vec{e}_y \int_{y=-R}^{R} \frac{H^2}{8}\sqrt{R^2-y^2} - \frac{H^2}{24R^2}\left(R^2-y^2\right)^{\frac{3}{2}}\ \mathrm{d}x\mathrm{d}y =$$

As in section I, $y = R\sin(\varphi) \Rightarrow \mathrm{d}y = R\cos(\varphi)\mathrm{d}\varphi$ is substituted and the magnetic moment for section II, $\vec{m}_2$, is calculated to

$$\vec{m}_2 = j\ \vec{e}_y \int_{\frac{-\pi}{2}}^{\frac{\pi}{2}} \frac{H^2}{8}R^2\cos(\varphi)^2 - \frac{H^2}{24R^2}R^4\cos(\varphi)^4\mathrm{d}\varphi =$$

$$= j\left[\frac{H^2}{8}\frac{R^2\pi}{2} - \frac{H^2}{24R^2}\frac{3\pi R^4}{8}\right]\vec{e}_y = \frac{jH^2R^2\pi}{16}\left(1-\frac{3}{12}\right)\vec{e}_y$$

$$\vec{m}_2 = \frac{3j\pi H^2R^2}{64}\ \vec{e}_y \tag{4.4}$$

is obtained. The total magnetization is calculated as the sum of all parts, where the parts III and IV are equal to the parts I and II

$$\vec{m}_{ges} = \vec{m}_1 + \vec{m}_2 + \vec{m}_3 + \vec{m}_4 = 2\left(\frac{jHR^3\pi}{16} + \frac{3j\pi H^2R^2}{64}\right)\vec{e}_y$$

$$\vec{m}_{ges} = \frac{j\pi HR^2}{32}\left(3H + 4R\right)\vec{e}_y \tag{4.5}$$

This is the final result for a finite cylinder with its main axis perpendicular to the magnetic field.

Infinitly long cylinder perpendicular to the magnetic field

For an infinitly long cylinder with its main axis that is perpendicular to the magnetic field, as seen in Fig. 4.4, formula (2.4) is used:

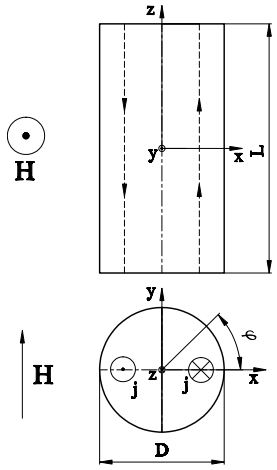

Figure 4.4.: An infinitly long cylinder with its longest side perpendicular to the magentic field. The critical current density flows in the $xz-$plane parallel to the length L of the cylinder. It is assumed that the current flows through the surface perpendicular to L.

$$\mathrm{d}\vec{m} = \mathrm{d}\vec{I}F = 2jLx\mathrm{d}x\mathrm{d}y\ \vec{e}_y \tag{4.6}$$

$\vec{I}$ denotes the current and F is the area between the $zy-$plane and the current.

$$\vec{m} = 2jL\ \vec{e}_y \int_{-R}^{R}\int_{0}^{\sqrt{R^2-y^2}} x\ \mathrm{d}x\mathrm{d}y = jL\ \vec{e}_y \int_{-R}^{R} R^2 - y^2\ \mathrm{d}y =$$

$$= jL\left[R^2y - \frac{y^3}{3}\right]_{-R}^{R}\vec{e}_y = jL\left[2R^3 - \frac{2}{3}R^3\right]\vec{e}_y$$

$$\vec{m} = \frac{4jLR^3}{3}\,\vec{e}_y \tag{4.7}$$

4.1.2. Cuboid

Finite Cuboid with length L parallel to the magnetic field

Analog to the cylinder, this geometry is divided into 4 sections, as seen in Fig. 4.5. First the magnetic moment in the sectors I and III is calculated. In order to apply formula (2.5) to calculate the magnetic moment, it is assumed that the width B and the height H are almost equal in length.

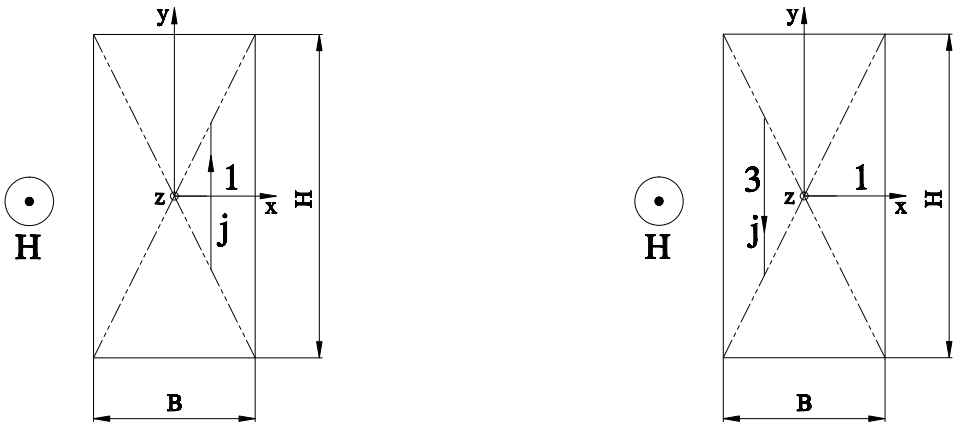

Figure 4.5.: A cuboid with its length L parallel to the magnetic field. In section I and III flows the critical current density parallel to the height H of the cuboid.

$$\begin{aligned}
\vec{m}_{I.III} &= \frac{1}{2}\int_{\frac{-L}{2}}^{\frac{L}{2}}\int_{0}^{\frac{B}{2}}\int_{-\frac{H}{B}x}^{\frac{H}{B}x}\begin{pmatrix}x\\y\\z\end{pmatrix}\times\begin{pmatrix}0\\j\\0\end{pmatrix}\,\mathrm{d}x\mathrm{d}y\mathrm{d}z = \\
&= \frac{jL}{2}\,\vec{e}_z\int_{0}^{\frac{B}{2}}\int_{\frac{-H}{B}x}^{\frac{H}{B}x} x\;\mathrm{d}y\mathrm{d}x = \frac{jL}{2}\,\vec{e}_z\int_{0}^{\frac{B}{2}}\frac{2H}{B}x^2\;\mathrm{d}x = \frac{2jLH}{2B}\left[\frac{x^3}{3}\right]_0^{\frac{B}{2}}\vec{e}_z = \\
&= \frac{jLHB^2}{24}\,\vec{e}_z
\end{aligned}$$

Next the magnetic moment in the sectors II and IV, as seen in Fig. 4.6, is calculated.

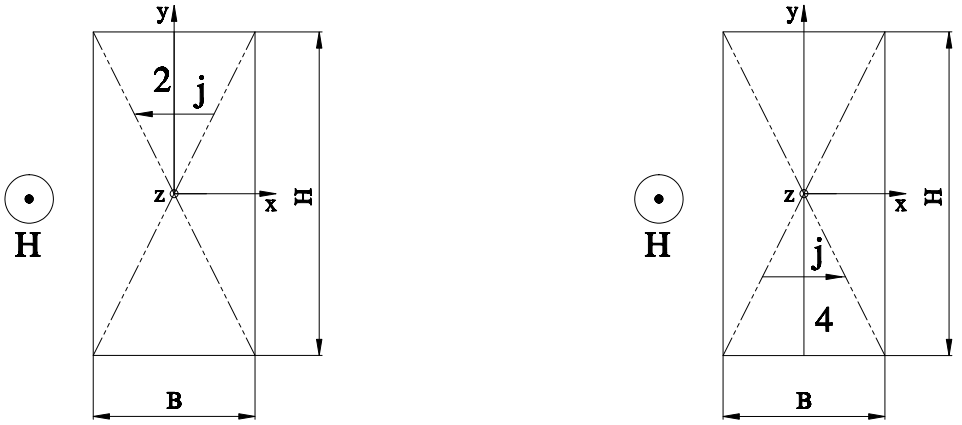

Figure 4.6.: A cuboid with its length L parallel to the magnetic field. In section II and IV flows the critical current density parallel to the width B of the cuboid.

$$\vec{m}_{II.IV} = 2\frac{1}{2}\int_{\frac{-L}{2}}^{\frac{L}{2}}\int_{0}^{\frac{B}{2}}\int_{\frac{H}{B}x}^{\frac{H}{2}} \begin{pmatrix} x \\ y \\ z \end{pmatrix} \times \begin{pmatrix} -j \\ 0 \\ 0 \end{pmatrix} \mathrm{d}z\mathrm{d}y\mathrm{d}x =$$

$$= jL\,\vec{e}_z \int_{0}^{\frac{B}{2}}\int_{\frac{H}{B}x}^{\frac{H}{2}} y\;\mathrm{d}y\mathrm{d}x = jL\,\vec{e}_z \int_{0}^{\frac{B}{2}} \frac{H^2}{8} - \frac{H^2}{2B^2}x^2\;\mathrm{d}x = jL\left[\frac{H^2}{8} - \frac{H^2}{6B^2}x^3\right]_0^{\frac{B}{2}} \vec{e}_z =$$

$$= jL\left[\frac{H^2B}{16} - \frac{H^2B^3}{6B^28}\right]\vec{e}_z = \frac{jLH^2B}{24}\,\vec{e}_z$$

The full magnetization of a finite cuboid is the sum of all four sections.

$$\vec{m} = \vec{m}_1 + \vec{m}_2 + \vec{m}_3 + \vec{m}_4 \tag{4.8}$$

$$\vec{m} = \frac{jL}{12}\left(B^2H + H^2B\right)\vec{e}_z \tag{4.9}$$

Infinitly long bar with its longest side perpendicular to the magnetic field

In the case where the cuboid has one side which is much longer than the other two sides and where this side is perpendicular to the magnetic field, as seen in Fig. 4.7, the same formula (2.4), like for the infinitly long cylinder perpendicular to the magnetic field is used.

$$\mathrm{d}\vec{m} = \mathrm{d}\vec{I}F = 2Lxj\mathrm{d}x\mathrm{d}y\,\vec{e}_y \tag{4.10}$$

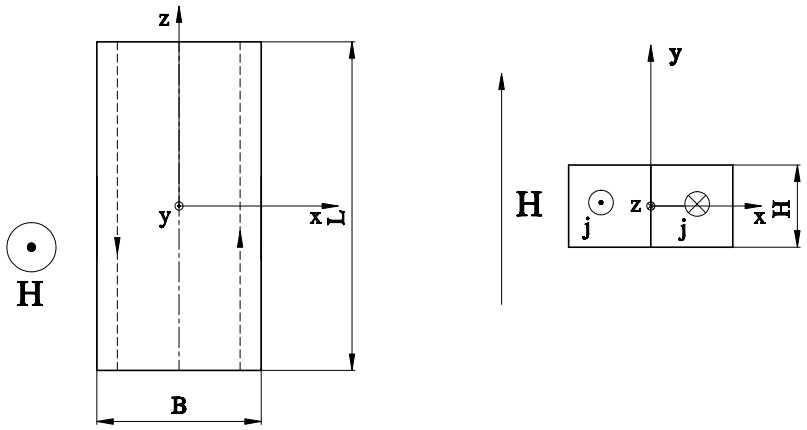

Figure 4.7.: An infinitly long bar, with its longest side L perpendicular to the magnetic field. The current density flows parallel to L. Since the bar is infinitly long, it can be assumed that the current flows through the surface perpendicular to L.

In this case the side L is much longer than the others and located parallel to the z-axis. I denotes the current and F is the area between the $yz-$plane and the current.

$$\vec{m} = 2jL\,\vec{e}_y \int_0^{\frac{B}{2}} \int_0^{H} x \,\mathrm{d}y\mathrm{d}x = 2jLH \left[\frac{x^2}{2}\right]_0^{\frac{B}{2}} \vec{e}_y$$

Therefore the magnetic moment calculates to

$$\vec{m} = \frac{1}{4} jLB^2H\,\vec{e}_y \tag{4.11}$$

4.1.3. Hollow cylinder

Hollow cylinder with its main axis parallel to the field

This geometry is finite and has a closed integration curve, as seen in Fig. 4.8. It is similar to the cylinder parallel to the magnetic field.

$$\vec{m} = \frac{1}{2} \int_V \vec{r} \times \vec{j}\,\mathrm{d}V \tag{4.12}$$

$$\vec{m} = \frac{1}{2} \int_0^L \int_0^{2\pi} \int_r^R \begin{pmatrix} \xi \cdot \cos(\varphi) \\ \xi \cdot \sin(\varphi) \\ z \end{pmatrix} \times \begin{pmatrix} -j \cdot \sin(\varphi) \\ j \cdot \cos(\varphi) \\ 0 \end{pmatrix} \cdot \xi \cdot \mathrm{d}\xi\mathrm{d}\varphi\mathrm{d}z =$$

$$= \frac{jL}{2}\,\vec{e}_z \int_r^R \int_0^{2\pi} \xi^2 \left[\cos(\varphi)^2 + \sin(\varphi)^2\right] \mathrm{d}\varphi\mathrm{d}\xi = jL\pi\vec{e}_z \int_r^R \xi^2 \mathrm{d}\xi$$

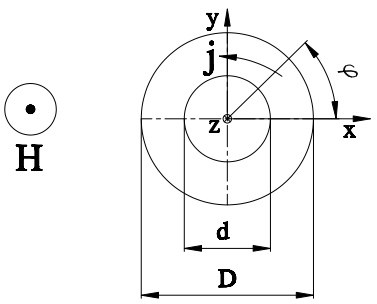

Figure 4.8.: A hollow cylinder with its main axis parallel to the magnetic field. The current flows in the $xy-$plane in direction of φ.

$$\vec{m} = \frac{1}{3} jL\pi(R^3 - r^3)\ \vec{e}_z \tag{4.13}$$

Long hollow cylinder with its main axis perpendicular to the field

Since it is assumed that the length L is much longer than the outer diameter $2R$ of the hollow cylinder, as seen in Fig. 4.9, formula (2.4) is used. In this case a more general formula is needed since the enclosed area by the current F is a function of the radius.

$$\mathrm{d}\vec{m} = F(\xi)\mathrm{d}\vec{I}(\xi) \tag{4.14}$$

$$\mathrm{d}\vec{I} = j\xi \mathrm{d}\varphi \mathrm{d}\xi\ \vec{e}_y \tag{4.15}$$

$$F = 2 \int_{z=0}^{L} \int_{s=0}^{\xi\cos(\varphi)} \mathrm{d}s\mathrm{d}z \tag{4.16}$$

The enclosed area and the current are both functions of ξ. Put together the magnetic moment calculates as follows

$$\vec{m} = 2j\ \vec{e}_y \int_{\xi=r}^{R} \int_{\varphi=\frac{-\pi}{2}}^{\frac{\pi}{2}} \int_{z=0}^{L} \int_{s=0}^{\xi\cos(\varphi)} \mathrm{d}s\mathrm{d}z\ \xi\ \mathrm{d}\varphi\mathrm{d}\xi =$$

$$= 2jL\ \vec{e}_y \int_{\xi=r}^{R} \int_{\varphi=\frac{-\pi}{2}}^{\frac{\pi}{2}} \xi^2 \cos(\varphi)\mathrm{d}\varphi\mathrm{d}\xi = 4jL\ \vec{e}_y \int_{\xi=r}^{R} \xi^2 \mathrm{d}\xi = \frac{4}{3} jL(R^3 - r^3)\ \vec{e}_y$$

$$\vec{m} = \frac{4}{3} jL(R^3 - r^3)\ \vec{e}_y \tag{4.17}$$

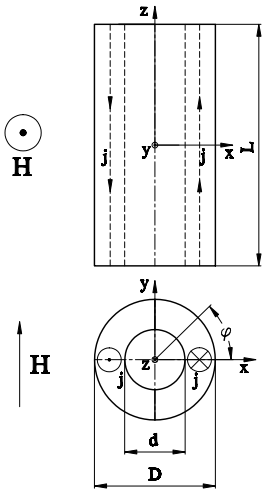

Figure 4.9.: A hollow cylinder with its main axis perpendicular to the magnetic field. The current flows in the $xz-$plane parallel to the length L.

This result is in perfect analogy to the infinite cylinder perpendicular to the magnetic field.

4.1.4. Elliptical cylinder

Elliptical cylinder with its main axis parallel to the field

In order to calculate the magnetic moment for elliptic geometries, elliptical coordinates are chosen. The geometry of the elliptical cylinder can be seen in Fig. 4.10. The calculation of the magnetic moment is analogue to the calculation of a cylinder with its main axis parallel to the magnetic field.

$$\begin{aligned}
\vec{m} &= \frac{1}{2}\int_0^L\int_0^{2\pi}\int_0^1 \begin{pmatrix} rb\cos(\varphi) \\ ra\sin(\varphi) \\ z \end{pmatrix} \times \begin{pmatrix} -j\sin(\varphi) \\ j\cos(\varphi) \\ 0 \end{pmatrix} abr \; \mathrm{d}r\mathrm{d}\varphi\mathrm{d}z = \\
&= \frac{jLab}{2}\,\vec{e}_z \int_0^{2\pi}\int_0^1 \cos(\varphi)^2 r^2 b + \sin(\varphi)^2 r^2 a \; \mathrm{d}r\mathrm{d}\varphi = \\
&= \frac{jLab}{6}\,\vec{e}_z \int_0^{2\pi} \cos(\varphi)^2 b + \sin(\varphi)^2 a \; \mathrm{d}\varphi = \frac{jLab}{6}\left[\frac{b\varphi}{2} + \frac{a\varphi}{2}\right]_0^{2\pi}\vec{e}_z
\end{aligned}$$

$$\vec{m} = \frac{j\pi Lab}{6}(a+b)\;\vec{e}_z \tag{4.18}$$

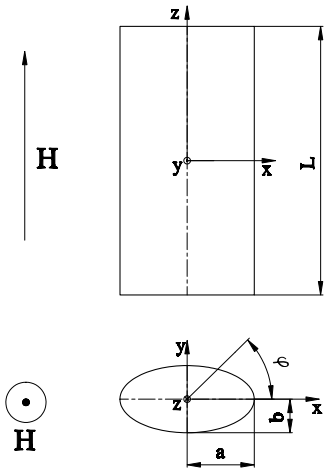

Figure 4.10.: An elliptical cylinder with its main axis parallel to the magnetic field. The current flows in the $xy-$plane in direction of φ.

If $a = b$ the result for the magnetic moment of a cylinder with its main axis parallel to the magnetic field, is obtained.

Infinite Elliptical cylinder with its main axis perpendicular to the field

Assume an elliptical cylinder with its length L much greater than its main axis, $2a$, as seen in Fig .4.11. The length L is perpendicular to the magnetic field, so formula (2.4) can be used

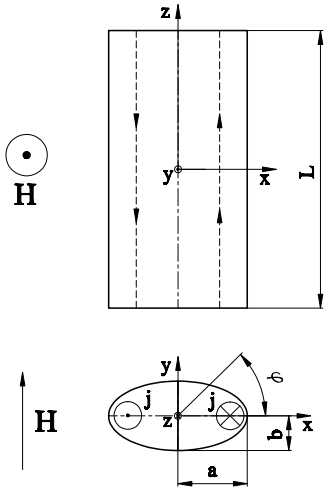

Figure 4.11.: A hollow cylinder with its main axis perpendicular to the magnetic field. The current flows in the $xz-$plane. Since L is much longer than $2a$, it can be assumed that the current only flows parallel to L.

$$\mathrm{d}\vec{m} = \mathrm{d}IF = 2jLx\mathrm{d}x\mathrm{d}y\ \vec{e}_y$$

$$\vec{m} = 2jL\ \vec{e}_y \int_{-a}^{a} \int_{0}^{a\sqrt{1-\frac{y^2}{b^2}}} x\ \mathrm{d}x\mathrm{d}y = jL\ \vec{e}_y \int_{-a}^{a} a^2 \left(1 - \frac{y^2}{b^2}\right)\ \mathrm{d}y =$$

$$= jLa^2 \left[y - \frac{y^3}{3b^2}\right]_{-a}^{a} \vec{e}_y = jLa^2 \left[2b - \frac{2b^3}{3b^2}\right] \vec{e}_y$$

$$\vec{m} = \frac{4}{3} jLa^2 b\ \vec{e}_y \tag{4.19}$$

This result is analog to the magnetic moment of a long cylinder with its main axis perpendicular to the magnetic field. If $a = b$ the results are equal.

4.1.5. Hollow elliptical cylinder with its main axis parallel to the field

This calculation is analog to the calculation of the magnetic moment of a hollow cylinder with its main axis parallel to the field. The geometry of the hollow elliptical cylinder can be seen in Fig. 4.12. The total magnetic moment is equal to the magnetic moment of a cylinder with radius R minus the magnetic moment of a cylinder with radius r, in the case of the hollow cylinder. Analog, the magnetic moment can be calculated using the formula for a elliptical cylinder with its main axis parallel to the magnetic field (2.5)

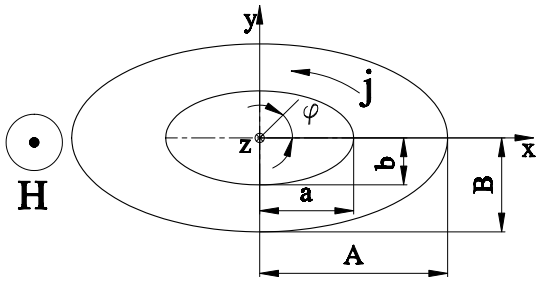

Figure 4.12.: A hollow elliptical cylinder with its main axis parallel to the magnetic field. The current flows in the $xy-$plane in direction of φ.

$$\vec{m} = \vec{m}_a - \vec{m}_i = \frac{j\pi LAB}{6}(A + B)\ \vec{e}_z - \frac{j\pi Lab}{6}(a + b)\ \vec{e}_z \tag{4.20}$$

$$\vec{m} = \frac{jL\pi}{6}\left[AB(A + B) - ab(a + b)\right] \vec{e}_z \tag{4.21}$$

4.1.6. Infinite hollow elliptical cylinder with its main axis perpendicular to the field

A good example to use the parallel axis theorem, of section 2.2.2, is the case of a hollow elliptical cylinder with its main axis perpendicular to the field. This geometry

can be seen in Fig. 4.13. First the centroid of the right half of the hollow elliptical cylinder is calculated

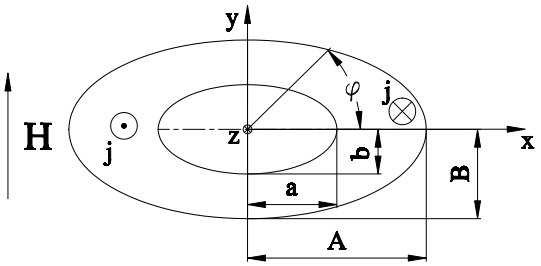

Figure 4.13.: Hollow elliptical cylinder with its main axis perpendicular to the magnetic field.

$$s_x = \frac{2}{A_E} \int_{\frac{-\pi}{2}}^{\frac{\pi}{2}} \int_{r(\varphi)}^{R(\varphi)} \xi^2 \cos(\varphi)\, \mathrm{d}\xi \mathrm{d}\varphi =$$

$$= \frac{2}{(AB-ab)\pi} \int_{\frac{-\pi}{2}}^{\frac{\pi}{2}} \frac{\left[R^3(\varphi) - r^3(\varphi)\right] \cos(\varphi)}{3}\, \mathrm{d}\varphi$$

In order to calculate s_x, the function $r(\varphi)$ of an ellipse needs to be deducted. The starting point is the elliptical equation

$$\frac{x^2}{a^2} + \frac{y^2}{b^2} = 1 \tag{4.22}$$

Next, polar coordinates are introduced: $x = r\cos(\varphi)$ and $y = r\cos(\varphi)$.

$$\Rightarrow \frac{r^2\cos(\varphi)^2}{a^2} + \frac{r^2\sin(\varphi)^2}{b^2} = 1$$
$$r^2\left[b^2\cos(\varphi)^2 + a^2\sin(\varphi)^2\right] = a^2b^2$$

This leads to

$$r(\varphi) = \frac{ab}{\sqrt{b^2\cos(\varphi)^2 + a^2\sin(\varphi)^2}} \tag{4.23}$$

$R(\varphi)$ is calculated analog. These relations are inserted into the calculation of s_x

$$s_x = \frac{2}{(AB-ab)\pi} \int_{\frac{-\pi}{2}}^{\frac{\pi}{2}} \frac{A^3B^3\cos(\varphi)}{3\left[B^2\cos(\varphi)^2 + A^2\sin(\varphi)^2\right]^{\frac{3}{2}}} - \frac{a^3b^3\cos(\varphi)}{3\left[b^2\cos(\varphi)^2 + a^2\sin(\varphi)^2\right]^{\frac{3}{2}}}\, \mathrm{d}\varphi =$$

$$= \frac{2}{(AB-ab)\pi} \int_{\frac{-\pi}{2}}^{\frac{\pi}{2}} \frac{A^3B^3\cos(\varphi)}{3\left[B^2 + (A^2-B^2)\sin(\varphi)^2\right]^{\frac{3}{2}}} - \frac{a^3b^3\cos(\varphi)}{3\left[b^2 + (a^2-b^2)\sin(\varphi)^2\right]^{\frac{3}{2}}}\, \mathrm{d}\varphi$$

The functions $\sin(x)$ and $\cos(x)$ are substituted with hypergeometric functions.

$$\sqrt{A^2 - B^2}\sin(\varphi) = B\sinh(u) \qquad \Rightarrow \quad \mathrm{d}\varphi = \frac{B\cosh(u)}{\sqrt{A^2 - B^2}\cos(\varphi)}\,\mathrm{d}u \tag{4.24}$$

$$\sqrt{a^2 - b^2}\sin(\varphi) = b\sinh(v) \qquad \Rightarrow \quad \mathrm{d}\varphi = \frac{b\cosh(v)}{\sqrt{a^2 - b^2}\cos(\varphi)}\,\mathrm{d}v \tag{4.25}$$

$$\begin{aligned}
s_x &= \frac{2}{(AB-ab)\pi}\int_{u_1}^{u_2}\frac{A^3B^3\cos(\varphi)B\cosh(u)}{3B^3\sqrt{A^2-B^2}\cos(\varphi)\cosh(u)^3}\,\mathrm{d}u - \\
&- \frac{2}{(AB-ab)\pi}\int_{v_1}^{v_2}\frac{a^3b^3\cos(\varphi)b\cosh(v)}{3b^3\sqrt{a^2-b^2}\cos(\varphi)\cosh(v)^3}\,\mathrm{d}v = \\
&= \frac{2}{3\pi(AB-ab)}\left[\int_{u_1}^{u_2}\frac{A^3B}{\sqrt{A^2-B^2}\cosh(u)^2}\,\mathrm{d}u - \int_{v_1}^{v_2}\frac{a^3b}{\sqrt{a^2-b^2}\cosh(v)^2}\,\mathrm{d}v\right] = \\
&= \frac{2}{3\pi(AB-ab)}\left[\frac{A^3B\tanh(u)}{\sqrt{A^2-B^2}} - \frac{a^3b\tanh(v)}{\sqrt{a^2-b^2}}\right]_{u_1.v_1}^{u_2.v_2}
\end{aligned}$$

The expressions to reverse the substitution are

$$u = \operatorname{arcsinh}\left(\frac{\sqrt{A^2-B^2}}{B}\sin(\varphi)\right) \tag{4.26}$$

$$v = \operatorname{arcsinh}\left(\frac{\sqrt{a^2-b^2}}{b}\sin(\varphi)\right) \tag{4.27}$$

Furthermore following relation is used

$$\tanh(\operatorname{arcsinh}(x)) = \frac{x}{\sqrt{1+x^2}} \tag{4.28}$$

After all above steps are made, s_x becomes

$$\begin{aligned}
s_x &= \frac{2}{3\pi(AB-ab)}\left[\frac{A^3B\frac{\sqrt{A^2-B^2}}{B}\sin(\varphi)}{\sqrt{A^2-B^2}\sqrt{1+\left(\frac{\sqrt{A^2-B^2}}{B}\sin(\varphi)\right)^2}}\right]_{\frac{-\pi}{2}}^{\frac{\pi}{2}} - \\
&- \frac{2}{3\pi(AB-ab)}\left[\frac{a^3b\frac{\sqrt{a^2-b^2}}{b}\sin(\varphi)}{\sqrt{a^2-b^2}\sqrt{1+\left(\frac{\sqrt{a^2-b^2}}{b}\sin(\varphi)\right)^2}}\right]_{\frac{-\pi}{2}}^{\frac{\pi}{2}} = \\
&= \frac{4}{3\pi(AB-ab)}\left[\frac{A^3}{\sqrt{1+\frac{A^2}{B^2}-1}} - \frac{a^3}{\sqrt{1+\frac{a^2}{b^2}-1}}\right] = \frac{4}{3\pi(AB-ab)}\left[A^2B - a^2b\right]
\end{aligned}$$

After having obtained the centroid in $x-$direction, it can be inserted into the main formula of section 2.2.2

$$\vec{m} = 2js_xV = j\frac{4}{3\pi(AB-ab)}\left[A^2B - a^2b\right] L(AB-ab)\pi\ \vec{e}_y \tag{4.29}$$

$$\vec{m} = \frac{4jL}{3}\left[A^2B - a^2b\right]\vec{e}_y \tag{4.30}$$

The solution is perfectly analog to the solution of the hollow cylinder perpendicular to the magnetic field.

4.2. Numerical calculations

In this section the results of the numerical calculations of the demagnetizing factors of a cylinder with its main axis parallel and perpendicular to the magnetic field and of an infinily long bar with its longest side perpendicular to the magnetic field are presented.

4.2.1. Cylinder

The results given were evaluated with MATHEMATICA since the FORTRAN program did not give results with satisfying accuracy, although the implementation was similar. A possible reason is that the LU decomposition routine or the pre written functions are not accurate enough. Since the results obtained with MATHEMATICA were accurate enough, this was not investigated further.

For a cylinder with its main axis parallel to the magnetic field, the characteristic number of segments in which the cylinder is cut is $p_{min} = N_s + N_l$. N_s is the number of segments in radial direction and N_l is the number of segments in direction of the length, which was explained in section 3.1. For a cylinder with its main axis perpendicular to the applied field, p_{min} is defined as $p_{min} = N_s + N_l - 1$. p_{min} should be as big as possible in order to achieve most accurate results. However the best number for practical purposes for $N_s + N_l$ was determined to be 16. For different values of the radius, a, to half length, b, ratios, γ ($\gamma = \frac{a}{b}$), N_s and N_l change their value. In general the longer the cylinder is, the bigger N_s has to be and the smaller N_l has to be [2, 3]. For some ratios of γ the best values of N_s and N_l are given in Tab. 4.1. The results of the demagnetizing factor if the applied field is parallel to the

Table 4.1.: The values for N_s and N_l give the number of segments in radial direction and in direction of the length respectively. For best accuracy these numbers change with the radius to half length ratio $\gamma = \frac{a}{b}$

.

	Cylinder parallel		**Cylinder perpendicular**	
γ	N_s	N_l	N_s	N_l
$\frac{1}{4}$	2	14	3	13
$\frac{1}{2}$	5	11	6	10
1	8	8	10	6
2	11	5	13	3
4	14	2	14	2

main axis (N_{mp}) and perpendicular to the main axis (N_{ms}) are presented in Tab.

4.2. The magnetic susceptibility for N_{mp} and N_{ms} is $\chi = -1$. The values for $\gamma = 0$ and $\gamma = \infty$ could not be calculated since the program returned no results. If these values are inserted into the program, there occurs a division by zero which either blows up the values or just returns with an error. The rest of the $\frac{\alpha_{tt}}{V\epsilon_0}$ and $\frac{\mu_0\beta_{tt}}{V}$ values are in good agreement to the values already calculated by Taylor [21, 22].

Table 4.2.: In this table are the demagnetizing factors of a cylinder with its main axis parallel (N_{mp}) and perpendicular (N_{ms}) to the field for different radius to half length ratios $\gamma = \frac{a}{b}$ listed. The factors are evaluated for $\chi = -1$. If the calculated values are compared to those calculated by Taylor [21, 22], they fit perfectly.

	Cylinder parallel			**Cylinder perpendicular**		
γ	$\frac{\alpha_{tt}}{V\epsilon_0}$	$\frac{\alpha_{tt}}{V\epsilon_0}$ [21]	$N_{mp}(-1)$	$\frac{\mu_0\beta_{tt}}{V}$	$\frac{\mu_0\beta_{tt}}{V}$ [22]	$N_{ms}(-1)$
0	–	2.0000	0.0000	–	−2.0000	0.6186
$\frac{1}{4}$	2.3151	2.3151	0.1361	−1.8506	−1.8506	0.4596
$\frac{3}{8}$	2.4653	–	0.1887	−1.7892	–	0.4411
$\frac{3}{7}$	2.5283	–	0.2090	−1.7650	–	0.4334
$\frac{1}{2}$	2.6115	2.6115	0.2342	−1.7351	−1.7351	0.4237
$\frac{6}{11}$	2.6639	–	0.2492	−1.7174	–	0.4177
$\frac{3}{5}$	2.7264	–	0.2664	−1.6973	–	0.4108
$\frac{3}{4}$	2.8956	–	0.3093	−1.6481	–	0.3932
$\frac{6}{7}$	3.0143	–	0.3365	−1.6165	–	0.3814
1	3.1707	3.1707	0.3692	−1.5795	−1.5795	0.3669
2	4.2173	4.2173	0.5258	−1.4140	−1.4140	0.2928
4	6.1814	6.1814	0.6764	−1.2716	−1.2716	0.2136
∞	–	∞	1.0000	–	−1.0000	0.0000

4.2.2. Infinite slab perpendicular to the field

The demagnetizing factors N_{ms} for an infinite long bar with its longest side perpendicular to the applied field were calculated. The bar has a rectangular cross section. a is half of the width in $x-$direction and b is half of the height in $y-$direction. The magnetic field is applied in $x-$direction. The program for this problem was written in FORTRAN. The implementation in MATHEMATICA is not advisable, since the calculation time and RAM needed for satisfying accuracy are much greater than for FORTRAN.

The output of the calculations can be seen in Tab. 4.3. The demagnetizing factors were calculated for $\chi = -1$. The first column is the width to height ratio $\frac{a}{b}$ of the bar. The second column contains the demagnetizing values numerically calculated in this thesis, compared to the values found in literature [23] at column three. The fourth column gives the relative error between these two. The relative error to the values of N_{ms} given in literature is below 1% for $a/b > 5$ and below 1‰ for $a/b \leq 5$. For this calculation the accuracy is sufficient enough. The reason for the discrepancy between the calculations is that in the above mentioned literature the surface was not divided into equally long cells. They used such an optimization, that a larger number of cells were located near the edge than in the middle. Regarding the calculations, the number of cells $n_x + n_y$ were between 8000 and 14000. In the original calculation by Chen et al. [24] only around 400 cells were needed. For further optimization of this program this has to be taken into account.

Table 4.3.: The demagnetizing values N_{ms} calculated (column 2) of an infinitly long bar with its longest side perpendicular to the magnetic field can be found for some ratios of $\frac{a}{b}$ (column 1) in this table. The values were calculated for $\chi = -1$ and compared to the values found in literature (column 3). In column 4 is the relative error, between the calculated value and the value found in literature, given [23].

a/b	$N_{ms}(-1)$	$N_{ms}(-1)$ [23]	rel. error
0.001	0.998 031	0.998 734	0.07%
0.002	0.996 860	0.997 478	0.06%
0.005	0.993 241	0.993 770	0.05%
0.01	0.987 275	0.987 752	0.05%
0.02	0.975 784	0.976 223	0.04%
0.05	0.944 297	0.944 731	0.05%
0.1	0.899 221	0.899 593	0.04%
0.2	0.826 669	0.826 972	0.04%
0.5	0.681 512	0.681 741	0.03%
1	0.542 767	0.543 053	0.05%
2	0.399 479	0.399 702	0.06%
5	0.237 051	0.237 276	0.09%
10	0.148 367	0.148 557	0.13%
20	0.088 442	0.088 647	0.23%
50	0.042 424	0.042 546	0.29%
100	0.023 692	0.023 778	0.36%
200	0.013 030	0.013 089	0.45%
500	0.005 802	0.005 848	0.79%
1000	0.003 120	0.003 150	0.95%

4.3. Magnetic flux measurements

In order to examine the influence of demagnetizing effects on the magnetization and the critical current density the magnetic moment of different samples were measured using magnetic flux measurements. In Tab. 4.4 the geometries of all measured samples are listed. The first test series had big discontinuities in the magnetic moment

Table 4.4.: Table of all geometries and dimensions of the first test series. The length l is the dimension parallel to the main axis of the geometry. All dimensions are in mm.

Cuboid l**x**b**x**h		**Cyl.** l**xØ**		**H. Cyl.** l**xØ**$_a$**xØ**$_i$	
par.	perp.	par.	perp.	par.	perp.
3x3x3	–	3x3	3x3	2.5x3x2	2.5x3x2
3.85x3x3	3.85x3x3	4x3	4x3	4x3x2	4x3x2
4.6x3x3	4.6x3x3	5x3	5x3	4.9x3x2	4.9x3x2
6x3x3	6x3x3	6x3	6x3	6x3x2	6x3x2
7x3x3	–	7x3	7x3	7x3x2	7x3x2
8x3x3	–	8x3	–	8x3x2	–

Table 4.5.: Table of all geometries and dimensions of the second test series. This test series was made to get rid of the big flux jumps which occurred in the magnetic moment hysteresis curves of the first test series. Also for the second test series is the length l the dimension parallel to the main axis of the geometries. All dimensions are in mm.

Cuboid l**x**b**x**h		**Cyl.** l**xØ**	
par.	perp.	par.	perp.
3x3.3x3.3	–	3x3	3x3
3.5x3.3x3.3	3.5x3.3x3.3	3.5x3	3.5x3
4x3.3x3.3	4x3.3x3.3	4x3	4x3
5x3.3x3.3	5x3.3x3.3	5x3	5x3
5.5x3.3x3.3	5.5x3.3x3.3	5.5x3	5.5x3
6x3.3x3.3	6x3.3x3.3	6x3	6x3

hysteresis curves. These discontinuities are assumed to be due to large flux jumps, since they appeared randomly during measurements.

A second test series was made in order to try to avoid these discontinuities. The samples were degased, at 1000°C and at a pressure of 10^{-5} bar, for 48 hours. This second series consisted only of cylinders and cuboids which were measured parallel and perpendicular to the field. The full set of all geometries measured in the second test series can be found in Tab. 4.5. The main length l is parallel to the main axis for all geometries. The width b and the height h for the cuboid and the diameter Ø for the cylinder are given in Tab. 4.4 and Tab. 4.5. Additionally, for the hollow cylinder in Tab. 4.4, the outer ($Ø_a$) and the inner ($Ø_i$) diameter is given.

In figure Fig. 4.14 a typical hysteresis (blue) is shown. As it can be seen, the flux jumps are too high to obtain any useful data for the width of the hysteresis necessary to calculate the critical current density. A curve was approximated to smoothen the graph and get rid of the flux jumps. Polynomials of order four to seven were used for the smoothed curves. Now formula (2.21) could be applied to Fig. 4.14 for the mag-

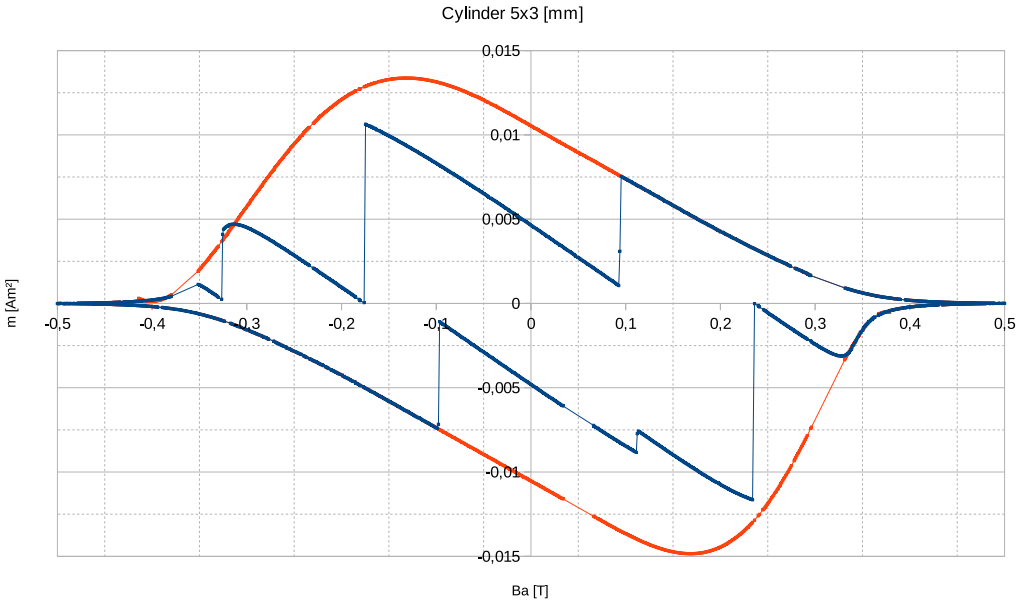

Figure 4.14.: A cylinder of the first test series with its main axis parallel to the magnetic field. The blue curve was measured, but since the flux jumps were too big a curve was approximated to smoothen the graph (orange line). The first digit of the label indicates the length of the dimension parallel to the main axis.

netic moment no longer to be a function of the applied field, but to be a function of

the internal field. The corresponding graph is shown in Fig. 4.15. The reason why the

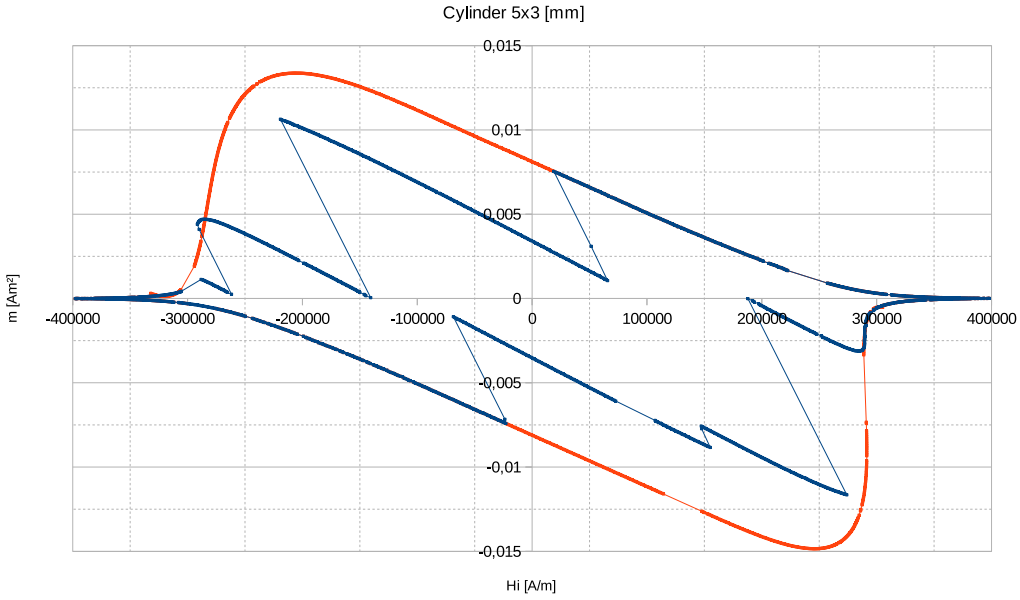

Figure 4.15.: The magnetization curve of a cylinder parallel to the magnetic field as function of the internal field. If demagnetizing effects are taken into account the magnetic moment is no longer a function of the applied field H_a, but a function of the internal field H_i. The first digit of the label indicates the length of the dimension parallel to the main axis.

hysteresis curve in Fig. 4.15 looks so different compared to Fig. 4.14 is the influence of the magnetization on the field H. The magnetization values which were at the applied field H_a shifted, due to formula (2.21), to another value of the internal field H_i. The difference of the magnetic moment ($\Delta m = m_{\text{up}} - m_{\text{down}}$), between upper and lower hysteresis curve, is big for a low absolute value of the applied field. Therefore, the correction of the applied field is big and the corresponding internal field is considerably different from the applied field. In contrary, magnetization values at a high absolute value of the applied field have a smaller influence on the correction of the applied field. The corresponding values of internal field, for those magnetization values, are almost equal to the values of the applied field.

Some of the hysteresis curves have a negative slope at high absolute values of the field which can be seen in appendix B. This physically impossible behavior occurs most likely because the smoothed curve is an approximation. Since the magnetic moment values at low absolute values of the internal field are more important in this thesis, the non physical behavior is not harmful. The second, degased, test series did not show these non physical behavior.

In case of the degased samples (2^{nd} test series), the opening of the hysteresis loops is more narrow, indicating a reduced superconducting volume. Only small reductions of flux jumps could be reached under the chosen degasing conditions. All measured magnetic moment hysteresis curves can be found in appendix B.

4.3.1. Magnetic susceptibility

The demagnetization factors in section 4.2 are all calculated for a susceptibility of $\chi = -1$. It is important to know if the tested samples have susceptibilities close to this value. The slopes of the virgin magnetic curves have been evaluated in order to calculate the measured susceptibilities. In Fig. 4.16 a typical virgin magnetic moment curve (blue) and the ideal slope (black) are illustrated. Tab. 4.6 shows the

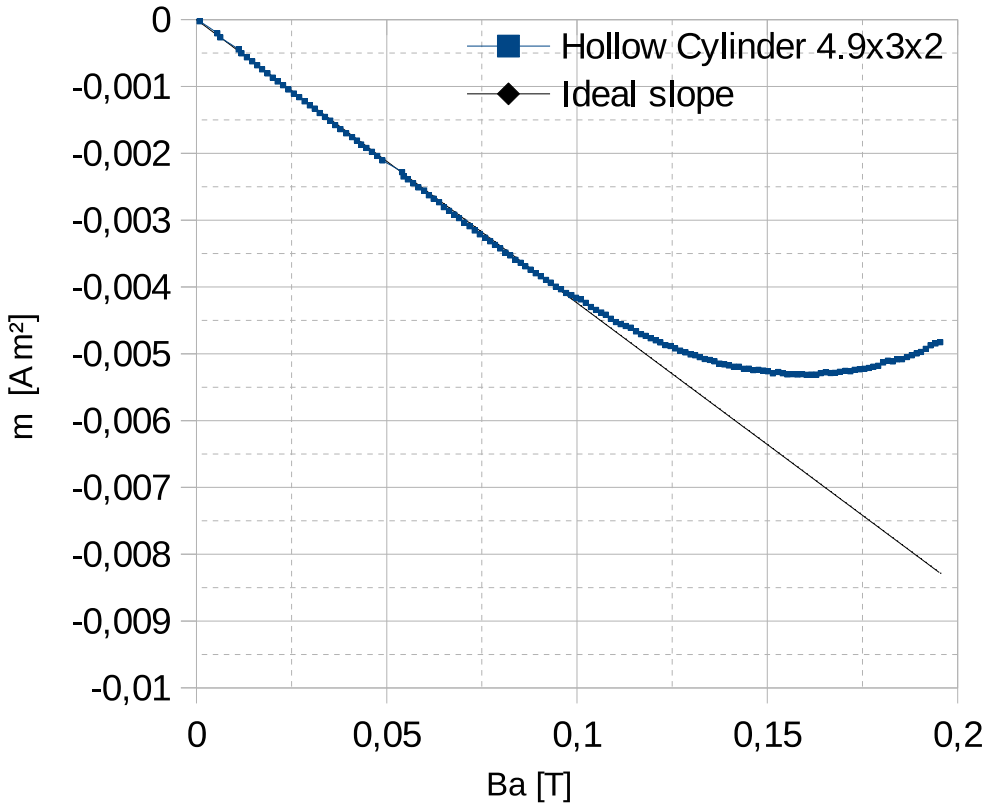

Figure 4.16.: The blue curve is the virgin magnetic curve of the magnetic moment of a hollow cylinder with its main axis perpendicular to the magnetic field. The black cure is the ideal slope of the virgin magnetic moment curve.

susceptibilities of all measured geometries. The susceptibilities are varying, as it can

Table 4.6.: Table of susceptibilities for all measured geometries, parallel and perpendicular to the magnetic field. The values are smaller than −1, which is due to demagnetizing effects.

length	**1st test series**						**2nd test series**			
[mm]	**Cuboid**		**Cylinder**		**Hollow Cyl.**		**Cuboid**		**Cylinder**	
	para.	perp.	para.	perp.	para.	perp.	para.	perp.	para.	perp.
2.50	–	–	–	–	-3.04	-2.19	–	–	–	–
3.00	-1.59	–	-1.62	-1.61	–	–	-1.31	–	-1.55	-1.36
3.50	–	–	–	–	–	–	-1.35	-1.39	-1.47	-1.62
3.85	-1.59	-1.84	–	–	–	–	–	–	–	–
4.00	–	–	-1.51	-1.79	-2.56	-2.60	-1.30	-1.49	-1.37	-1.64
4.60	-1.46	-1.80	–	–	–	–	–	–	–	–
4.90	–	–	–	–	-2.39	-2.77	–	–	–	–
5.00	–	–	-1.39	-1.77	–	–	-1.24	-1.55	-1.32	-1.75
5.50	–	–	–	–	–	–	-1.21	-1.60	-1.29	-1.68
6.00	-1.37	-1.91	-1.30	-1.79	-2.21	-2.85	-1.15	-1.56	-1.21	-1.74
7.00	-1.28	–	-1.24	-1.89	-2.14	-2.95	–	–	–	–
8.00	-1.17	–	-1.11	-1.85	-1.91	–	–	–	–	–

bee seen from this table and are all smaller than −1. This is not surprising, since the susceptibility is object to the demagnetizing factor as mentioned in subsection 2.3.5. For the numerical calculations a χ of −1 was assumed. For the cylinder and the cuboid are the values close enough to the assumed value. The magnetic susceptibility of the hollow cylinder is far from the ideal value. All virgin magnetic moment curves can be found in appendix C.

4.3.2. Magnetization

Values for the magnetization as a function of applied and internal field have been evaluated for cuboids and cylinders of various dimensions, for both test series. The goal was to see if deviations between the obtained magnetization curves are smaller if demagnetization factors are taken into account. As magnetization is an intrinsic property of the material and all samples are made of the same niobium rod, the obtained differences are due to not correctly considering the different geometries of the samples.

Magnetization of the first test series

The magnetization values as functions of the applied field for cylinders of the first test series with their main axes parallel and perpendicular to the magnetic field are shown in Figs. 4.17 and 4.18. Tab. 4.7 shows the magnetization values, at zero applied field, of the cuboids, cylinders and hollow cylinders with their main axes parallel and perpendicular to the magnetic field.

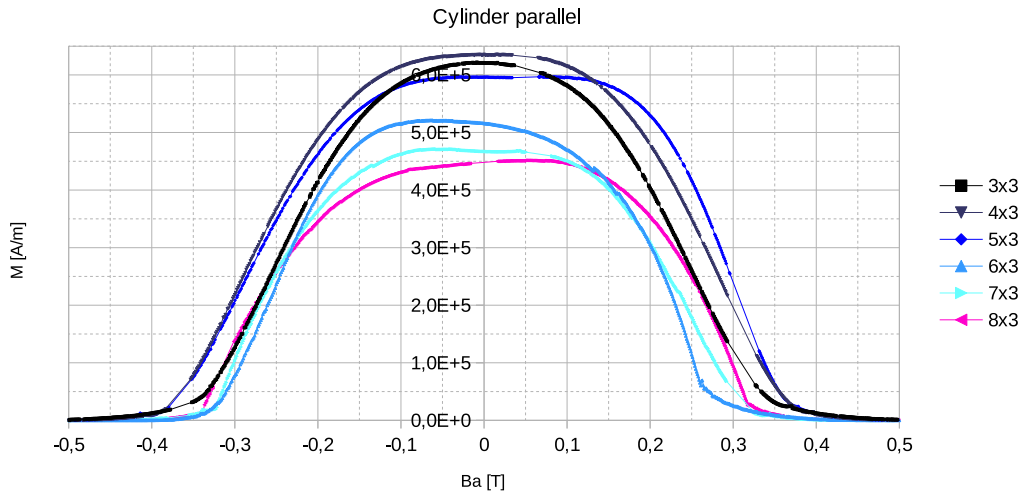

Figure 4.17.: Magnetization curves versus the applied field of the cylinders of the first test series with their main axes parallel to the magnetic field. The first digit of every label indicates the length of the dimension parallel to the main axis.

At zero field, differences between 7 and 16% are obtained for the magnetization of the samples. No systematic concerning length of cylinder nor field direction is found.

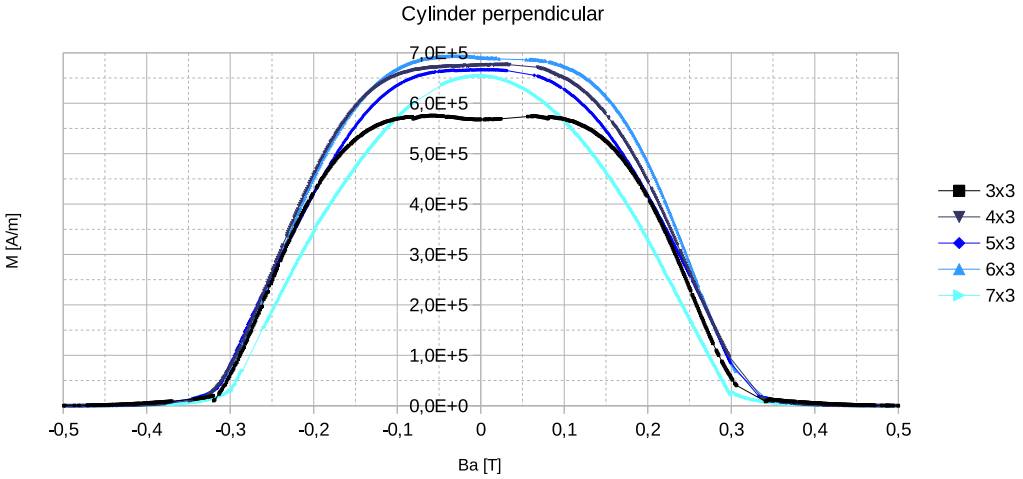

Figure 4.18.: Magnetization curves versus the applied field of the cylinders of the first test series with their main axes perpendicular to the magnetic field. The first digit of every label indicates the length of the dimension parallel to the main axis.

Table 4.7.: Magnetization values of the first test series at zero applied field for different values of the length, which also indicates the main axis. Magnetization values are divided by a factor of 10^5. The unit of the magnetization values is [A/m].

length	Cuboid		Cylinder		H. Cylinder	
[mm]	para.	perp.	para.	perp.	para.	perp.
2.50	–	–	–	–	9.484	6.285
3.00	4.580	4.580	6.210	5.678	–	–
3.85	5.824	6.191	–	–	–	–
4.00	-	–	6.356	6.755	9.501	7.365
4.60	5.447	6.194	–	–	–	–
4.90	-	–	–	–	9.123	8.045
5.00	-	–	5.962	6.663	–	–
6.00	5.447	6.748	5.156	6.761	9.061	8.876
7.00	5.116	–	4.672	6.543	8.548	9.294
8.00	4.908	–	4.495	–	7.831	–

Magnetization of the first test series after demagnetization effects are considered

The demagnetization effects could only be considered for the cylinders with their main axes parallel and perpendicular to the magnetic field. If Fig. 4.17 is compared with Fig. 4.19 and Fig. 4.18 is compared with Fig. 4.20, it can be seen that the appliance of the demagnetization factor causes the magnetization curves at zero field to lie closer to each other. Differences, at zero internal field, are now 9% instead of 15% for the field parallel to the cylinder axis and 3% instead of 7% for the field perpendicular to the cylinder axis. The values of the magnetization of the first test series with the magnetization factor applied can be found in Tab. 4.8.

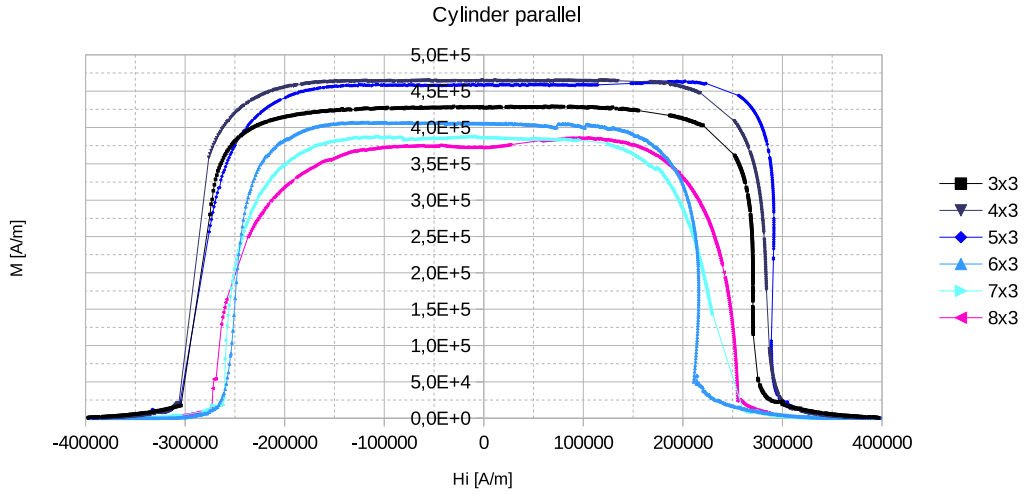

Figure 4.19.: Magnetization curves, after demagnetization effects are considered, versus the internal field of the cylinders of the first test series with their main axes parallel to the magnetic field. The first digit of every label indicates the length of the dimension parallel to the main axis.

The asymmetry of the magnetization curves with respect to the $M-$axis in Figs. 4.19 and 4.20 is due to the approximation of the magnetic hysteresis curves. The smoothed curves were applied to the upper and lower part of the hysteresis curve separately. As mentioned before, the non physical negative slopes of the magnetization curves at high absolute values of the internal fields are due to the approximation of the smoothed curves of the magnetic hysteresis curves.

The different values of the magnetization are averaged for every geometry, and the standard deviation of this average is calculated. These statistic values are gathered in Tab. 4.9. The average of the magnetization where the demagnetizing factor had been applied scattered much less than the average of the magnetization without the

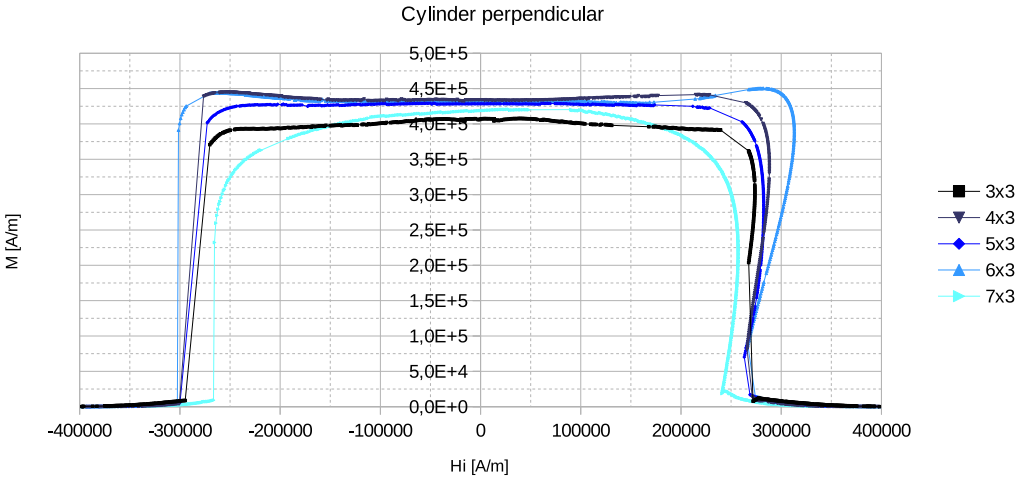

Figure 4.20.: Magnetization curves, after demagnetization effects are considered, versus the internal field of the cylinders of the first test series with their main axes perpendicular to the magnetic field. The first digit of every label indicates the length of the dimension parallel to the main axis.

corrections of demagnetizing effects. This is at least true for the cylinders with their main axes parallel and perpendicular to the magnetic field.

Table 4.8.: Magnetization values of the cylinders of the first test series with their main axis parallel and perpendicular to the field. The demagnetization factor has been applied. The magnetization values are divided by a factor of 10^5. The unit of the magnetization values is [A/m].

length [mm]	3.00	4.00	5.00	6.00	7.00	8.00
parallel	4.282	4.653	4.584	4.055	3.860	3.728
perpendicular	4.062	4.341	4.284	4.285	4.073	–

Table 4.9.: Comparison of the mean and the standard deviation of the magnetization of the first test series. Values are divided by a factor of 10^5. The unit for the magnetization values is [A/m].

1^{st} test series - magnetization				
	field not corrected		field corrected	
Cylinder	para.	perp.	para.	perp.
$\mu\ [A/m]$	5.48	6.48	4.19	4.21
$\sigma\ [A/m]$	0.81	0.46	0.38	0.13
Cuboid	para.	perp.	para.	perp.
$\mu\ [A/m]$	5.22	5.93	–	–
$\sigma\ [A/m]$	0.44	0.94	–	–
H. Cylinder	para.	perp.	para.	perp.
$\mu\ [A/m]$	8.92	5.93	–	–
$\sigma\ [A/m]$	0.64	0.12	–	–

Magnetization of the second test series

The samples of the second test series were degased in order to get rid of the flux jumps in the magnetic moment curves. The magnetization curves of the cylinders of the second test series with their main axes parallel and perpendicular to the magnetic field are shown in Fig. 4.21 and Fig. 4.22.

At zero field, differences between 5% and 11% are obtained for the magnetization of the samples. No systematic concerning length of cylinder nor field direction is found. Tab. 4.10 shows the magnetization values of the second test series. In that series only cuboids and cylinders with their main axes parallel and perpendicular to the magnetic field were measured.

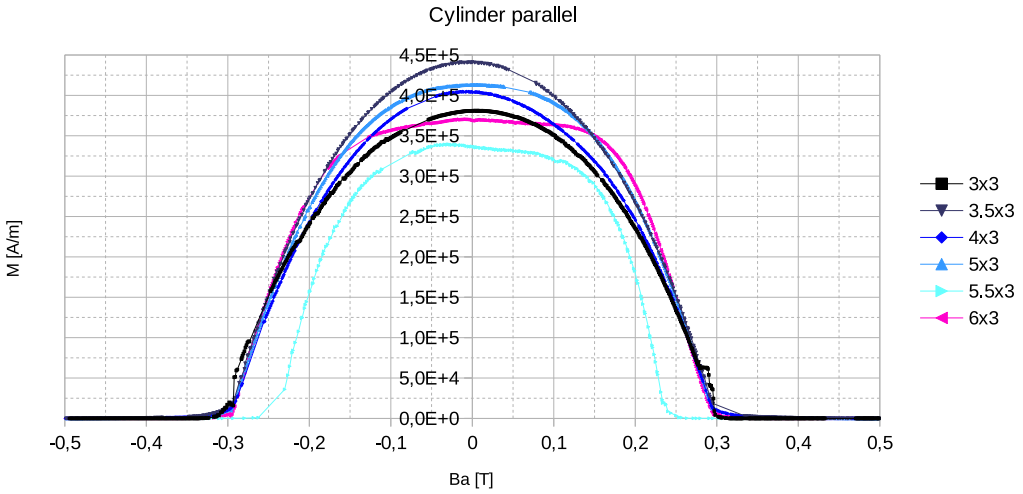

Figure 4.21.: Magnetization curves versus the applied field of the cylinders of the second test series with their main axes parallel to the magnetic field. The first digit of every label indicates the length of the dimension parallel to the main axis.

Magnetization of the second test series after demagnetization effects are considered

After the demagnetization factor is applied, the magnetization curves lie closer to each other. This can be seen if Fig. 4.21 is compared with Fig. 4.23 and Fig. 4.22 is compared with Fig. 4.24. The difference of magnetization curves is now 7% instead of 9% for the field parallel to the cylinder axis. The percentual difference of the magnetization curves at zero applied field of the cylinders perpendicular to the magnetic field did not change. It is 11%. All magnetization values of the second test series where the demagnetization factor has been applied can be found in Tab. 4.11.

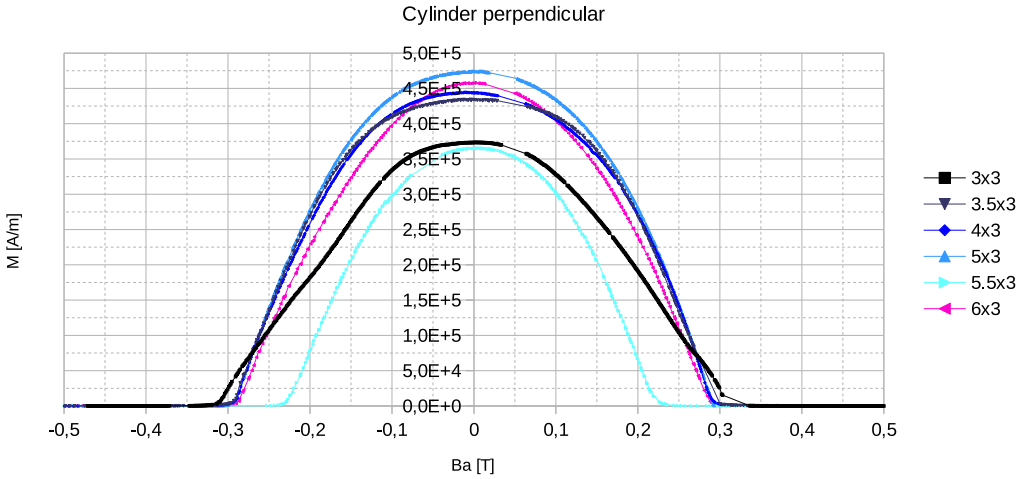

Figure 4.22.: Magnetization curves versus applied field of the cylinders of the second test series with their main axes perpendicular to the magnetic field. The first digit of every label indicates the length of the dimension parallel to the main axis.

Table 4.10.: Magnetization values of cylinders and cuboids of the second test series with their main axes parallel and perpendicular to the magnetic field, at zero applied field. The magnetization values are divided by a factor of 10^5. The unit of the magnetization values is [A/m].

length	Cuboid		Cylinder	
[mm]	para.	perp.	para.	perp.
3.00	3.707	3.707	3.808	3.730
3.50	4.037	3.909	4.404	4.342
4.00	3.834	4.150	4.046	4.437
5.00	3.861	4.400	4.128	4.738
5.50	3.593	4.254	3.368	3.646
6.00	3.592	4.252	3.701	4.569

The different values of the magnetization are averaged for every geometry, and the standard deviation from this average is calculated. These statistic values are gathered in Tab. 4.12. The average of the magnetization where the demagnetizing

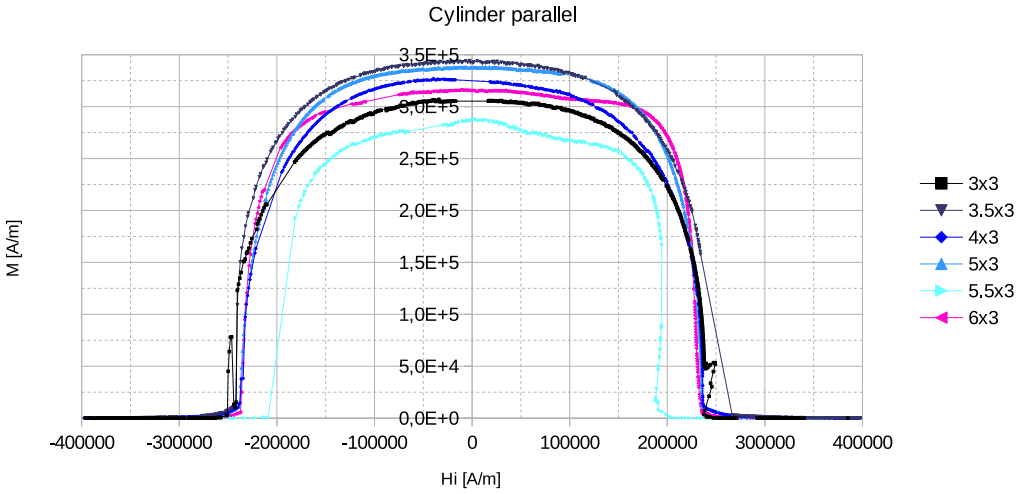

Figure 4.23.: Magnetization curves, after demagnetization effects are considered, versus the internal field of the cylinders of the second test series, with their main axes parallel to the magnetic field. The first digit of every label indicates the length of the dimension parallel to the main axis.

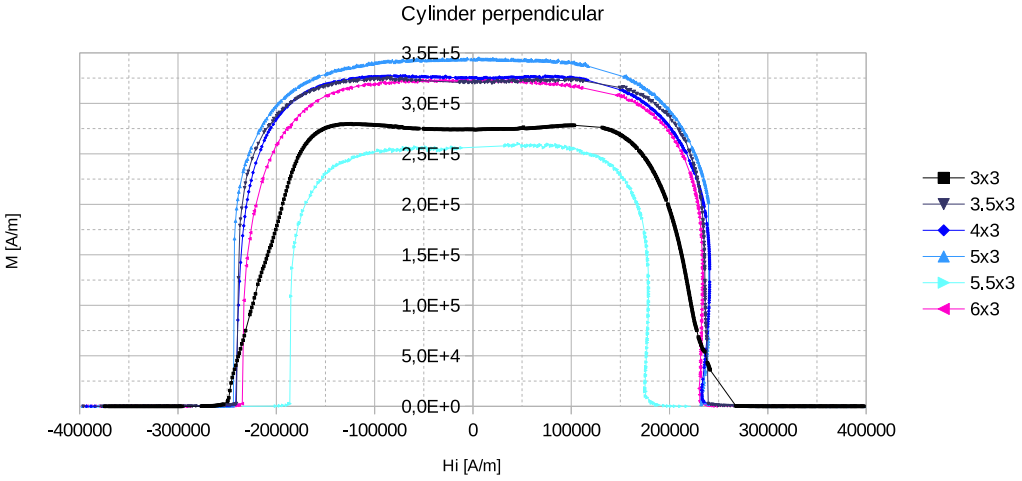

Figure 4.24.: Magnetization curves, after demagnetization effects are considered, versus the internal field of the cylinders of the second test series, with their main axes perpendicular to the magnetic field. The first digit of every label indicates the length of the dimension parallel to the main axis.

Table 4.11.: Magnetization values of the cylinders of the second test series with their main axes parallel and perpendicular to the field. The demagnetization factor has been applied. The magnetization values are divided by a factor of 10^5. The unit of the magnetization values is [A/m].

length [mm]	3.00	3.50	4.00	5.00	5.50	6.00
parallel	3.053	3.443	3.259	3.376	2.865	3.157
perpendicular	2.743	3.254	3.219	3.414	2.579	3.206

factor had been applied scattered less than the average of the magnetization without the corrections of demagnetizing effects. This is true for both the cylinder with its main axis parallel and perpendicular to the magnetic field. The negative slopes of the magnetic curves are most likely due to the approximation made when the magnetic hysteresis curves were smoothed. The improvement after the demagnetization factor was applied, is not so big compared to the first test series. This is surprising, because better material properties were expected from the degased niobium. It was found by DeSorbo [25, 26] that sample impurities have great influence on the superconducting properties of niobium.

Table 4.12.: Comparison of the mean and the standard deviation value of the magnetization of the second test series. Values are divided by a factor of 10^5.

2^{nd} test series - magnetization				
	not field corrected		field corrected	
Cylinder	para.	perp.	para.	perp.
$\mu\ [A/m]$	3.91	4.24	3.19	3.07
$\sigma\ [A/m]$	0.36	0.45	0.21	0.33
Cuboid	para.	perp.	para.	perp.
$\mu\ [A/m]$	3.76	4.11	–	–
$\sigma\ [A/m]$	0.19	0.26	–	–

4.3.3. Current density

More important than the magnetization is the critical current density j_c which should also be dimension independent. The j_c values were corrected for demagnetization effects of the cylinder samples in the same way as the magnetization values. The corrected values of the current density did indeed show less scatter.

The problem with the current density is that the current flows, in rectangular cross sections that are perpendicular to the magnetic field, only in circles if the cross section is square like. In cross sections, perpendicular to the magnetic field, where one of the two sides is much longer than the other one, the current flows parallel to the longer side and closes only at the edges. The effects of the samples having a slightly longer dimension in one direction, perpendicular to the magnetic field, seems to have a big influence. That is especially true for the degased test series.

A calculation of the critical current densities according to the new approach from section 2.4 gives an even better agreement for the cylinders. The values are approximately 65% higher than in the case of calculations with formula (2.5). Details are given in the following.

Critical current densities of the first test series

The critical current density was calculated from the magnetic moment by formula (2.5) since the cross section perpendicular to the applied field of the geometries was square like. The critical current densities have been calculated for cuboids, cylinders and hollow cylinders with their main axes parallel and perpendicular to the magnetic field. An example of the critical current density curves as functions of the applied field can be seen in Fig. 4.25.

Furthermore, the theory developed in section 2.4 has been used to calculate the critical current density in order to compare the j_c values with those obtained by formula (2.5). Fig. 4.26 shows the critical current density curves obtained by the method from section 2.4 as a function of the applied field. Tab. 4.13 shows the evaluated values of the critical current density for all geometries measured.

At zero applied field, differences of the current densites are between 7% and 16% for the different samples. With the method of section 2.4, the difference of the current density of the cylinders perpendicular to the magnetic field is 6% instead of 16%. Then, the average value of the current density is 65% higher compared to the average of the current densities calculated by formula (2.5).

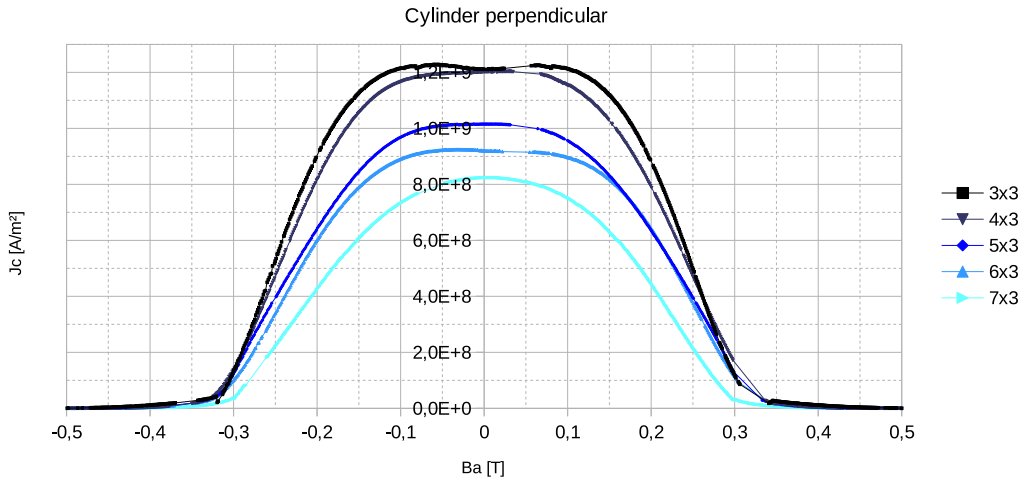

Figure 4.25.: Critical current density curves calculated by formula (2.5) versus the applied field of the cylinders of the first test series with their main axes perpendicular to the magnetic field. The first digit of every label indicates the length of the dimension parallel to the main axis.

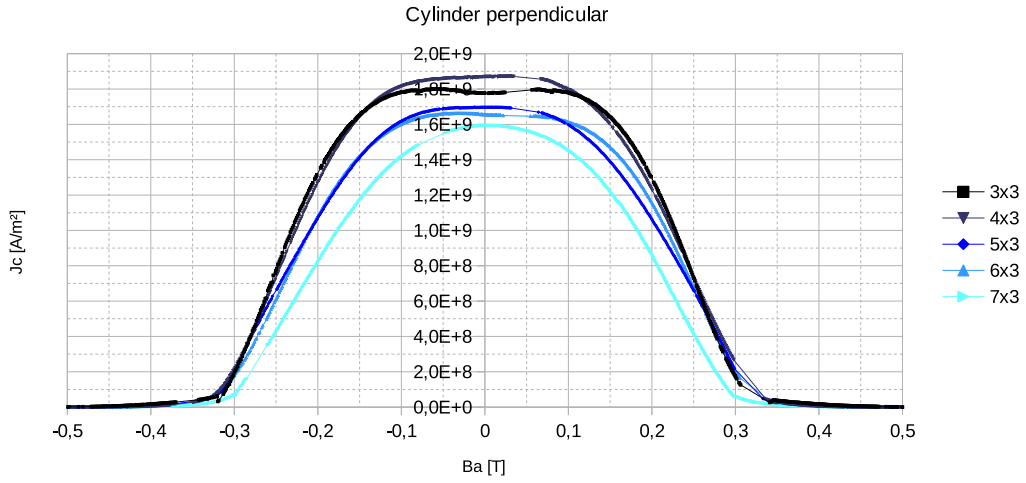

Figure 4.26.: Critical current density calculated with the adjusted formula of section 2.4. The curves are plotted versus the applied field of the cylinders of the first test series with their main axes perpendicular to the magnetic field. The first digit of every label indicates the length of the dimension parallel to the main axis.

Table 4.13.: Critical current densities of the first test series at zero applied field. Values are divided by a factor of 10^9. The current density values in column "adj.", were calculated with the method introduced in section 2.4 for the cylinders with their main axes perpendicular to the magnetic field. The unit of the current density is $[A/m^2]$

	Cuboid		Cylinder			Hollow Cyl.	
length	para.	perp.	para.	perp.	adj.	para.	perp.
2.50	–	–	–	–	–	1.499	0.779
3.00	0.916	0.916	1.242	1.211	1.777	–	–
3.85	1.164	1.238	–	–	–	–	–
4.00	–	–	1.269	1.211	1.870	1.513	0.913
4.60	1.089	1.239	–	–	–	–	–
4.90	–	–	–	–	–	1.440	0.998
5.00	–	–	1.192	1.015	1.697	–	–
6.00	1.086	1.235	1.032	0.920	1.655	1.432	1.100
7.00	1.023	–	0.934	0.824	1.595	1.348	1.140
8.00	0.982	–	0.899	–	–	1.239	–

Critical current densities of the first test series after demagnetization effects are considered

The demagnetization factor has been applied to the cylinders with their main axes parallel and perpendicular to the magnetic field. Fig. 4.27 shows the critical current density curves as a function of the internal field for the cylinders perpendicular to the magnetic field. The adjustment method of the critical current density from section 2.4 has been used and the resulting curves of the cylinders perpendicular to the magnetic field can be seen in Fig. 4.28 as functions of the internal field. All values of the critical current density of the first test series, after the demagnetization effects have been applied, can be found in Tab. 4.14.

The averages of the critical current densities for every geometry were made and the standard deviation was calculated. These values can be found in Tab. 4.15. At zero applied field, differences of the current densites are now between 10%, for cylinders parallel to the field, and 22%, for cylinders perpendicular to the field, instead of 15% and 16% for the different samples after demagnetization effects have been considered. With the method of section 2.4, the difference of the current density of the cylinders perpendicular to the magnetic field is 12% instead of 22%. Then, the aver-

age value of the current density is 66% higher compared to the average of the current densities calculated by formula (2.5). It can be seen that after the demagnetization effects were applied, the averages and standard deviations of the critical current densities decreased for the cylinders parallel to the field. The adjusted formula for the current density increased the current density and the standard deviation was reduced for the cylinders perpendicular to the field. A negative slope in the critical

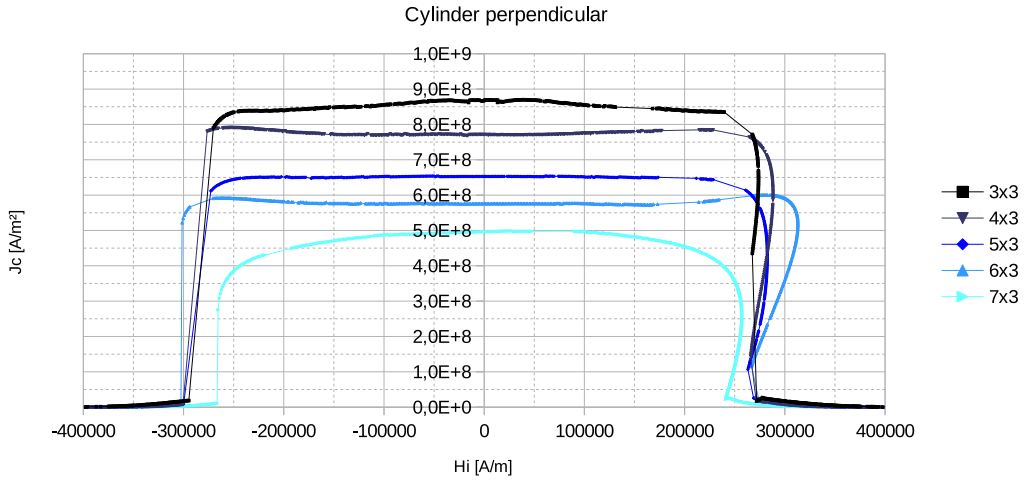

Figure 4.27.: Critical current density curves calculated according to formula (2.5) versus the internal field of the cylinders of the first test series with their main axes perpendicular to the magnetic field, after demagnetization effects were considered. The first digit of every label indicates the length of the dimension parallel to the main axis.

current density curves can be seen in Figs. 4.27 and 4.28 for high fields. This non physical behavior is most likely due to the approximation made as the magnetic hysteresis curves were smoothed.

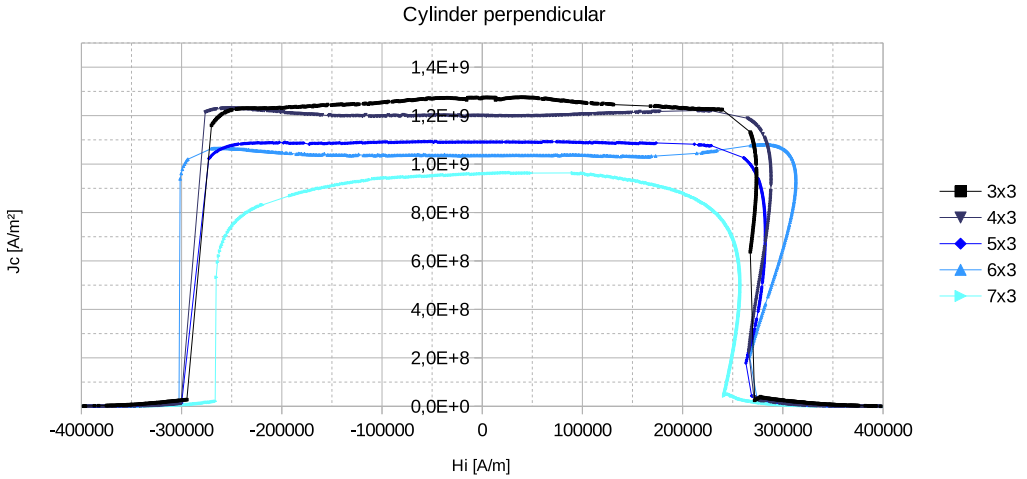

Figure 4.28.: Critical current density calculated with the adjusted formula of section 2.4. The curves are plotted versus the internal field of the cylinders of the first test series with their main axes perpendicular to the magnetic field, after demagnetization effects were considered. The first digit of every label indicates the length of the dimension parallel to the main axis.

Table 4.14.: Critical current densities of cylinders of various length at zero internal field. Values are divided by a factor of 10^9. The current density values in the row "adjusted perp." were calculated with the method introduced in section 2.4. The unit of the current density is [A/m^2].

length [mm]	3.00	4.00	5.00	6.00	7.00	8.00
parallel	0.856	0.929	0.916	0.811	0.772	0.744
perpendicular	0.867	0.772	0.653	0.576	0.496	–
adjusted perp.	1.275	1.201	1.091	1.036	0.960	–

Table 4.15.: Comparison of the mean and the standard deviation value of the critical current density of the first test series. Values are divided by a factor of 10^9. The current density values in columns "adj.", were calculated with the method introduced in section 2.4 for the cylinders with their main axes perpendicular to the magnetic field.

1^{st} test series - current density						
	not field corrected			field corrected		
Cylinder	para.	perp.	adj.	para.	perp.	adj.
$\mu\ [A/m^2]$	1.09	1.04	1.72	0.84	0.67	1.11
$\sigma\ [A/m^2]$	0.16	0.17	0.11	0.08	0.15	0.13
Cuboid	para.	perp.	adj.	para.	perp.	adj.
$\mu\ [A/m^2]$	1.04	1.16	–	–	–	–
$\sigma\ [A/m^2]$	0.09	0.16	–	–	–	–
Hollow Cyl.	para.	perp.	adj.	para.	perp.	adj.
$\mu\ [A/m^2]$	1.41	0.99	–	–	–	–
$\sigma\ [A/m^2]$	0.10	0.15	–	–	–	–

Critical current densities of the second test series

Also for the second test series, which was degased, the critical current densities were evaluated. They were calculated with formula (2.5) for cuboids and cylinders, with their main axes parallel and perpendicular to the magnetic field. An example for the critical current curves as functions of the applied field can be seen in Fig. 4.29.

A difference of 4% and 18% is found between calculated values by formula (2.5) for both field directions in case of cuboids and cylinders. The scattering of the cylinders parallel to the field dropped from 15% to 10%, compared to the first test series. The difference of the cylinders perpendicular to the field increased from 16% to 18%, compared to the first test series. The scattering of the cuboids dropped from 9% to 6%, in the case where the longest side is parallel to the applied field, and from 14% to 4% in the case where the longest side is perpendicular to the applied field, compared to the first test series.

Additionally, for the cylinders with their main axes perpendicular to the magnetic field, the adjusted critical current approach from section 2.4 was used. These curves as functions of the applied field are illustrated in Fig. 4.30. Analyses with the approach of section 2.4 give much higher j_c values. They are 48% higher for the shortest cylinder and increase systematically with cylinder length until they reach 90% for 6 mm length. The difference of the current densities of the cylinders perpendicular to the field calculated by the method of section 2.4 is 10% instead of 18%. The whole set of critical current values at zero applied field for all measured geometries of the second test series can be found in Tab. 4.16.

Table 4.16.: Critical current densities of the second test series at zero applied field. Values are divided by a factor of 10^9. The current density values in column "adj." were calculated with the method introduced in section 2.4 for the cylinders, with their main axes perpendicular to the magnetic field. The unit of the current density is [A/m^2]

	Cuboid		Cylinder		
length	para.	perp.	para.	perp.	adj.
3.00	0.741	0.741	0.762	0.796	1.168
3.50	0.741	0.711	0.882	0.842	1.269
4.00	0.698	0.752	0.737	0.790	1.227
5.00	0.697	0.798	0.809	0.722	1.168
5.50	0.670	0.773	0.672	0.519	0.934
6.00	0.654	0.755	0.762	0.610	1.168

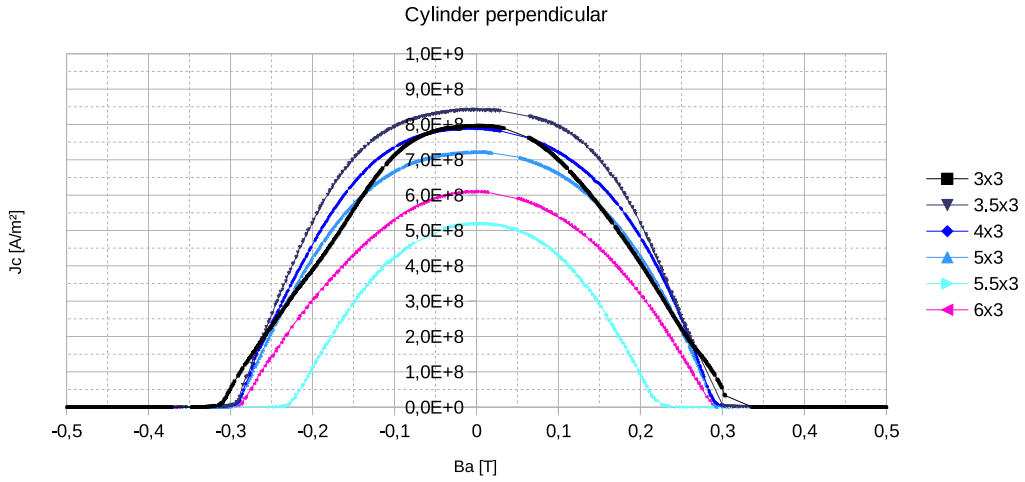

Figure 4.29.: Critical current density determined by formula (2.5) versus the applied field of the cylinders of the second test series with their main axes perpendicular to the magnetic field. The first digit of every label indicates the length of the dimension parallel to the main axis.

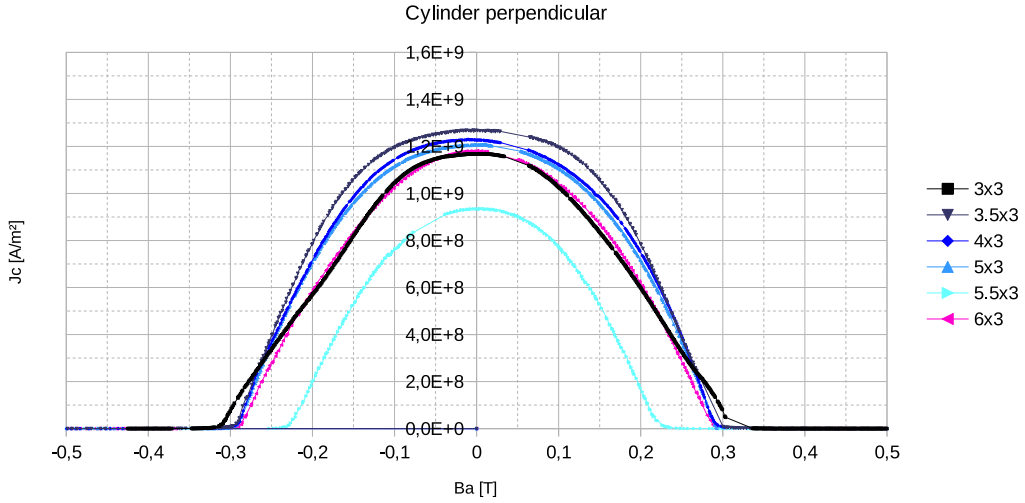

Figure 4.30.: Critical current density calculated with the adjusted formula of section 2.4. The curves are plotted versus the applied field of the cylinders of the second test series with their main axes perpendicular to the magnetic field. The first digit of every label indicates the length of the dimension parallel to the main axis.

Critical current densities of the second test series after demagnetization effects are considered

The demagnetization factor has been applied to the second test series. The resulting curves of the cylinders, with their main axes perpendicular to the magnetic field as functions of the internal field can be seen in Fig. 4.31. The critical current density curves calculated with the alternative Ansatz from section 2.4 are illustrated in Fig. 4.32. The calculated values of the critical current densities at zero internal field for all measured geometries can be seen in Tab. 4.17.

The average of the critical current densities for the cylinders was made and their standard deviation was calculated. It can be seen from Tab. 4.18 that the critical current density values and the standard deviation values decrease if demagnetization effects are considered. This is analog to the cylinders parallel to the field of to the first test series. The difference of the cylinders parallel to the field is 6% after demagnetization effects are considered instead of 10%. The difference of the cylinders perpendicular to the field is 19% after demagnetization effects are considered instead of 18%. With the adjusted method of section 2.4, the difference of the current densities is 13% instead of 19%. The adjusted formula for the critical current density does not decrease the standard deviation, in the same amount, like for the first test series, but also increased the values for the current densities. The average value of the current densities is 66% higher compared to the average of the current densities calculated by formula (2.5). No significant difference concerning deviation between different field densities and different analysis methods is found compared to the case where demagnetization effects are not taken into account.

Table 4.17.: Critical current densities of cylinders of various length calculated by formula (2.5) at zero internal field. Values are divided by a factor of 10^9. The current density values in the row "adjusted perp." were calculated with the method introduced in section 2.4. The unit of the current density is [A/m^2].

length [mm]	3.00	3.50	4.00	5.00	5.50	6.00
parallel	0.611	0.685	0.648	0.675	0.573	0.631
perpendicular	0.585	0.622	0.579	0.523	0.367	0.429
adjusted perp.	0.858	0.937	0.900	0.874	0.636	0.775

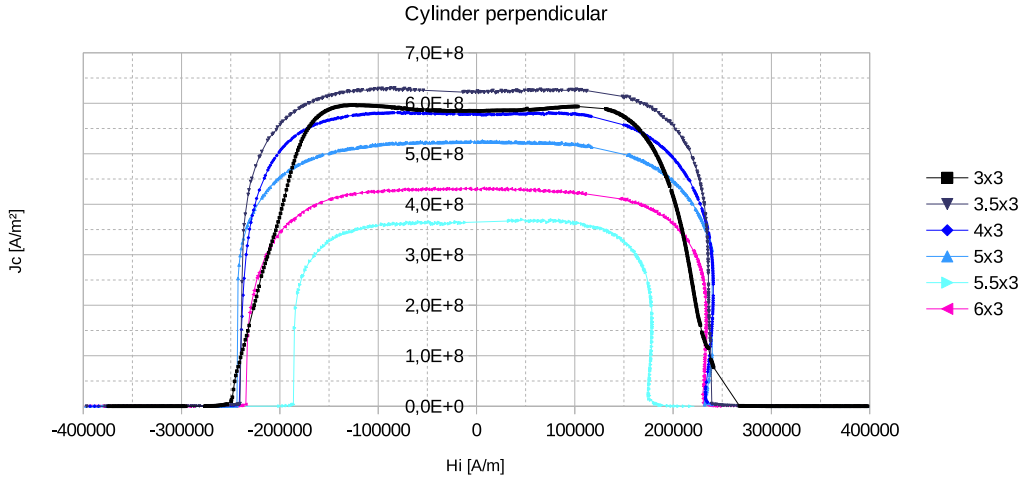

Figure 4.31.: Critical current density curves versus the internal field of the cylinders of the second test series with their main axes perpendicular to the magnetic field to the magnetic field. Demagnetization effects have been considered. The first digit of every label indicates the length of the dimension parallel to the main axis.

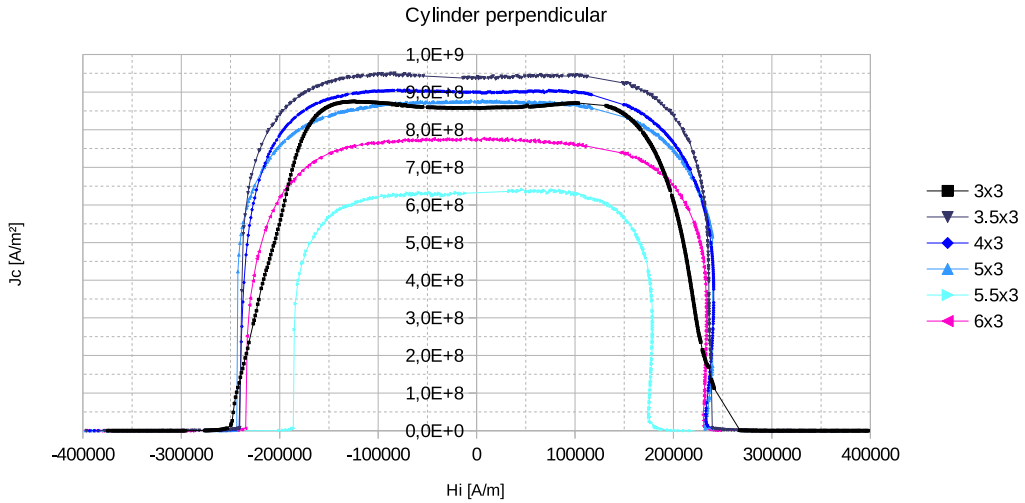

Figure 4.32.: Critical current density calculated with the adjusted formula of section 2.4, after demagnetization effects have been considered. The curves are plotted versus the internal field of the cylinders of the second test series with their main axes perpendicular to the magnetic field to the magnetic field. The first digit of every label indicates the length of the dimension parallel to the main axis.

Table 4.18.: Comparison of the mean and the standard deviation value of the critical current density of the second test series. The current density values in column "adj." were calculated with the method introduced in section 2.4 for the cylinders with their main axes perpendicular to the magnetic field. Values are divided by a factor of 10^9.

2^{nd} test series - current density						
	not field corrected			field corrected		
Cylinder	para.	perp.	adj.	para.	perp.	adj.
$\mu\ [A/m^2]$	0.77	0.71	1.16	0.64	0.52	0.83
$\sigma\ [A/m^2]$	0.07	0.13	0.12	0.04	0.10	0.11
Cuboid	para.	perp.	adj.	para.	perp.	adj.
$\mu\ [A/m^2]$	0.70	0.76	–	–	–	–
$\sigma\ [A/m^2]$	0.04	0.03	–	–	–	–

5. Conclusion

For indirect critical current density measurements the geometry of the current flow, which for a homogeneous superconductor should be identical with the sample geometry, has to be known. The motivation for this thesis was to compare the theoretical magnetization and critical current densities, obtained by formulas, with the real magnetization and current densities for type-II superconductors. This is done in order to help to estimate the error for indirect magnetic flux measurements, in particular for magnesium diboride wires.

On the theoretical side, detailed calculations of the magnetic moment as a function of the current density have been given for cuboids, cylinders, hollow cylinders, elliptical and elliptical hollow cylinders parallel as well as perpendicular to the magnetic field. These calculations and the parallel axis theorem can provide a basis for future calculations for much more complex profiles and geometries. Also the usually used two formulas for calculating the magnetic moment from the critical current density have been compared. The first formula is used to calculate profiles where one side is much longer than the others and is located perpendicular to the applied field. The other formula is used to calculate profiles with a cross section perpendicular to the magnetic field that is rather squarish. It has been shown that these formulas can also calculate the case of the other cross section if applied correctly.

The numerical calculations of the demagnetization factor for cylinders, with their main axes parallel and perpendicular to the magnetic field have been done and are complete for a susceptibility of minus one. Since the susceptibilities of type-II superconductors are subject to demagnetizing effects, numerical calculations similar to the calculations of the cuboid will be necessary in the future. A program calculating the demagnetization factor of an infinitly long bar with its main axis perpendicular to the magnetic field has been written. The program returns the correct values of the demagnetization factors for all values of the susceptibility. The program could be optimized through better subdivision of the sample surface. Finally, a program for a general cuboid was written but, at the moment, it does not return correct values of the demagnetization factor. This program has to be finished in the future.

The magnetic moment of two test series was measured. The first test series included the geometries of cylinders, cuboids and hollow cylinders with their main axes parallel and perpendicular to the magnetic field. A second test series was made for cylinders and cuboids with their main axes parallel and perpendicular to the magnetic field. The second test series was degased before measurement in order to

reduce the big flux jumps that appeared in the first test series. Unfortunately, there was only a little reduction of flux jumps. The magnetization values have been calculated for all geometries measured. The results show that the standard deviation of the average of the magnetization values of the cylinders was halved after demagnetization effects have been considered. The standard deviation of the average of the magnetization of the second test series was also reduced but not as much as for the first series.

Since the demagnetization factors have been computed for a susceptibility of minus one, the susceptibilities of the measured geometries have been evaluated. For the cylinder and cuboid the approximation of the susceptibility with minus one can be said to be rather good, whereas for the hollow cylinder this approximation is rather bad.

The critical current densities for both test series have been calculated with the classic formula from the magnetic moment and with a new approach for the current densities of cylinders with their main axes perpendicular to the magnetic field. It could be shown that for the first test series the application of demagnetization effects reduced the percentual spreading of the critical current densities of the cylinders parallel to the field. For the cylinder perpendicular to the field, the application of the demagnetizing effects increased the percentual scattering. Although the new approach to calculate the critical current density reduced the spreading, this effect became smaller for the current densities where demagnetization effects have been considered. In case of the second test series, the application of demagnetizing effects reduced the percentual scattering of the cylinders parallel to the field and increased the percentual scattering of the cylinders perpendicular to the field. The adjusted approach for the cylinder perpendicular to the field reduced the percentual scattering, but increased the average values. This new approach needs more time to be studied in greater detail in the future.

A. Program code

In chapter 3 the implementation methods of programs to calculate the demagnetization factor were discussed. The program code regarding these methods can be found in this appendix.

A.1. Cylinder parallel to the magnetic field

This program code calculates the demagnetization factor of a cylinder of susceptibility $\chi = -1$ with its main axis parallel to the applied magnetic field. Lines (4) to (8) initialize the program. In lines (10) to (20) parameters relevant for the calculations, such as the length and the diameter, have to be given by the user in mm. N_s and N_l are the numbers of sections in which the cylinder is cut in radial direction and in direction of the length respectively. In line (31) the subroutine Zylinder_parallel is called, which initialises the linear set of equations given by formula (3.1) to (3.3). After the initialising process has been finished the subroutine DGESV from the LAPACK [16] package is called, which solves the linear set of equations by using a lower upper (LU) decomposition routine and returns a vector with the values for the solved coefficients, solvec. The values for the coefficients are printed on the console (lines (51)-(63)). With the solution vector and the function alpha_tt, the demagnetization factor can be calculated in line (80)-(82). To calculate the error for the coefficients the subroutine Testing is called in line (90).

```
1  Program Entmag_Zylinder_parallel
2    implicit none
3
4   integer :: N,i,j,mode,Nl,Ns,p,INFO
5   integer,allocatable,dimension(:,:) :: IPIV
6   real*8 :: a,b,length,diam,m,nu,alphatt
7   real*8,allocatable,dimension(:) :: solvec
8   real*8,allocatable,dimension(:,:) :: eqnarray
9
10     Write(*,*) "Diameter of the cylinder [mm]:"
11     Read(*,*) diam
12     Write(*,*) "Length of the cylinder [mm]:"
13     Read(*,*) length
14     a=diam/2D0
15     b=length/2D0
16
17     write(*,*)"Number of coefficents for the length:"
18     Read(*,*)Ns
19     write(*,*)"Number of coefficents for the radius:"
```

```
20      Read(*,*)Nl
21
22      Allocate(IPIV(0:Nl+Ns+1,0:Ns+Nl+1))
23      Allocate(solvec(0:Nl+Ns+1))
24      Allocate(eqnarray(0:Nl+Ns+1,0:Nl+Ns+1))
25
26      IPIV=0
27      solvec=0D0
28      solvec(1)=1D0
29      eqnarray=0D0
30
31      Call Zylinder_parallel(a,b,Nl,Ns,eqnarray,solvec)
32
33      write(*,*)"*********************************************************************"
34      write(*,*)"*  DGESV OUTPUT:          *"
35      write(*,*)"*********************************************************************"
36      write(*,*)"* INFO = 0 , DGESV was successfull         *"
37      write(*,*)"* INFO = -i, the i-th argument had an illegal value         *"
38      write(*,*)"* INFO = i, U(i,i) is exactly zero. The factorization has    *"
39      write(*,*)"*      been completed, but the factor U is exactly singular, *"
40      write(*,*)"* so the solution could not be computed.   *"
41      write(*,*)"*********************************************************************"
42
43      Call DGESV( Ns+Nl+2, 1, eqnarray, Ns+Nl+2, IPIV,solvec, Ns+Nl+2, INFO )
44
45      Write(*,*)"* INFO = ",INFO,"*"
46      write(*,*)"***********************"
47      write(*,*)""
48      write(*,*)"*******************************"
49      Write(*,*)"*     Koeffizienten:       *"
50      write(*,*)"*******************************"
51
52      write(*,'(A10,E20.12,A2)')"* sb    = ",solvec(0)," *"
53      Do i=2,Ns+1
54        Write(*,'(A4,I2,A4,E20.12,A2)')"* s[",i-2,"] = ",solvec(i)," *"
55      End Do
56
57      Write(*,*)"*     *     *     *     *     *"
58      write(*,'(A10,E20.12,A2)')"* wb    = ",solvec(1)," *"
59
60      Do i=Ns+2,Ns+Nl+1
61        Write(*,'(A4,I2,A4,E20.12,A2)')"* w[",i-Ns-2,"] = ",solvec(i)," *"
62      End Do
63
64      write(*,*)"*******************************"
65      write(*,*)""
66      write(*,*)"*******************************"
67      write(*,*)"* Demagnetizing Factor   *"
68      write(*,*)"*******************************"
69      write(*,'(A12,F15.12,A5)')"*     att = ",&
70      &alphatt(a,b,solvec(0),solvec(1),solvec(2),solvec(Ns+2)),"    *"
71      write(*,'(A12,F15.12,A5)')"*      Np = "&
72      &,-(2D0-alphatt(a,b,solvec(0),solvec(1),solvec(2),solvec(Ns+2)))/&
```

```
73      &alphatt(a,b,solvec(0),solvec(1),solvec(2),solvec(Ns+2)),"    *"
74
75      write(*,*)"*****************************"
76      write(*,*)""
77      write(*,*)"*********************************"
78      write(*,*)"*       Testing            *"
79      write(*,*)"*********************************"
80
81      Call Testing(a,b,Ns,Nl,solvec,mode)
82
83      write(*,*)"*********************************"
84
85    Deallocate(IPIV)
86    Deallocate(solvec)
87    Deallocate(eqnarray)
88
89  End Program
90
91  !*******************************************************************************************
92  !*******************************************************************************************
93  !*******************************************************************************************
94
95  real*8 FUNCTION Gammaf(arg1)
96    implicit none
97    real*8 :: arg1, gammasol
98
99      Call Gamma(arg1,gammasol)
100     Gammaf = gammasol
101
102 END FUNCTION Gammaf
103
104  real*8 FUNCTION Hypergeometric2F1(arg1, arg2, arg3, arg4)
105   implicit none
106   real*8 :: arg1, arg2, arg3, arg4, hypersol
107
108     call hygfx(arg1,arg2,arg3,arg4,hypersol)
109     Hypergeometric2F1 = hypersol
110
111 End FUNCTION Hypergeometric2F1
112
113 !*******************************************************************************************
114
115 SUBROUTINE Zylinder_parallel(a,b,Nl,Ns,eqnarray,solvec)
116   implicit none
117   integer :: Nl,Ns,i,j
118   real*8 :: a,b,eqnarray(0:Nl+Ns+1,0:Nl+Ns+1),solvec(0:Nl+Ns+1),Ypsm,Yplm,nu
119
120     eqnarray(0,0)=0D0
121     eqnarray(0,1)=0D0
122
123     Do i=2,Ns+1
124       eqnarray(0,i)=1D0
125     End Do
```

```
126
127     Do i=Ns+2,Ns+Nl+1
128       eqnarray(0,i)=-(a/b)**(0.33333333333333333D0)
129     End Do
130
131     Do i=1,Ns+Nl+1
132       eqnarray(i,0)=Ypsm(a,b,DBLE(i-1),0D0,0D0)
133     End Do
134
135     Do i=1,Ns+Nl+1
136       eqnarray(i,1)=Yplm(a,b,DBLE(i-1),0D0,0D0)
137     End Do
138
139     Do i=1,Ns+Nl+1
140       Do j=2,Ns+1
141 eqnarray(i,j)=Ypsm(a,b,DBLE(i-1),DBLE(j-2),-0.33333333333333333D0)
142       End do
143     End Do
144
145     Do i=1,Ns+Nl+1
146       Do j=Ns+2,Ns+Nl+1
147       eqnarray(i,j)=Yplm(a,b,DBLE(i-1),DBLE(j-Ns-2),-0.33333333333333333D0)
148       End do
149     End Do
150
151 End SUBROUTINE Zylinder_parallel
152
153 !*****************************************************************************************
154
155 real*8 FUNCTION Ypsm(a,b,p,m,nu)
156   implicit none
157   real*8 :: m,p,nu,a,b
158   real*8 :: gammaf,Hypergeometric2F1
159
160     Ypsm=(-1)**(p+m)*2D0**(2D0*p-nu)*Gammaf(m+p+1.5D0)*Gammaf(m+p+0.5D0)*&
161       &(a**2D0/(b*Sqrt(a**2D0+b**2D0)))*(b/Sqrt(a**2D0+b**2D0))**(2D0*m+2D0)*&
162       &Hypergeometric2F1(m+p+1.5D0,m-p+1D0+nu,2D0*m+1.5D0+nu,b**2D0/(a**2D0+b**2D0))/&
163       &(Gammaf(0.5D0)*Gammaf(2D0*p+3D0)*Gammaf(2D0*m+1.5D0+nu))
164
165 End FUNCTION Ypsm
166
167 real*8 FUNCTION Yplm(a,b,p,m,nu)
168   implicit none
169   real*8 :: m,p,nu,a,b
170   real*8 :: gammaf,Hypergeometric2F1
171
172     Yplm=(-1)**Int(m)*2D0**(2D0*p-nu)*Gammaf(m+p+1.5D0)*Gammaf(m+p+2)*&
173 &(a/Sqrt(a**2D0+b**2D0))*(a/Sqrt(a**2D0+b**2D0))**(2D0*m+2D0)*&
174 &Hypergeometric2F1(m+p+1.5D0,m-p+1D0+nu,2D0*m+3D0+nu,a**2D0/(a**2D0+b**2D0))/&
175 &(Gammaf(0.5D0)*Gammaf(2D0*p+3D0)*Gammaf(a*m+3D0+nu))
176
177 End FUNCTION Yplm
178
```

```
179 real*8 FUNCTION Ys(a,b,p,Ns,Nl,solvec)
180   implicit none
181   integer :: i,Ns,Nl
182   real*8 :: a,b,p,nu,erg,Ypsm,solvec(0:INT(Ns+Nl+1))
183 
184     erg=0D0
185 
186     Do i=2,Ns+1
187       erg=erg+solvec(i)*Ypsm(a,b,p,DBLE(i-2),-0.33333333333333333D0)
188     End Do
189 
190     Ys=erg
191 
192 End FUNCTION Ys
193 
194 real*8 FUNCTION Yl(a,b,p,Ns,Nl,solvec)
195   implicit none
196   integer :: i,Ns,Nl
197   real*8 :: a,b,p,nu,erg,Yplm,solvec(0:INT(Ns+Nl+1))
198 
199     erg=0D0
200 
201     Do i=Ns+2,Ns+Nl+1
202       erg=erg+solvec(i)*Yplm(a,b,p,DBLE(i-Ns-2),-0.33333333333333333D0)
203     End Do
204 
205     Yl=erg
206 
207 End FUNCTION Yl
208 
209 real*8 FUNCTION alphatt(a,b,sb,wb,s0,w0)
210   implicit none
211   real*8 :: a,b,sb,wb,s0,w0,Gammaf
212 
213     alphatt=(sb+Gammaf(0.5D0)/(2**0.66666666666666666D0*&
214 &Gammaf(1.16666666666666666D0))*s0)+a/b*(0.25D0*wb+1D0/&
215 &(2D0**0.66666666666666666D0*Gammaf(2.66666666666666666D0))*w0)
216 
217 End FUNCTION alphatt
218 
219 !*******************************************************************************************
220 
221 SUBROUTINE Testing(a,b,Ns,Nl,solvec,mode)
222   implicit none
223   integer :: i,mode,Ns,Nl
224   real*8 :: a,b,solp,Ypsm,Yplm,Ys,Yl,solvec(0:Ns+Nl+1),tol
225 
226     tol=0D0
227     solp=0D0
228 
229     Do i=2,Ns+1
230       solp=solp+solvec(i)
231     End Do
```

```
232
233     Do i=Ns+2,Ns+Nl+1
234       solp=solp-a/b**(0.33333333333333333D0)*solvec(i)
235     End Do
236
237     write(*,'(A11,F20.17,A3)')"* Edgek. : ",solp,"  *"
238
239     Do i=1,Ns+Nl+1
240       solp=0D0
241       solp=solvec(0)*Ypsm(a,b,DBLE(i-1),0D0,0D0)+solvec(1)*Yplm(a,b,DBLE(i-1),0D0,0D0)+&
242   &Ys(a,b,DBLE(i-1),Ns,Nl,solvec)+Yl(a,b,DBLE(i-1),Ns,Nl,solvec)
243
244       write(*,'(A6,I2,A3,F20.17,A3)')"* p = ",i," : ",solp,"  *"
245     End Do
246
247 End SUBROUTINE Testing
248
249 !*************************************************************************************
250 !*********************************   END   *******************************************
251 !*************************************************************************************
```

A.2. Cylinder perpendicular to the magnetic field

This program code calculates the demagnetization factor of a cylinder of susceptibility $\chi = -1$ with its main axis perpendicular to the applied magnetic field. Lines (4) to (8) initialize the program. In lines (10) to (20) parameters relevant for the calculations, such as the length and the diameter, both in mm, have to be given by the user. N_s and N_l are the numbers of sections in which the cylinder is cut in radial direction and in direction of the length respectively. In line (31) the subroutine Zylinder_senkrecht is called, which initialises the linear set of equations given by formula (3.11) to (3.13). After the initialising process has been finished the subroutine DGESV from the LAPACK [16] package is called, which solves the linear set of equations by using a lower upper (LU) decomposition routine and returns a vector with the values for the solved coefficients, solvec. The values for the coefficients are printed on the console (lines (50)-(61)). With the solution vector and the function beta_tt, the demagnetization factor can be calculated in line (68)-(69). To calculate the error for the coefficients the subroutine Testing is called in line (77).

```
1  Program Entmag_Zylinder_senkrecht
2    implicit none
3
4    integer :: N,i,j,mode,Nl,Ns,p,INFO
5    integer,allocatable,dimension(:,:) :: IPIV
6    real*8 :: a,b,length,diam,m,nu,betatt
7    real*8,allocatable,dimension(:) :: solvec
8    real*8,allocatable,dimension(:,:) :: eqnarray
9
10     Write(*,*) "Diameter of the cylinder [mm]:"
11     Read(*,*) diam
12     Write(*,*) "Length of the cylinder [mm]:"
13     Read(*,*) length
14     a=diam/2D0
15     b=length/2D0
16
17     write(*,*)"Number of coefficents for the length:"
18     Read(*,*)Ns
19     write(*,*)"Number of coefficents for the radius:"
20     Read(*,*)Nl
21
22     Allocate(IPIV(0:Nl+Ns,0:Ns+Nl))
23     Allocate(solvec(0:Nl+Ns))
24     Allocate(eqnarray(0:Nl+Ns,0:Nl+Ns))
25
26     solvec=0D0
27     solvec(1)=1D0
28     eqnarray=0D0
29
30     Call Zylinder_senkrecht(a,b,Nl,Ns,eqnarray,solvec)
31
32     write(*,*)"*****************************************************************"
33     write(*,*)"*  DGESV OUTPUT:          *"
```

```
34      write(*,*)"*********************************************************************"
35      write(*,*)"* INFO = 0 , DGESV was successfull         *"
36      write(*,*)"* INFO = -i, the i-th argument had an illegal value         *"
37      write(*,*)"* INFO = i, U(i,i) is exactly zero. The factorization has    *"
38      write(*,*)"*      been completed, but the factor U is exactly singular, *"
39      write(*,*)"* so the solution could not be computed.   *"
40      write(*,*)"*********************************************************************"
41
42      Call DGESV( Ns+Nl+1, 1, eqnarray, Ns+Nl+1, IPIV,solvec, Ns+Nl+1, INFO )
43
44      Write(*,*)"* INFO = ",INFO,"*"
45      write(*,*)"***********************"
46      write(*,*)""
47      write(*,*)"*******************************"
48      Write(*,*)"*   Koeffizienten:         *"
49      write(*,*)"*******************************"
50      write(*,'(A10,E20.12,A2)')"* sb    = ",solvec(0)," *"
51
52      Do i=1,Ns
53        Write(*,'(A4,I2,A4,E20.12,A2)')"* s[",i-1,"] = ",solvec(i)," *"
54      End Do
55
56      Write(*,*)"*     *     *     *     *     *"
57
58      Do i=Ns+1,Ns+Nl
59        Write(*,'(A4,I2,A4,E20.12,A2)')"* w[",i-Ns-1,"] = ",solvec(i)," *"
60      End Do
61
62      write(*,*)"*******************************"
63      write(*,*)""
64      write(*,*)"*******************************"
65      write(*,*)"* Demagnetizing Factor   *"
66      write(*,*)"*******************************"
67
68      write(*,'(A12,F15.12,A5)')"*      Ns = "&
69  &,(betatt(a,b,solvec(0),solvec(1))+1)/betatt(a,b,solvec(0),solvec(1)),"    *"
70
71      write(*,*)"*******************************"
72      write(*,*)""
73      write(*,*)"*********************************"
74      write(*,*)"*       Testing            *"
75      write(*,*)"*********************************"
76
77      Call Testing(a,b,Ns,Nl,solvec)
78
79      write(*,*)"*********************************"
80
81      Deallocate(IPIV)
82      Deallocate(solvec)
83      Deallocate(eqnarray)
84
85  End Program
86
```

```
87 !*****************************************************************************************
88 !*****************************************************************************************
89 !*****************************************************************************************
90
91 real*8 FUNCTION Gammaf(arg1)
92   implicit none
93   real*8 :: arg1, gammasol
94
95     Call Gamma(arg1,gammasol)
96     Gammaf = gammasol
97
98 END FUNCTION Gammaf
99
100 real*8 FUNCTION Hypergeometric2F1(arg1, arg2, arg3, arg4)
101   implicit none
102   real*8 :: arg1, arg2, arg3, arg4, hypersol
103
104     call hygfx(arg1,arg2,arg3,arg4,hypersol)
105     Hypergeometric2F1 = hypersol
106
107 End FUNCTION Hypergeometric2F1
108
109 !*****************************************************************************************
110
111 SUBROUTINE Zylinder_senkrecht(a,b,Nl,Ns,eqnarray,solvec)
112  implicit none
113  integer :: Nl,Ns,i,j
114  real*8 :: a,b,eqnarray(0:Nl+Ns,0:Nl+Ns),solvec(0:Nl+Ns),Zpsm,Zplm,nu
115
116     eqnarray(0,0)=0D0
117     eqnarray(0,1)=0D0
118
119     Do i=1,Ns
120       eqnarray(0,i)=1D0
121     End Do
122
123     Do i=Ns+1,Ns+Nl
124       eqnarray(0,i)=(b/a)**(0.66666666666666666D0)
125     End Do
126
127     Do i=1,Ns+Nl
128       eqnarray(i,0)=Zpsm(a,b,DBLE(i-1),0D0,0D0)+Zplm(a,b,DBLE(i-1),0D0,0D0)
129     End Do
130
131
132     Do i=1,Ns+Nl
133       Do j=1,Ns
134 eqnarray(i,j)=Zpsm(a,b,DBLE(i-1),DBLE(j-1),0.66666666666666666D0)
135       End do
136     End Do
137
138     Do i=1,Ns+Nl
139       Do j=Ns+1,Ns+Nl
```

```
140       eqnarray(i,j)=Zplm(a,b,DBLE(i-1),DBLE(j-Ns-1),0.66666666666666666D0)
141       End do
142     End Do
143
144 End SUBROUTINE Zylinder_senkrecht
145
146 !*****************************************************************************************
147
148 real*8 FUNCTION Zs(a,b,p,Ns,Nl,solvec)
149   implicit none
150   integer :: i,Ns,Nl
151   real*8 :: a,b,p,nu,erg,Zpsm,solvec(0:Ns+Nl)
152
153     erg=0D0
154
155     Do i=1,Ns
156       erg=erg+solvec(i)*Zpsm(a,b,p,DBLE(i-1),0.66666666666666666D0)
157     End Do
158
159     Zs=erg
160
161 End FUNCTION Zs
162
163 real*8 FUNCTION Zl(a,b,p,Ns,Nl,solvec)
164   implicit none
165   integer :: i,Ns,Nl
166   real*8 :: a,b,p,nu,erg,Zplm,solvec(0:Ns+Nl)
167
168     erg=0D0
169
170     Do i=Ns+1,Ns+Nl
171       erg=erg+solvec(i)*Zplm(a,b,p,DBLE(i-Ns-1),0.66666666666666666D0)
172     End Do
173
174     Zl=erg
175
176 End FUNCTION Zl
177
178 real*8 FUNCTION betatt(a,b,sb,s0)
179   implicit none
180   real*8 :: a,b,sb,s0,Gammaf
181
182     betatt=-(sb+Gammaf(0.5D0)/(2D0**1.66666666666666666D0*&
183   &Gammaf(2.16666666666666666D0))*s0)
184
185 End FUNCTION betatt
186
187 !*****************************************************************************************
188
189 SUBROUTINE Testing(a,b,Ns,Nl,solvec)
190   implicit none
191   integer :: i,mode,Ns,Nl
192   real*8 :: a,b,solp,Zpsm,Zplm,Zs,Zl,solvec(0:Ns+Nl),tol
```

```
193
194       tol=0D0
195       solp=0D0
196
197       Do i=1,Ns
198         solp=solp+solvec(i)
199       End Do
200
201       Do i=Ns+1,Ns+Nl
202         solp=solp+(b/a)**(0.66666666666666666D0)*solvec(i)
203       End Do
204
205       write(*,'(A11,F20.17,A3)')"* Edgek. : ",solp,"  *"
206
207       Do i=1,Ns+Nl
208         solp=0D0
209         solp=solvec(0)*(Zpsm(a,b,DBLE(i-1),0D0,0D0)+Zplm(a,b,DBLE(i-1),0D0,0D0))+&
210     &Zs(a,b,DBLE(i-1),Ns,Nl,solvec)+Zl(a,b,DBLE(i-1),Ns,Nl,solvec)
211
212         write(*,'(A6,I2,A3,F20.17,A3)')"* p = ",i," : ",solp,"  *"
213       End Do
214
215   End SUBROUTINE Testing
216
217   real*8 FUNCTION Zpsm(a,b,p,m,nu)
218     implicit none
219     real*8 :: m,p,nu,a,b
220     real*8 :: gammaf,Hypergeometric2F1
221
222       Zpsm=(-1)**(p+m)*2D0**(2D0*p+1D0-nu)*Gammaf(m+p+1.5D0)*Gammaf(m+p+0.5D0)*&
223       &(a**2D0/(b*Sqrt(a**2D0+b**2D0)))*(b/Sqrt(a**2D0+b**2D0))**(2D0*m+2)*&
224       &(0.5D0*Hypergeometric2F1(m+p+1.5D0,m-p+1D0+nu,2D0*m+1.5D0+nu,b**2D0/(a**2D0+b**2D0))&
225       &+(m+p+0.5D0)*Hypergeometric2F1(m+p+1.5D0,m-p+nu,2D0*m+1.5D0+nu,b**2D0/(a**2+b**2)))/&
226       &(Gammaf(0.5D0)*Gammaf(2D0*p+3D0)*Gammaf(2D0*m+1.5D0+nu))
227
228   End FUNCTION Zpsm
229
230   real*8 FUNCTION Zplm(a,b,p,m,nu)
231     implicit none
232     real*8 :: m,p,nu,a,b
233     real*8 :: gammaf,Hypergeometric2F1
234
235       Zplm=(-1)**Int(m)*2D0**(2D0*p+1D0-nu)*Gammaf(m+p+2.5D0)*Gammaf(m+p+2D0)*&
236           &(b/Sqrt(a**2D0+b**2D0))*(a/Sqrt(a**2D0+b**2D0))**(2D0*m+4)*&
237           &Hypergeometric2F1(m+p+2.5D0,m-p+1D0+nu,2D0*m+3D0+nu,a**2D0/(a**2D0+b**2D0))/&
238           &(Gammaf(0.5D0)*Gammaf(2D0*p+3D0)*Gammaf(a*m+3D0+nu))
239
240   End FUNCTION Zplm
241
242   !*****************************************************************************************
243   !*********************************   END   ***********************************************
244   !*****************************************************************************************
```

A.3. Infinite bar perpendicular to the magnetic field

This program calculates the demagnetization value for an infinite long bar with its longest side perpendicular to the magnetic field. Lines (3) to (11) initialise the program. In lines (13) to (34) parameters relevant for the calculations, such as width and height of the cross section of the bar, all in mm, have to be given by the user. The program only needs to know whether the width or the length is longer and the number of sections in which the shorter side should be divided. The field is applied in $x-$direction, parallel to side a. A maximum number of sections is defined, if the ratio of longer to shorter side is to big. In line (63) the subroutine Quader is called, which initialises the linear set of equation defined by formula (3.34) and (3.35). The subroutine DGESV from the LAPACK [16] package in line (75) solves the system of linear equations by using a lower upper (LU) decomposition routine. The subroutine returns the values for the solved coefficients in the vector solvec. The demagnetization factor is calculated in line (87) by the subroutine calcNm with the formulas (3.33), (3.32) and (3.25).

Not included in the program code are the definitions of the functions $N_a^{l\pm m'_\pm}$. In the program code they appear for example as Nxipjm. This convention is equal to the convention in formulas (3.43)-(3.46). The x denotes the direction of the field (x, y, z). p and m mean algebraic plus and minus respectively.

```
1  Program Entmag_Quader_parallel
2  implicit none
3   integer :: i,j,jp,ip,nx,ny,nz,INFO
4   integer,allocatable,dimension(:,:) :: IPIV
5   real*8 :: a,b,xs,ys,xp,yp,mu,chi,Ha,dx,dy,x,y
6   real*8,allocatable,dimension(:) :: solvec,sigmax,sigmay
7   real*8,allocatable,dimension(:,:) :: eqnarray
8
9    nx=200
10   ny=200
11   Ha=1D0
12
13    Write(*,*)"Length parallel to the field [mm]"
14    Read(*,*)b
15    Write(*,*)"Shorter side perpendicular to the field [mm]"
16    Read(*,*)a
17    Write(*,*)"Magnetic suscebtibility"
18    Read(*,*)chi
19
20   If(b>a) Then
21     Write(*,*)"Number of FEM elements for the shorter side [200+]"
22     Read(*,*),nx
23     ny=int(b/a)*nx
24   End If
25
26   If(a>b) Then
27     Write(*,*)"Number of FEM elements for the shorter side [200+]"
```

```
28      Read(*,*),ny
29      nx=int(a/b)*ny
30    End if
31
32    If(a==b) Then
33      Write(*,*)"Number of FEM elements for the shorter side [200+]"
34      Read(*,*),nx
35      ny=nx
36    End If
37
38    If(nx>12000) Then
39      nx=12000
40    End If
41
42    If(ny>12000) Then
43      ny=12000
44    End if
45
46    write(*,*)"nx: ",nx
47    write(*,*)"ny: ",ny
48
49    dx=a/(0.5D0 + nx)
50    dy=b/(ny)
51
52    Allocate(IPIV(1:nx+ny,1:nx+ny))
53    Allocate(solvec(1:nx+ny))
54    Allocate(sigmax(1:ny))
55    Allocate(sigmay(1:nx))
56    Allocate(eqnarray(1:nx+ny,1:nx+ny))
57
58    solvec=0D0
59    eqnarray=0D0
60
61    write(*,*)"*********************************************************************"
62    write(*,*)"*  INITALISING SYSTEM:           *"
63    write(*,*)"*********************************************************************"
64
65    Call  Quader(a,b,nx,ny,Ha,chi,eqnarray,solvec,dx,dy)
66
67    write(*,*)"*********************************************************************"
68    write(*,*)"*  DGESV OUTPUT:           *"
69    write(*,*)"*********************************************************************"
70    write(*,*)"* INFO =  0, DGESV was successfull         *"
71    write(*,*)"* INFO = -i, the i-th argument had an illegal value         *"
72    write(*,*)"* INFO =  i, U(i,i) is exactly zero. Factorization has been   *"
73    write(*,*)"*     completed, but the factor U is exactly singular   *"
74    write(*,*)"*      so the solution could not be computed.   *"
75    write(*,*)"*********************************************************************"
76    Write(*,*)"SOLVING MATRIX..."
77    Call DGESV( nx+ny, 1, eqnarray, nx+ny, IPIV, solvec, nx+ny, INFO )
78    write(*,*)"INFO = ",INFO
79
80    Do j=1,ny
```

```
81      sigmax(j)=solvec(j)
82    End Do
83
84    Do i=ny+1,nx+ny
85      sigmay(i-ny)=solvec(i)
86    End Do
87
88
89    Call calcNm(a,b,nx,ny,Ha,chi,sigmax,sigmay,dx,dy)
90
91    Deallocate(IPIV)
92    Deallocate(solvec)
93    Deallocate(eqnarray)
94
95  End Program
96
97  !*****************************************************************************************
98  !*****************************************************************************************
99  !*****************************************************************************************
100
101 SUBROUTINE calcNm(a,b,nx,ny,Ha,chi,sigmax,sigmay,dx,dy)
102  implicit none
103  integer :: i,j,jp,ip,nx,ny
104  real*8 :: a,b,xs,ys,xp,yp,mu,chi,Ha,Nms,dx,dy,Md,Mvol
105  real*8 :: sigmax(1:ny),sigmay(1:nx)
106
107   Md=Mvol(sigmax,sigmay,a,b,nx,ny,dx,dy)
108
109   Nms = Ha/(Md) - 1/chi
110
111   Write(*,'(A,E25.17)')"Nms: ",Nms
112
113 End SUBROUTINE
114
115 !*****************************************************************************************
116
117 SUBROUTINE Quader(a,b,nx,ny,Ha,chi,eqnarray,solvec,dx,dy)
118  implicit none
119  integer :: i,j,jp,ip,nx,ny
120  real*8 :: a,b,xs,ys,xp,yp,mu,chi,Ha,dx,dy
121  real*8 :: Nxjpjp,Nxjpjm,Nxjmjp,Nxjmjm,Nxjpip,Nxjpim,Nxjmip,Nxjmim,Nxipip,Nxipim,Nximip,Nximim
122  real*8 :: Nyipip,Nyipim,Nyimip,Nyimim,Nyipjp,Nyipjm,Nyimjp,Nyimjm,
123  real*8 :: eqnarray(1:nx+ny,1:nx+ny),solvec(1:nx+ny)
124  mu=0.0000012566370614D0
125
126   Do j=1,ny
127     solvec(j)=mu*Ha
128   End Do
129
130   Do,j=1,ny
131
132     Do,jp=1,ny
133     eqnarray(j,jp)=-(Nxjpjp(ys(j,dy),yp(jp,dy),a,dy)+Nxjmjp(ys(j,dy),yp(jp,dy),a,dy)&
```

```
 &-Nxjpjm(ys(j,dy),yp(jp,dy),a,dy)-Nxjmjm(ys(j,dy),yp(jp,dy),a,dy))

 If(j==jp) Then
 eqnarray(j,jp)=eqnarray(j,jp)+1D0/chi
 End If
    End Do

    Do,ip=ny+1,nx+ny
    eqnarray(j,ip)=-(Nxjpip(ys(j,dy),xp(ip-ny,dx),a,b,dx)+Nxjpim(ys(j,dy),xp(ip-ny,dx),a,b,dx)&
 &-Nxjmip(ys(j,dy),xp(ip-ny,dx),a,b,dx)-Nxjmim(ys(j,dy),xp(ip-ny,dx),a,b,dx))
    End Do

  End Do

  Do,i=ny+1,nx+ny

    Do,jp=1,ny
    eqnarray(i,jp)=-(Nyipjp(xs(i-ny,dx),yp(jp,dy),a,b,dy)+Nyimjp(xs(i-ny,dx),yp(jp,dy),a,b,dy)&
 &-Nyipjm(xs(i-ny,dx),yp(jp,dy),a,b,dy)-Nyimjm(xs(i-ny,dx),yp(jp,dy),a,b,dy))
    End Do

    Do,ip=ny+1,nx+ny
    eqnarray(i,ip)=-(Nyipip(xs(i-ny,dx),xp(ip-ny,dx),b,dx)+Nyipim(xs(i-ny,dx),xp(ip-ny,dx),b,dx)&
 &-Nyimip(xs(i-ny,dx),xp(ip-ny,dx),b,dx)-Nyimim(xs(i-ny,dx),xp(ip-ny,dx),b,dx))

 If(i==ip) Then
 eqnarray(i,ip)=eqnarray(i,ip)+1D0/chi
 End If
    End Do

  End Do


End SUBROUTINE

!*****************************************************************************************

real*8 FUNCTION Mmid(sigmax,sigmay,b,nx,ny,dx,dy)
 implicit none
 integer :: i,j,ny,nx
 real*8 :: b,dx,dy,summe,mu,sigmax(1:ny),sigmay(1:nx)
 mu=0.0000012566370614D0
 summe=0D0

 Do i=1,nx
 summe=summe+sigmay(i)*dx
 End Do

 Do j=1,ny
 summe=summe+sigmax(j)*dy
 End Do

 Mmid=1D0/(mu*b)*summe
```

```
187
188 End FUNCTION
189
190
191
192 real*8 FUNCTION Mvol(sigmax,sigmay,a,b,nx,ny,dx,dy)
193  implicit none
194  integer :: i,ip,jp,j,ny,nx,perc
195  real*8 :: a,b,dx,dy,sigmax(1:ny),sigmay(1:nx),summe1,summe2,summe3,mu,Mmid
196  mu=0.0000012566370614D0
197  summe1=0D0
198  summe2=0D0
199  summe3=0D0
200  perc=0
201  write(*,*)"CALCULATING Mvol:"
202  Do ip=1,nx
203  summe1=summe1+0.5D0*sigmay(ip)*dx*dx
204  End Do
205
206  Do ip=1,nx
207   Do i=ip+1,nx
208     If(i>nx) Then
209       Goto 100
210     End If
211   summe2=summe2+sigmay(i)*dx*dx
212   100 End Do
213   perc=perc+1
214   Write(*,'(A,I4,A)',advance="no")"\b\b\b\b\b\b",Int(Real(perc)/(nx+nx)*100)," %"
215  End Do
216
217  Do ip=1,nx
218   Do j=1,ny
219   summe3=summe3+sigmax(j)*dx*dy
220   End Do
221     perc=perc+1
222    Write(*,'(A,I4,A)',advance="no")"\b\b\b\b\b\b",Int(Real(perc)/(nx+nx)*100)," %"
223  End Do
224  write(*,*)""
225  write(*,*)"Mvol FINISHED!"
226  Mvol=1D0/(mu*a*b)*(summe1+summe2+summe3+0.5D0*Mmid(sigmax,sigmay,b,nx,ny,dx,dy)*b*dx*mu)
227
228 End FUNCTION
229
230  !*****************************************************************************************
231
232  real*8 FUNCTION xs(i,dx)
233   implicit none
234   integer :: i
235   real*8 :: dx
236     xs=dx*DBLE(i)
237  End FUNCTION
238
239  real*8 FUNCTION ys(j,dy)
```

```
240   implicit none
241   integer :: j
242   real*8 :: dy
243     ys=dy*(2D0*DBLE(j)-1)/2
244  End FUNCTION
245
246  real*8 FUNCTION xp(ip,dx)
247   implicit none
248   integer :: ip
249   real*8 :: dx
250     xp=dx*DBLE(ip)
251  End FUNCTION
252
253  real*8 FUNCTION yp(jp,dy)
254   implicit none
255   integer :: jp
256   real*8 :: dy
257     yp=dy*(2D0*DBLE(jp)-1)/2
258  End FUNCTION
259
260 !*****************************************************************************************
261 !*********************************   END   ***********************************************
262 !*****************************************************************************************
```

A.4. Square bar

This program should calculate the demagnetization factor of a square bar. Unfortunately the program does not return proper values. Nevertheless a short introduction of the code is given. Lines (2) to (44) initialise the program. Values regrading the length, height and width have to be in mm. The user has to give some data to the program, which are important for the calculation. Length c is parallel to the magnetic field. n_1, n_2 and n_3 are the number of segments in which each surface is divided. The subroutine Quader initialises the linear set of equations in line (49), defined by formula (3.54) to (3.56). The subroutine DGESV from the LAPACK [16] package in line (75) solves the linear system of equations by using a lower upper (LU) decomposition routine. The subroutine returns the values for the solved coefficients in the vector solvec. The demagnetization factor is calculated in line (92) by the subroutine calcNm using formula (3.25) and (3.73).

Not included in the program code are the definitions of the functions $N_a^{lm,\pm u'\pm v'_\pm}$. In the program code they appear for example as Nzijpipkm.This convention is equal to the convention in formulas (3.60)-(3.68). The z denotes the direction of the field (x, y, z). p and m mean algebraic plus and minus respectively.

```
1  Program Entmag_Quader_parallel
2  implicit none
3   integer :: nx,ny,nz,n1,n2,n3,np,i,j,INFO
4   integer,allocatable,dimension(:,:) :: IPIV
5   real*8 :: Ha,chi,dx,dy,dz,a,b,c
6   real*8,allocatable,dimension(:) :: solvec,sigmax,sigmay,sigmaz
7   real*8,allocatable,dimension(:,:) :: eqnarray
8
9    Ha=1D0
10   chi=-1D0
11   Write(*,*)"Length parallel to field (c) [mm]"
12   read(*,*)c
13   Write(*,*)"Length perpendicular to field (b) [mm]"
14   read(*,*)b
15   Write(*,*)"Length perpendicular to field (a) [mm]"
16   read(*,*)a
17   Write(*,*)"Magnetic susceptibility"
18   read(*,*)chi
19   Write(*,*)"Number of segments for (c)"
20   read(*,*)nz
21   Write(*,*)"Number of segments for (b)"
22   read(*,*)ny
23   Write(*,*)"Number of segments for (a)"
24   read(*,*)nx
25
26   dx=a/(2D0*nx)
27   dy=b/(2D0*ny)
28   dz=c/(1D0 + 2D0*nz)
29
30   n1=ny*nz
```

```
31  n2=nx*nz
32  n3=nx*ny
33  np=n1+n2+n3
34
35  Allocate(IPIV(1:np,1:np))
36  Allocate(solvec(1:np))
37  Allocate(sigmax(1:n1))
38  Allocate(sigmay(1:n2))
39  Allocate(sigmaz(1:n3))
40  Allocate(eqnarray(1:np,1:np))
41
42  IPIV=0
43  solvec=0D0
44  eqnarray=0D0
45
46  write(*,*)"**********************************************************************"
47  write(*,*)"*  INITALISING SYSTEM:           *"
48  write(*,*)"**********************************************************************"
49  Call Quader(a,b,c,dx,dy,dz,Ha,chi,nx,ny,nz,np,eqnarray,solvec)
50  write(*,*)"**********************************************************************"
51  write(*,*)"*  DGESV OUTPUT:           *"
52  write(*,*)"**********************************************************************"
53  write(*,*)"* INFO =  0, DGESV was successfull         *"
54  write(*,*)"* INFO = -i, the i-th argument had an illegal value         *"
55  write(*,*)"* INFO =  i, U(i,i) is exactly zero. Factorization has been   *"
56  write(*,*)"*     completed, but the factor U is exactly singular   *"
57  write(*,*)"*      so the solution could not be computed.   *"
58  write(*,*)"**********************************************************************"
59  Write(*,*)"SOLVING MATRIX..."
60
61  Call DGESV( np, 1, eqnarray, np, IPIV, solvec, np, INFO )
62  Write(*,*)"INFO = ",INFO
63
64  Do i=1,n1
65    sigmax(i)=solvec(i)
66  End Do
67
68  Do i=n1+1,n1+n2
69    sigmay(i-n1)=solvec(i)
70  End Do
71
72  Do i=n1+n2+1,np
73    sigmaz(i-n1-n2)=solvec(i)
74  End Do
75
76  write(*,*)"**********************************************************************"
77  write(*,*)"*  CALCULATING Nm:           *"
78  write(*,*)"**********************************************************************"
79
80  Call calcNm(sigmax,sigmay,sigmaz,a,b,c,Ha,chi,nx,ny,n1,n2,n3,dx,dy,dz)
81
82  Deallocate(IPIV)
83  Deallocate(solvec)
```

```
84    Deallocate(sigmax)
85    Deallocate(sigmay)
86    Deallocate(sigmaz)
87    Deallocate(eqnarray)
88
89  End Program
90
91  !*****************************************************************************************
92  !*****************************************************************************************
93  !*****************************************************************************************
94
95  SUBROUTINE calcNm(sigmax,sigmay,sigmaz,a,b,c,Ha,chi,nx,ny,n1,n2,n3,dx,dy,dz)
96    implicit none
97    integer ::i,u,v,w,nx,ny,nz,n1,n2,n3,np,perc
98    real*8 :: Ha,chi,a,b,c,ap,bp,cp,xi,yi,zi,Hd,mu,HxzV,HyzV,HzzV,HxzzV,HyzzV
99    real*8 :: sigmax(1:n1),sigmay(1:n2),sigmaz(1:n3),Nmv,Nms,Mag
100   real*8 :: Hxx,Hyx,Hzx,Hxy,Hyy,Hzy,Hxz,Hyz,Hzz,dx,dy,dz,yj,zk,Md,Mvol
101
102     mu=0.0000012566370614D0
103
104     Md=Mvol(sigmax,sigmay,sigmaz,a,b,c,nx,ny,n1,n2,n3,dx,dy,dz)
105     Nms=Ha/Md-1/chi
106
107     Write(*,'(A6,F20.17)')" Md= ",Md
108     Write(*,*)""
109     Write(*,'(A6,F20.17)')" Nms= ",Nms
110 END SUBROUTINE
111
112 !*****************************************************************************************
113
114 real*8 FUNCTION Mmid(sigmax,sigmay,sigmaz,a,b,n1,n2,n3,dx,dy,dz)
115  implicit none
116  integer :: i,n1,n2,n3
117  real*8 :: a,b,dx,dy,dz,summe,mu,sigmax(1:n1),sigmay(1:n2),sigmaz(1:n3)
118
119   mu=0.0000012566370614D0
120   summe=0D0
121
122   Do i=1,n1
123     summe=summe+sigmax(i)*dy*dz
124   End Do
125
126   Do i=1,n2
127     summe=summe+sigmay(i)*dx*dz
128   End Do
129
130   Do i=1,n3
131     summe=summe+sigmaz(i)*dx*dy
132   End Do
133
134  Mmid=1D0/(mu*a*b)*summe
135
136 End FUNCTION
```

```
137
138  real*8 FUNCTION Mvol(sigmax,sigmay,sigmaz,a,b,c,nx,ny,n1,n2,n3,dx,dy,dz)
139   implicit none
140   integer :: i,k,ny,nx,perc,n1,n2,n3,v,w
141   real*8 :: a,b,c,dx,dy,dz,summe1,summe2,summe3,mu,Mmid,zk,xi,yj
142   real*8 :: sigmax(1:n1),sigmay(1:n2),sigmaz(1:n3)
143
144     mu=0.00000125663706l4D0
145     summe1=0D0
146     summe2=0D0
147     summe3=0D0
148     perc=0
149
150     write(*,*)"CALCULATING Mvol:"
151     k=1
152     Do i=1,n1
153       summe1=summe1+zk(k,dz)*sigmax(i)*dy*dz
154
155       If(mod(i,ny)==0)Then
156  k=k+1
157       End if
158
159       perc=perc+1
160       Write(*,'(A,I4,A)',advance="no")"\b\b\b\b\b\b",Int(Real(perc)/(n1+n2+n3)*100)," %"
161     End Do
162
163     k=1
164     Do i=1,n2
165       summe2=summe2+zk(k,dz)*sigmay(i)*dx*dz
166
167       If(mod(i,nx)==0 )Then
168  k=k+1
169       End If
170
171       perc=perc+1
172       Write(*,'(A,I4,A)',advance="no")"\b\b\b\b\b\b",Int(Real(perc)/(n1+n2+n3)*100)," %"
173     End Do
174
175     Do i=1,n3
176       summe3=summe3+c*sigmaz(i)*dx*dy
177
178       perc=perc+1
179       Write(*,'(A,I4,A)',advance="no")"\b\b\b\b\b\b",Int(Real(perc)/(n1+n2+n3)*100)," %"
180     End Do
181
182     write(*,*)""
183     write(*,*)"Mvol FINISHED!"
184
185     Mvol=1D0/(mu*a*b*c)*(summe1+summe2+summe3)
186
187  End FUNCTION
188
189  !*****************************************************************************************
```

```
190
191 SUBROUTINE Quader(a,b,c,dx,dy,dz,Ha,chi,nx,ny,nz,np,eqnarray,solvec)
192   implicit none
193   integer :: i,j,u,v,w,nx,ny,nz,n1,n2,n3,np,up,vp,wp
194   real*8 :: eqnarray(1:np,1:np),solvec(1:np)
195   real*8 :: Ha,chi,mu,a,b,c,ap,bp,cp,xi,yi,zi,dx,dy,dz,yj,zk,xp,yp,zp
196   real*8 :: Nxjkpjpkp,Nxjkpjmkp,Nxjkmjpkp,Nxjkmjmkp,Nxjkpjpkm,Nxjkpjmkm,Nxjkmjpkm,Nxjkmjmkm
197   real*8 :: Nxjkpipkp,Nxjkpimkp,Nxjkmipkp,Nxjkmimkp,Nxjkpipkm,Nxjkpimkm,Nxjkmipkm,Nxjkmimkm
198   real*8 :: Nxjkpipjp,Nxjkpimjp,Nxjkmipjp,Nxjkmimjp,Nxjkpipjm,Nxjkpimjm,Nxjkmipjm,Nxjkmimjm
199   real*8 :: Nyikpjpkp,Nyikpjmkp,Nyikmjpkp,Nyikmjmkp,Nyikpjpkm,Nyikpjmkm,Nyikmjpkm,Nyikmjmkm
200   real*8 :: Nyikpipkp,Nyikpimkp,Nyikmipkp,Nyikmimkp,Nyikpipkm,Nyikpimkm,Nyikmipkm,Nyikmimkm
201   real*8 :: Nyikpipjp,Nyikpimjp,Nyikmipjp,Nyikmimjp,Nyikpipjm,Nyikpimjm,Nyikmipjm,Nyikmimjm
202   real*8 :: Nzijpjpkp,Nzijpjmkp,Nzijmjpkp,Nzijmjmkp,Nzijpjpkm,Nzijpjmkm,Nzijmjpkm,Nzijmjmkm
203   real*8 :: Nzijpipkp,Nzijpimkp,Nzijmipkp,Nzijmimkp,Nzijpipkm,Nzijpimkm,Nzijmipkm,Nzijmimkm
204   real*8 :: Nzijpipjp,Nzijpimjp,Nzijmipjp,Nzijmimjp,Nzijpipjm,Nzijpimjm,Nzijmipjm,Nzijmimjm
205
206   mu=0.0000012566370614D0
207
208   n1=ny*nz
209   n2=nx*nz
210   n3=nx*ny
211
212   Do i=n1+n2+1,np
213     solvec(i)=mu*Ha
214   End Do
215
216   Write(*,*)"SOLUTION VECTOR INITIALISED!"
217   Write(*,*)"INITALISING MATRIX..."
218
219   u=1
220   v=1
221   w=1
222
223   Do i=1,n1
224
225     up=1
226     vp=1
227     wp=1
228
229     Do j=1,n1
230
231          eqnarray(i,j)=(Nxjkpjpkp(yj(v,dy),yp(vp,dy),zk(w,dz),zp(wp,dz),a,dy,dz)&
232       &-Nxjkpjmkp(yj(v,dy),yp(vp,dy),zk(w,dz),zp(wp,dz),a,dy,dz)&
233       &+Nxjkmjpkp(yj(v,dy),yp(vp,dy),zk(w,dz),zp(wp,dz),a,dy,dz)&
234       &-Nxjkmjmkp(yj(v,dy),yp(vp,dy),zk(w,dz),zp(wp,dz),a,dy,dz)&
235       &+Nxjkpjpkm(yj(v,dy),yp(vp,dy),zk(w,dz),zp(wp,dz),a,dy,dz)&
236       &-Nxjkpjmkm(yj(v,dy),yp(vp,dy),zk(w,dz),zp(wp,dz),a,dy,dz)&
237       &+Nxjkmjpkm(yj(v,dy),yp(vp,dy),zk(w,dz),zp(wp,dz),a,dy,dz)&
238       &-Nxjkmjmkm(yj(v,dy),yp(vp,dy),zk(w,dz),zp(wp,dz),a,dy,dz))
239
240           If(i==j)Then
241     eqnarray(i,j)=eqnarray(i,j)+1D0/chi
242           End If
```

```
243
244             vp=vp+1
245
246    If(vp==ny+1)Then
247      vp=1
248      wp=wp+1
249    End if
250      End Do
251
252      up=1
253      vp=1
254      wp=1
255
256      Do j=n1+1,n1+n2
257
258   eqnarray(i,j)=(Nxjkpipkp(xp(up,dx),zk(w,dz),zp(wp,dz),yj(v,dy),a,b,dx,dz)&
259        &-Nxjkpimkp(xp(up,dx),zk(w,dz),zp(wp,dz),yj(v,dy),a,b,dx,dz)&
260        &+Nxjkmipkp(xp(up,dx),zk(w,dz),zp(wp,dz),yj(v,dy),a,b,dx,dz)&
261        &-Nxjkmimkp(xp(up,dx),zk(w,dz),zp(wp,dz),yj(v,dy),a,b,dx,dz)&
262        &+Nxjkpipkm(xp(up,dx),zk(w,dz),zp(wp,dz),yj(v,dy),a,b,dx,dz)&
263        &-Nxjkpimkm(xp(up,dx),zk(w,dz),zp(wp,dz),yj(v,dy),a,b,dx,dz)&
264        &+Nxjkmipkm(xp(up,dx),zk(w,dz),zp(wp,dz),yj(v,dy),a,b,dx,dz)&
265        &-Nxjkmimkm(xp(up,dx),zk(w,dz),zp(wp,dz),yj(v,dy),a,b,dx,dz))
266
267             up=up+1
268
269    If(up==nx+1)Then
270      up=1
271      wp=wp+1
272    End if
273      End Do
274
275      up=1
276      vp=1
277      wp=1
278
279      Do j=n1+n2+1,np
280
281           eqnarray(i,j)=(Nxjkpipjp(xp(up,dx),yj(v,dy),yp(vp,dy),zk(w,dz),a,c,dx,dy)&
282        &+Nxjkpimjp(xp(up,dx),yj(v,dy),yp(vp,dy),zk(w,dz),a,c,dx,dy)&
283        &+Nxjkmipjp(xp(up,dx),yj(v,dy),yp(vp,dy),zk(w,dz),a,c,dx,dy)&
284        &+Nxjkmimjp(xp(up,dx),yj(v,dy),yp(vp,dy),zk(w,dz),a,c,dx,dy)&
285        &-Nxjkpipjm(xp(up,dx),yj(v,dy),yp(vp,dy),zk(w,dz),a,c,dx,dy)&
286        &-Nxjkpimjm(xp(up,dx),yj(v,dy),yp(vp,dy),zk(w,dz),a,c,dx,dy)&
287        &-Nxjkmipjm(xp(up,dx),yj(v,dy),yp(vp,dy),zk(w,dz),a,c,dx,dy)&
288        &-Nxjkmimjm(xp(up,dx),yj(v,dy),yp(vp,dy),zk(w,dz),a,c,dx,dy))
289
290             up=up+1
291
292    If(up==nx+1)Then
293      up=1
294      vp=vp+1
295    End if
```

```
296     End Do
297
298     v=v+1
299
300     If(v==ny+1)Then
301       v=1
302       w=w+1
303     End if
304
305     Write(*,'(A,I4,A2)',advance="no")"\b\b\b\b\b\b",Int(Real(i)/np*100)," %"
306   End Do
307
308   u=1
309   v=1
310   w=1
311
312   Do i=n1+1,n1+n2
313
314     up=1
315     vp=1
316     wp=1
317
318     Do j=1,n1
319
320          eqnarray(i,j)=(Nyikpjpkp(yp(vp,dy),zk(w,dz),zp(wp,dz),xi(u,dx),a,b,dy,dz)&
321       &-Nyikpjmkp(yp(vp,dy),zk(w,dz),zp(wp,dz),xi(u,dx),a,b,dy,dz)&
322       &+Nyikmjpkp(yp(vp,dy),zk(w,dz),zp(wp,dz),xi(u,dx),a,b,dy,dz)&
323       &-Nyikmjmkp(yp(vp,dy),zk(w,dz),zp(wp,dz),xi(u,dx),a,b,dy,dz)&
324       &+Nyikpjpkm(yp(vp,dy),zk(w,dz),zp(wp,dz),xi(u,dx),a,b,dy,dz)&
325       &-Nyikpjmkm(yp(vp,dy),zk(w,dz),zp(wp,dz),xi(u,dx),a,b,dy,dz)&
326       &+Nyikmjpkm(yp(vp,dy),zk(w,dz),zp(wp,dz),xi(u,dx),a,b,dy,dz)&
327       &-Nyikmjmkm(yp(vp,dy),zk(w,dz),zp(wp,dz),xi(u,dx),a,b,dy,dz))
328
329 vp=vp+1
330
331 If(vp==ny+1)Then
332   vp=1
333   wp=wp+1
334 End if
335     End Do
336
337     up=1
338     vp=1
339     wp=1
340
341     Do j=n1+1,n1+n2
342
343          eqnarray(i,j)=(Nyikpipkp(xi(u,dx),xp(up,dx),zk(w,dz),zp(wp,dz),b,dx,dz)&
344       &-Nyikpimkp(xi(u,dx),xp(up,dx),zk(w,dz),zp(wp,dz),b,dx,dz)&
345       &+Nyikmipkp(xi(u,dx),xp(up,dx),zk(w,dz),zp(wp,dz),b,dx,dz)&
346       &-Nyikmimkp(xi(u,dx),xp(up,dx),zk(w,dz),zp(wp,dz),b,dx,dz)&
347       &+Nyikpipkm(xi(u,dx),xp(up,dx),zk(w,dz),zp(wp,dz),b,dx,dz)&
348       &-Nyikpimkm(xi(u,dx),xp(up,dx),zk(w,dz),zp(wp,dz),b,dx,dz)&
```

```
349       &+Nyikmipkm(xi(u,dx),xp(up,dx),zk(w,dz),zp(wp,dz),b,dx,dz)&
350       &-Nyikmimkm(xi(u,dx),xp(up,dx),zk(w,dz),zp(wp,dz),b,dx,dz))
351
352           If(i==j)Then
353     eqnarray(i,j)=eqnarray(i,j)+1D0/chi
354           End If
355
356   up=up+1
357
358   If(up==nx+1)Then
359     up=1
360     wp=wp+1
361   End if
362     End Do
363
364     up=1
365     vp=1
366     wp=1
367
368     Do j=n1+n2+1,np
369
370         eqnarray(i,j)=(Nyikpipjp(yp(vp,dy),xi(u,dx),xp(up,dx),zk(w,dz),b,c,dx,dy)&
371       &+Nyikpimjp(yp(vp,dy),xi(u,dx),xp(up,dx),zk(w,dz),b,c,dx,dy)&
372       &+Nyikmipjp(yp(vp,dy),xi(u,dx),xp(up,dx),zk(w,dz),b,c,dx,dy)&
373       &+Nyikmimjp(yp(vp,dy),xi(u,dx),xp(up,dx),zk(w,dz),b,c,dx,dy)&
374       &-Nyikpipjm(yp(vp,dy),xi(u,dx),xp(up,dx),zk(w,dz),b,c,dx,dy)&
375       &-Nyikpimjm(yp(vp,dy),xi(u,dx),xp(up,dx),zk(w,dz),b,c,dx,dy)&
376       &-Nyikmipjm(yp(vp,dy),xi(u,dx),xp(up,dx),zk(w,dz),b,c,dx,dy)&
377       &-Nyikmimjm(yp(vp,dy),xi(u,dx),xp(up,dx),zk(w,dz),b,c,dx,dy))
378
379 up=up+1
380
381 If(up==nx+1)Then
382   up=1
383   vp=vp+1
384 End if
385     End Do
386
387     u=u+1
388
389     If(u==nx+1)Then
390       u=1
391       w=w+1
392     End if
393
394     Write(*,'(A,I4,A2)',advance="no") "\b\b\b\b\b\b",Int(Real(i)/np*100)," %"
395   End Do
396
397   u=1
398   v=1
399   w=1
400
401   Do i=n1+n2+1,np
```

```
402
403       up=1
404       vp=1
405       wp=1
406
407       Do j=1,n1
408
409            eqnarray(i,j)=(Nzijpjpkp(zp(wp,dz),yj(v,dy),yp(vp,dy),xi(u,dx),a,c,dy,dz)&
410         &-Nzijpjmkp(zp(wp,dz),yj(v,dy),yp(vp,dy),xi(u,dx),a,c,dy,dz)&
411         &+Nzijmjpkp(zp(wp,dz),yj(v,dy),yp(vp,dy),xi(u,dx),a,c,dy,dz)&
412         &-Nzijmjmkp(zp(wp,dz),yj(v,dy),yp(vp,dy),xi(u,dx),a,c,dy,dz)&
413         &+Nzijpjpkm(zp(wp,dz),yj(v,dy),yp(vp,dy),xi(u,dx),a,c,dy,dz)&
414         &-Nzijpjmkm(zp(wp,dz),yj(v,dy),yp(vp,dy),xi(u,dx),a,c,dy,dz)&
415         &+Nzijmjpkm(zp(wp,dz),yj(v,dy),yp(vp,dy),xi(u,dx),a,c,dy,dz)&
416         &-Nzijmjmkm(zp(wp,dz),yj(v,dy),yp(vp,dy),xi(u,dx),a,c,dy,dz))
417
418    vp=vp+1
419
420    If(vp==ny+1)Then
421      vp=1
422      wp=wp+1
423    End if
424      End Do
425
426       up=1
427       vp=1
428       wp=1
429
430       Do j=n1+1,n1+n2
431
432            eqnarray(i,j)=(Nzijpipkp(zp(wp,dz),xi(u,dx),xp(up,dx),yj(v,dy),b,c,dx,dz)&
433         &-Nzijpimkp(zp(wp,dz),xi(u,dx),xp(up,dx),yj(v,dy),b,c,dx,dz)&
434         &+Nzijmipkp(zp(wp,dz),xi(u,dx),xp(up,dx),yj(v,dy),b,c,dx,dz)&
435         &-Nzijmimkp(zp(wp,dz),xi(u,dx),xp(up,dx),yj(v,dy),b,c,dx,dz)&
436         &+Nzijpipkm(zp(wp,dz),xi(u,dx),xp(up,dx),yj(v,dy),b,c,dx,dz)&
437         &-Nzijpimkm(zp(wp,dz),xi(u,dx),xp(up,dx),yj(v,dy),b,c,dx,dz)&
438         &+Nzijmipkm(zp(wp,dz),xi(u,dx),xp(up,dx),yj(v,dy),b,c,dx,dz)&
439         &-Nzijmimkm(zp(wp,dz),xi(u,dx),xp(up,dx),yj(v,dy),b,c,dx,dz))
440
441  up=up+1
442
443  If(up==nx+1)Then
444    up=1
445    wp=wp+1
446  End if
447       End Do
448
449       up=1
450       vp=1
451       wp=1
452
453       Do j=n1+n2+1,np
454
```

```
455           eqnarray(i,j)=(Nzijpipjp(xi(u,dx),xp(up,dx),yj(v,dy),yp(vp,dy),c,dx,dy)&
456         &+Nzijpimjp(xi(u,dx),xp(up,dx),yj(v,dy),yp(vp,dy),c,dx,dy)&
457         &+Nzijmipjp(xi(u,dx),xp(up,dx),yj(v,dy),yp(vp,dy),c,dx,dy)&
458         &+Nzijmimjp(xi(u,dx),xp(up,dx),yj(v,dy),yp(vp,dy),c,dx,dy)&
459         &-Nzijpipjm(xi(u,dx),xp(up,dx),yj(v,dy),yp(vp,dy),c,dx,dy)&
460         &-Nzijpimjm(xi(u,dx),xp(up,dx),yj(v,dy),yp(vp,dy),c,dx,dy)&
461         &-Nzijmipjm(xi(u,dx),xp(up,dx),yj(v,dy),yp(vp,dy),c,dx,dy)&
462         &-Nzijmimjm(xi(u,dx),xp(up,dx),yj(v,dy),yp(vp,dy),c,dx,dy))
463
464             If(i==j)Then
465       eqnarray(i,j)=eqnarray(i,j)+1D0/chi
466      End If
467
468           up=up+1
469
470   If(up==nx+1)Then
471     up=1
472     vp=vp+1
473   End if
474       End Do
475
476       u=u+1
477
478       If(u==nx+1)Then
479         u=1
480         v=v+1
481       End if
482
483       Write(*,'(A,I4,A2)',advance="no")"\b\b\b\b\b\b",Int(Real(i)/np*100)," %"
484     End Do
485       Write(*,*)""
486       Write(*,*)"MATRIX INITIALISED!"
487   END SUBROUTINE
488
489   !*****************************************************************************************
490
491   real*8 FUNCTION xi(i,dx)
492     implicit none
493     real*8 :: dx
494     integer :: i,nx
495       xi=(2D0*i-1D0)*dx
496   End FUNCTION xi
497
498   real*8 FUNCTION yj(j,dy)
499     implicit none
500     real*8 :: dy
501     integer :: j,ny
502       yj=(2D0*j-1D0)*dy
503   End FUNCTION yj
504
505   real*8 FUNCTION zk(k,dz)
506     implicit none
507     real*8 :: dz
```

```
508   integer :: k,nz
509     zk=2D0*dz*k
510 End FUNCTION zk
511 
512 real*8 FUNCTION xp(i,dx)
513   implicit none
514   real*8 :: dx
515   integer :: i,nix
516     xp=(2D0*i-1D0)*dx
517 End FUNCTION xp
518 
519 real*8 FUNCTION yp(j,dy)
520   implicit none
521   real*8 :: dy
522   integer :: j,niy
523     yp=(2D0*j-1D0)*dy
524 End FUNCTION yp
525 
526 real*8 FUNCTION zp(k,dz)
527   implicit none
528   real*8 :: dz
529   integer :: k,niz
530     zp=2D0*dz*k
531 End FUNCTION zp
532 
533 !*****************************************************************************************
534 !**********************************   END   ********************************************
535 !*****************************************************************************************
```

B. Hysteresis curves

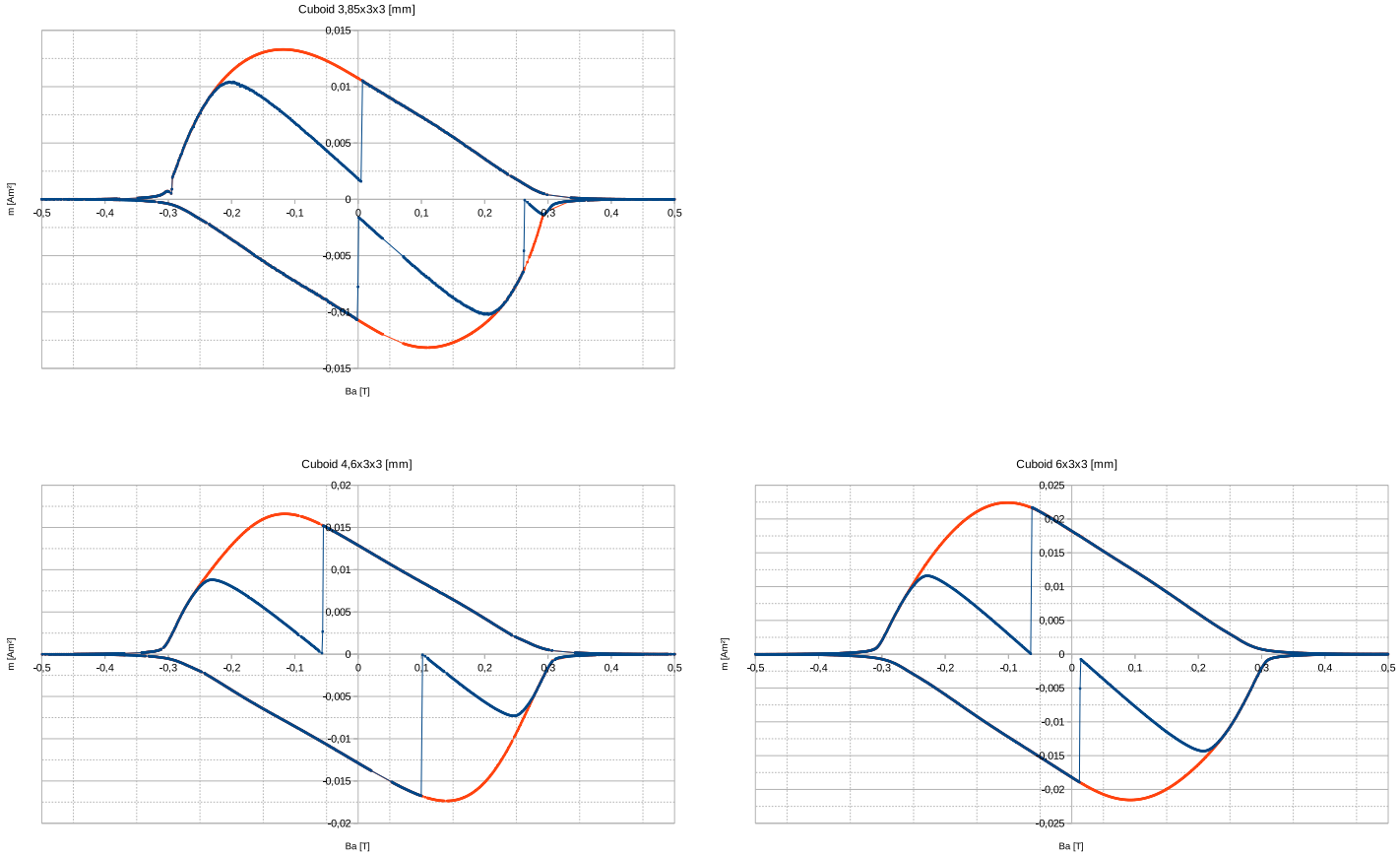

Figure B.1.: Hysteresis curves of cuboids with different geometries with their longest side perpendicular to the magnetic field. The first digit of every label indicates the length of the dimension perpendicular to the field.

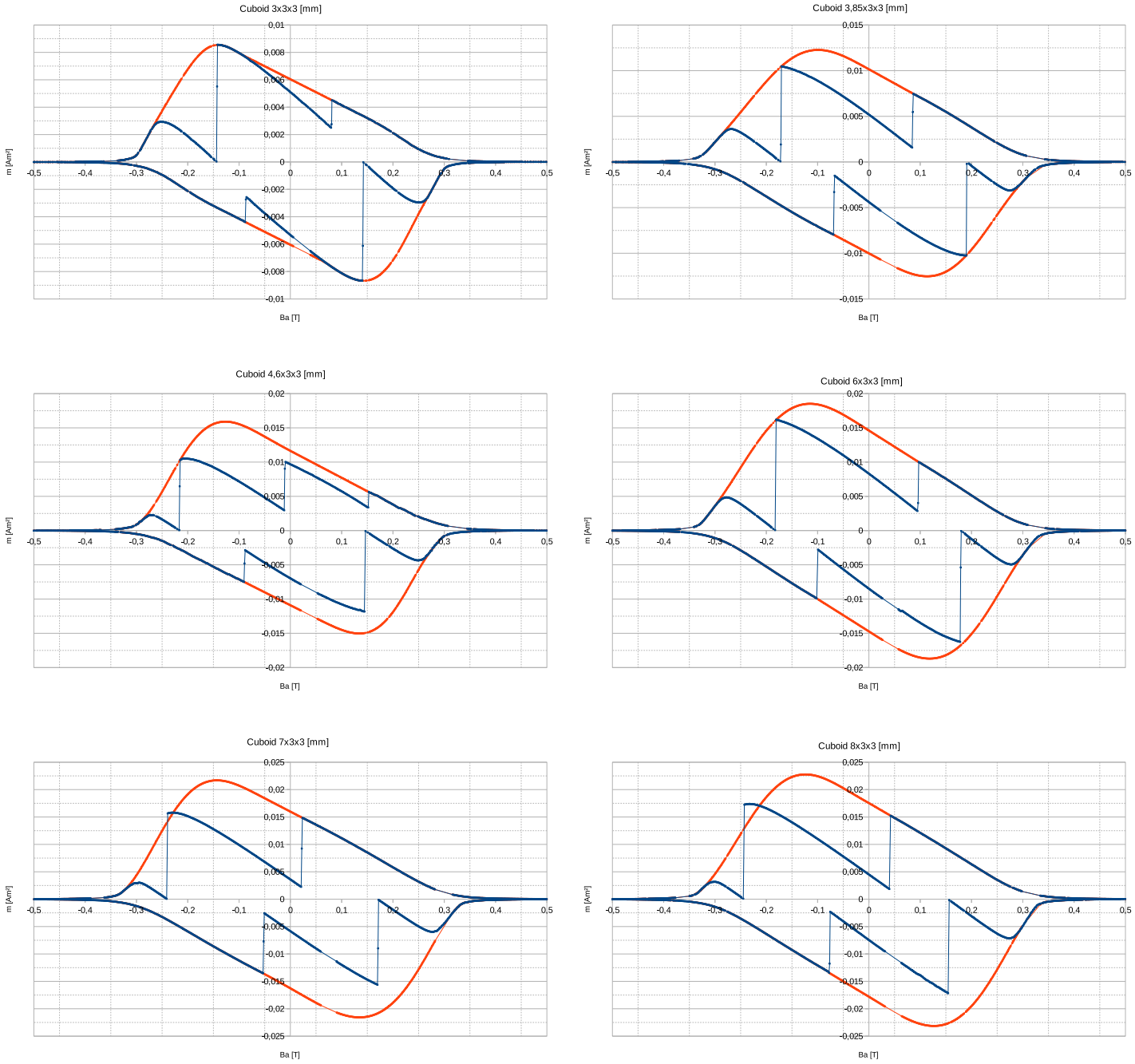

Figure B.2.: Hysteresis curves of cuboids with different geometries with their longest side parallel to the magnetic field. The first digit of every label indicates the length of the dimension parallel to the field.

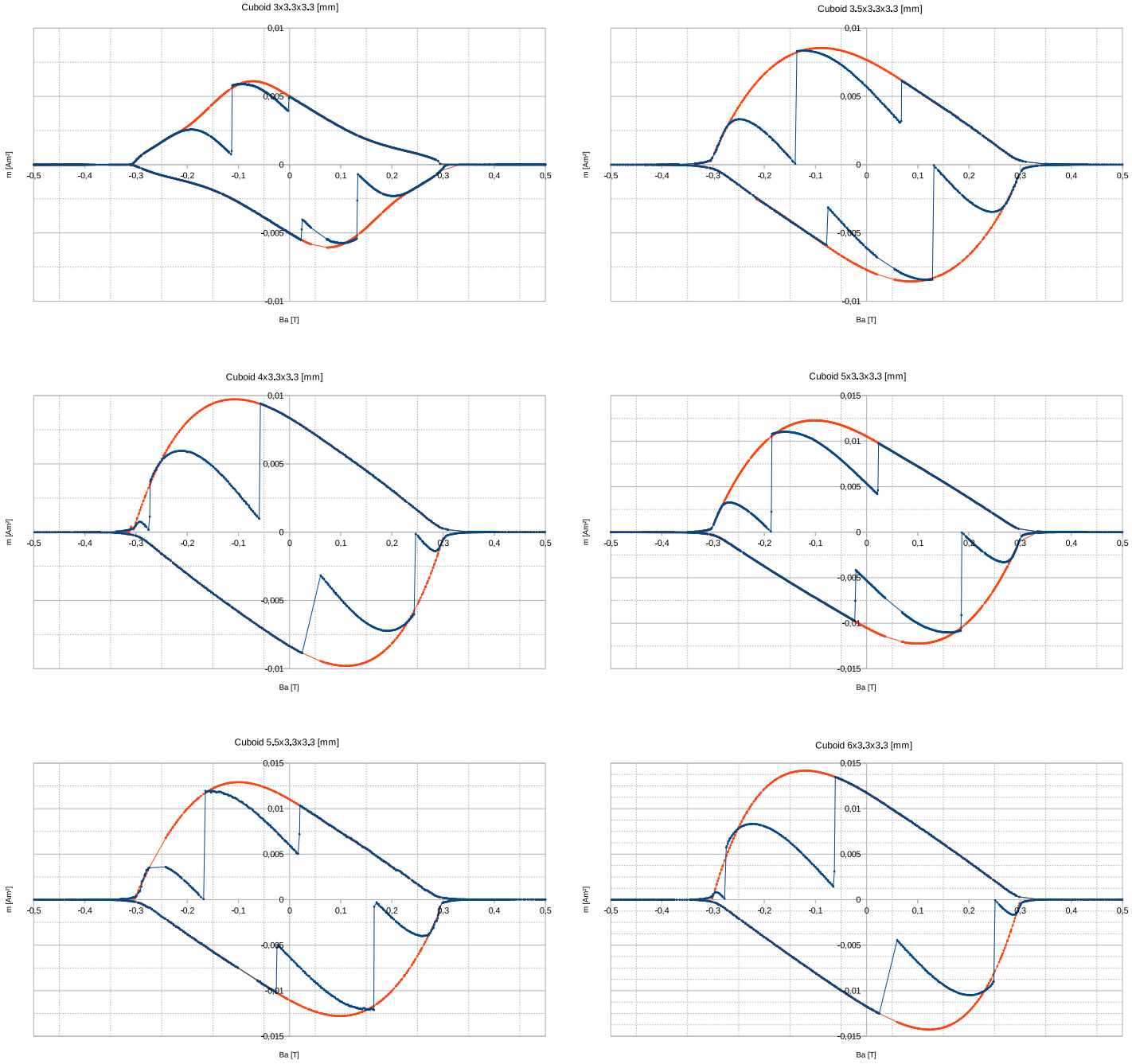

Figure B.3.: Hysteresis curves of degased cuboids with different geometries with their longest side parallel to the magnetic field. The first digit of every label indicates the length of the dimension parallel to the field.

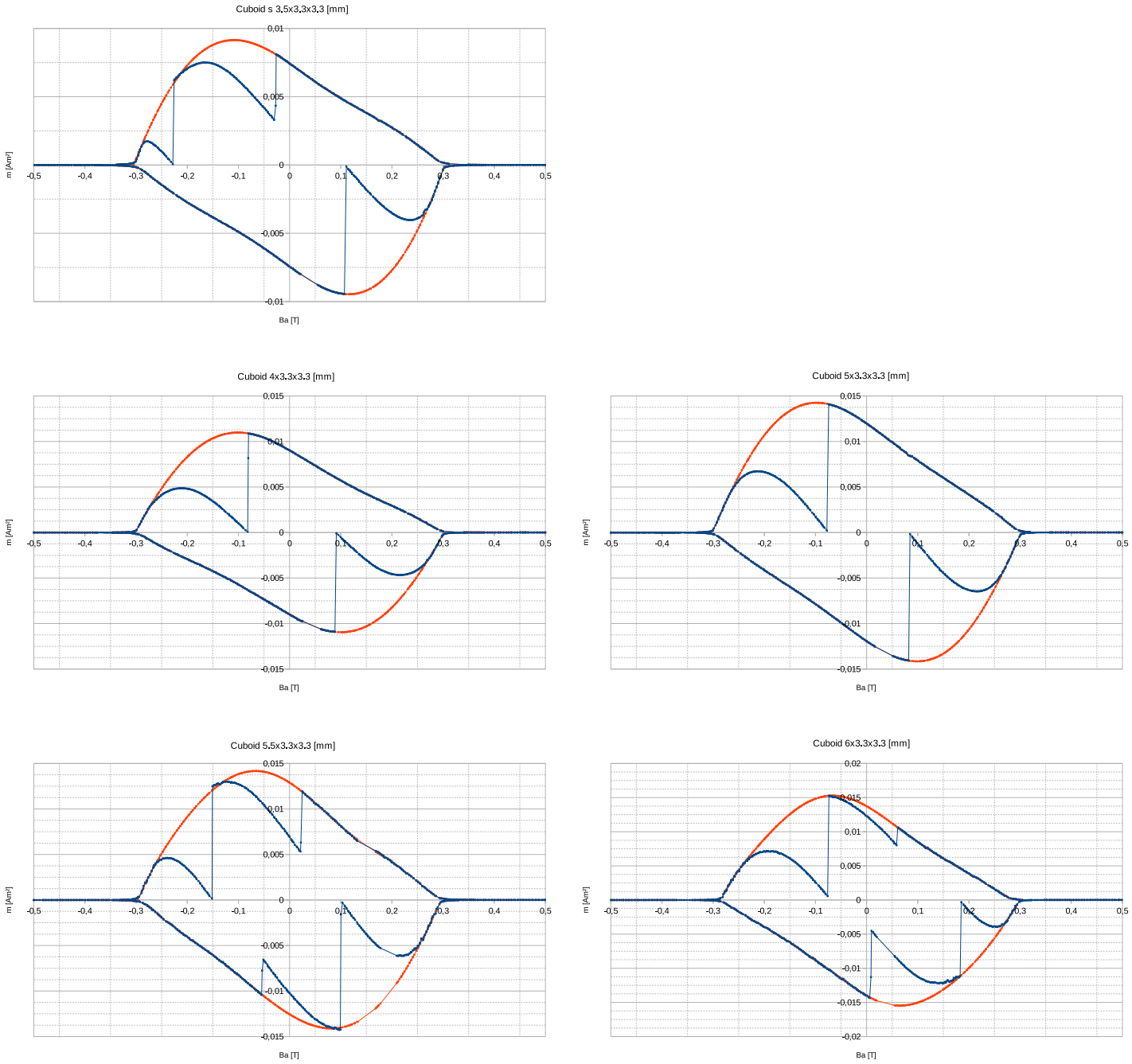

Figure B.4.: Hysteresis curves of degased cuboids with different geometries with their longest side perpendicular to the magnetic field. The first digit of every label indicates the length of the dimension perpendicular to the field.

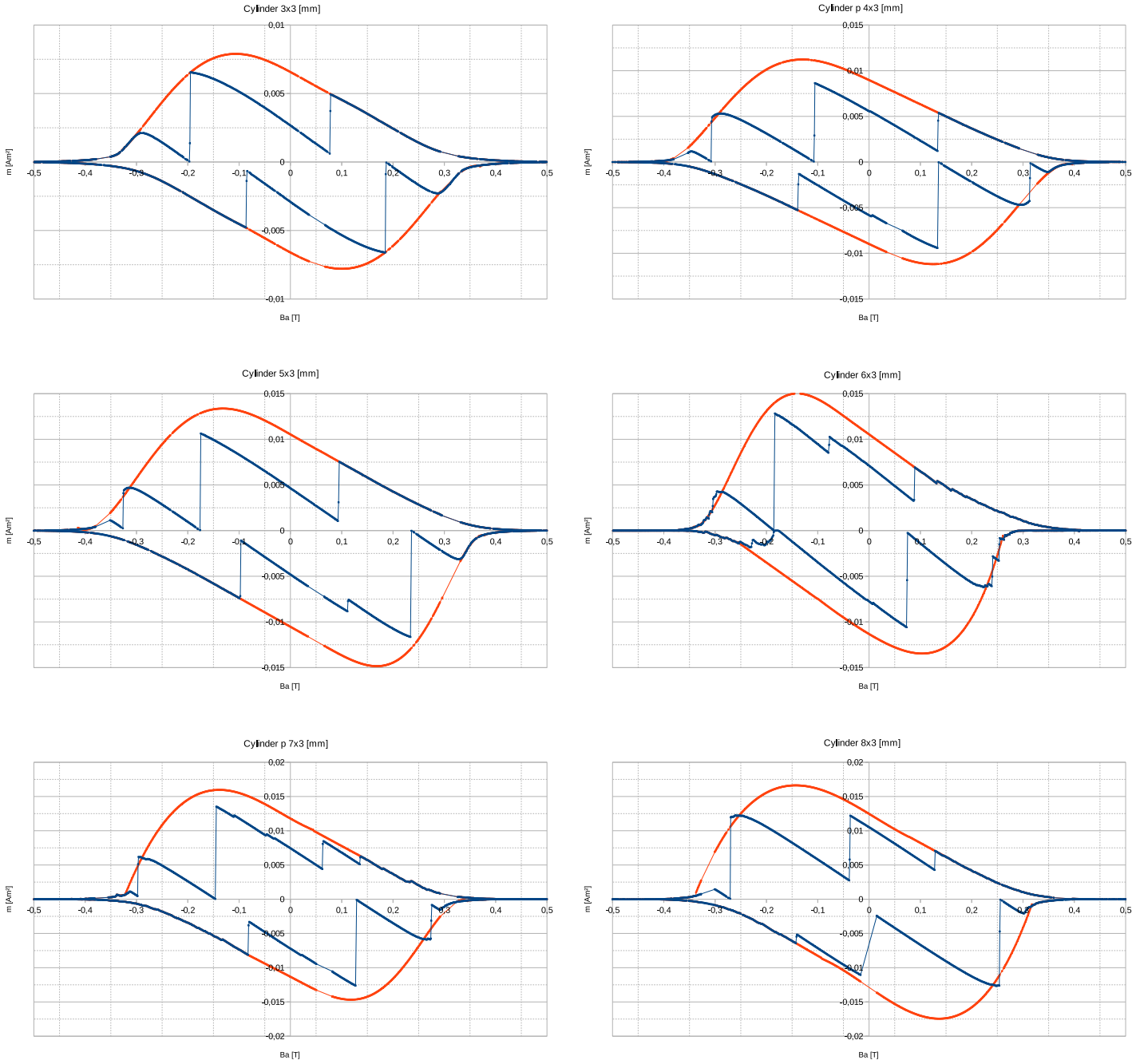

Figure B.5.: Hysteresis curves of cylinders with different geometries with their main axes parallel to the magnetic field, plotted against applied field. The first digit of every label indicates the length of the dimension parallel to the main axis.

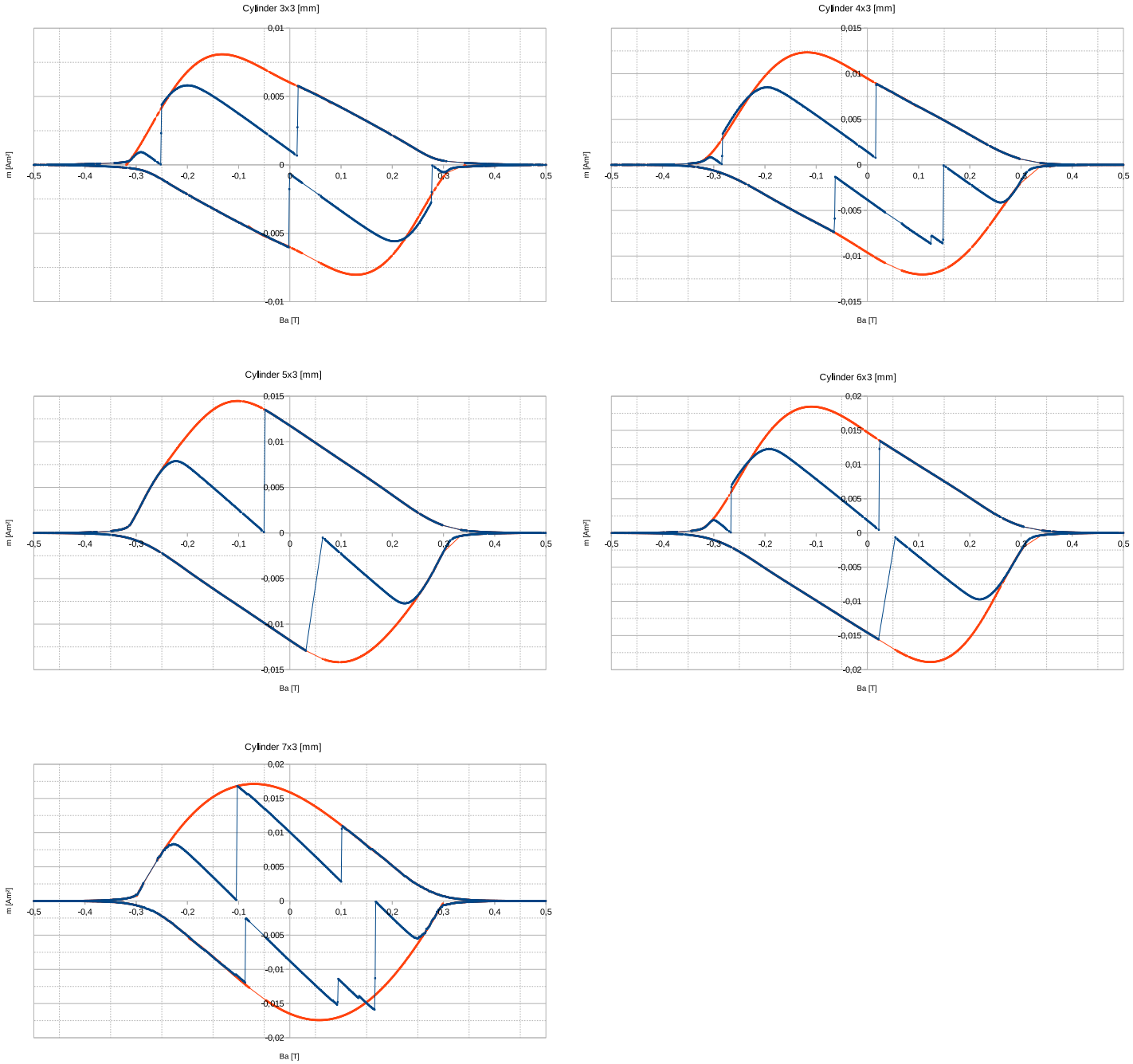

Figure B.6.: Hysteresis curves of cylinders with different geometries with their main axes perpendicular to the magnetic field, plotted against applied field. The first digit of every label indicates the length of the dimension parallel to the main axis.

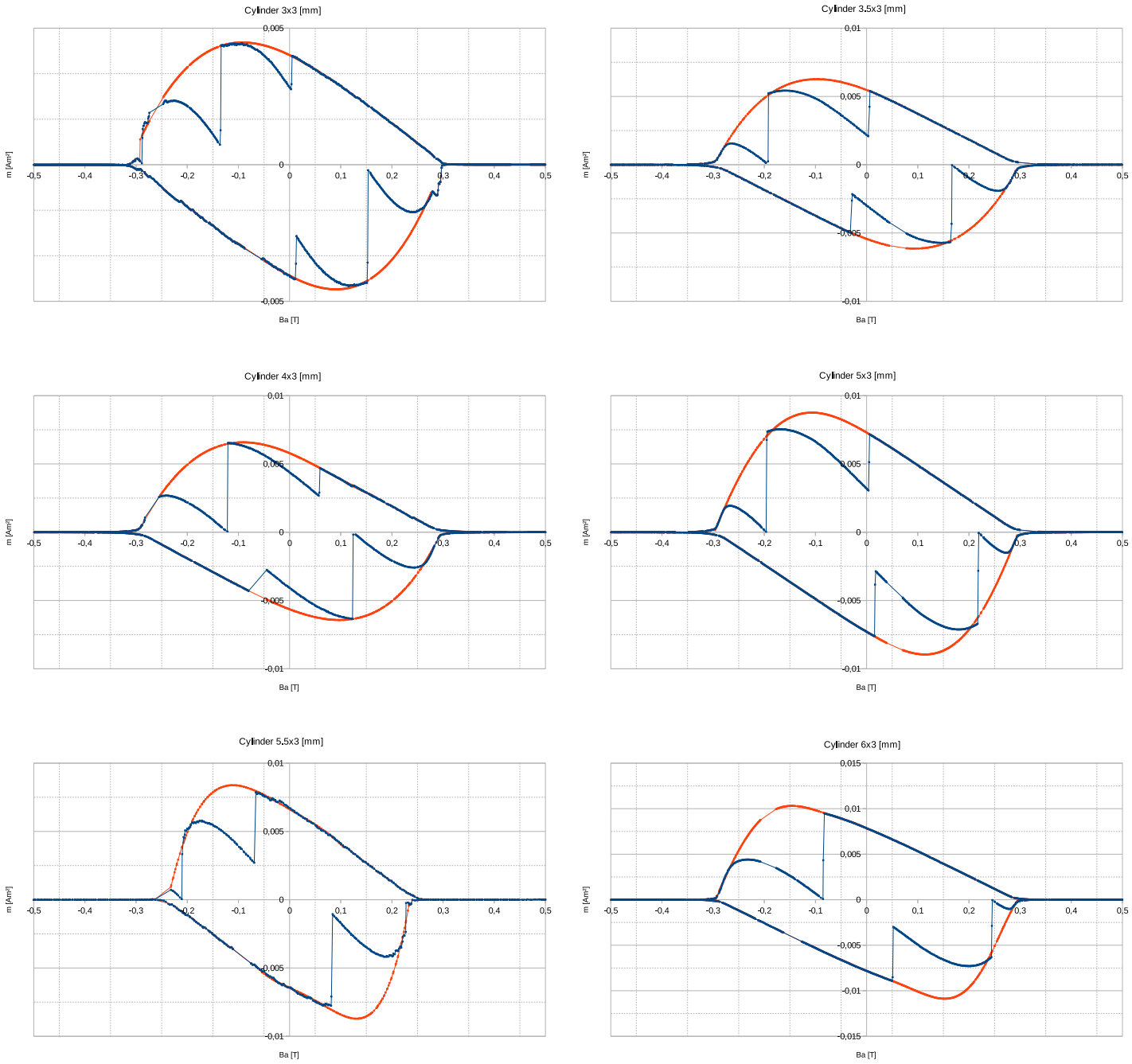

Figure B.7.: Hysteresis curves of degased cylinders with different geometries with their main axes parallel to the magnetic field, plotted against applied field. The first digit of every label indicates the length of the dimension parallel to the main axis.

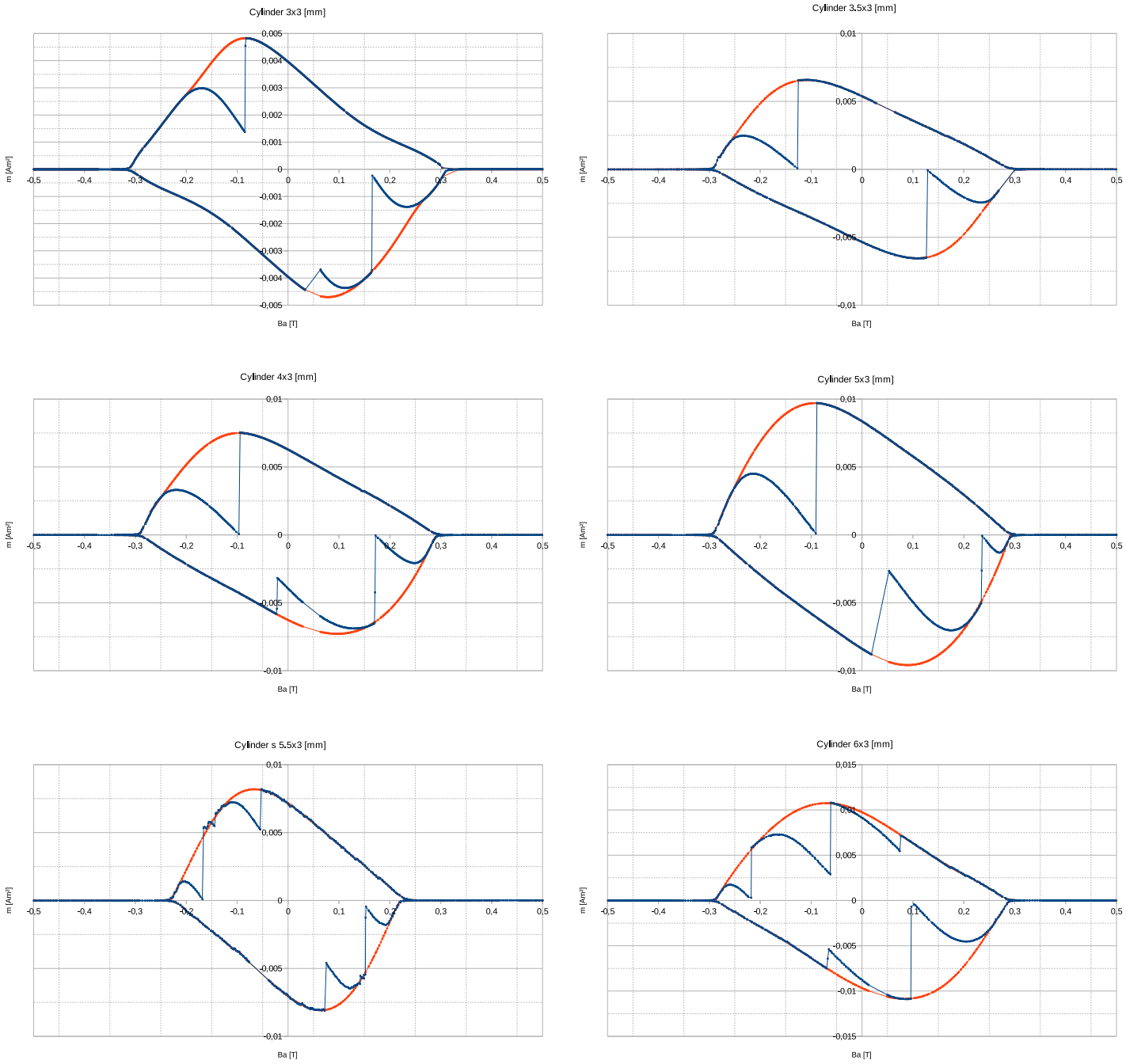

Figure B.8.: Hysteresis curves of degased cylinders with different geometries with their main axes perpendicular to the magnetic field, plotted against applied field. The first digit of every label indicates the length of the dimension parallel to the main axis.

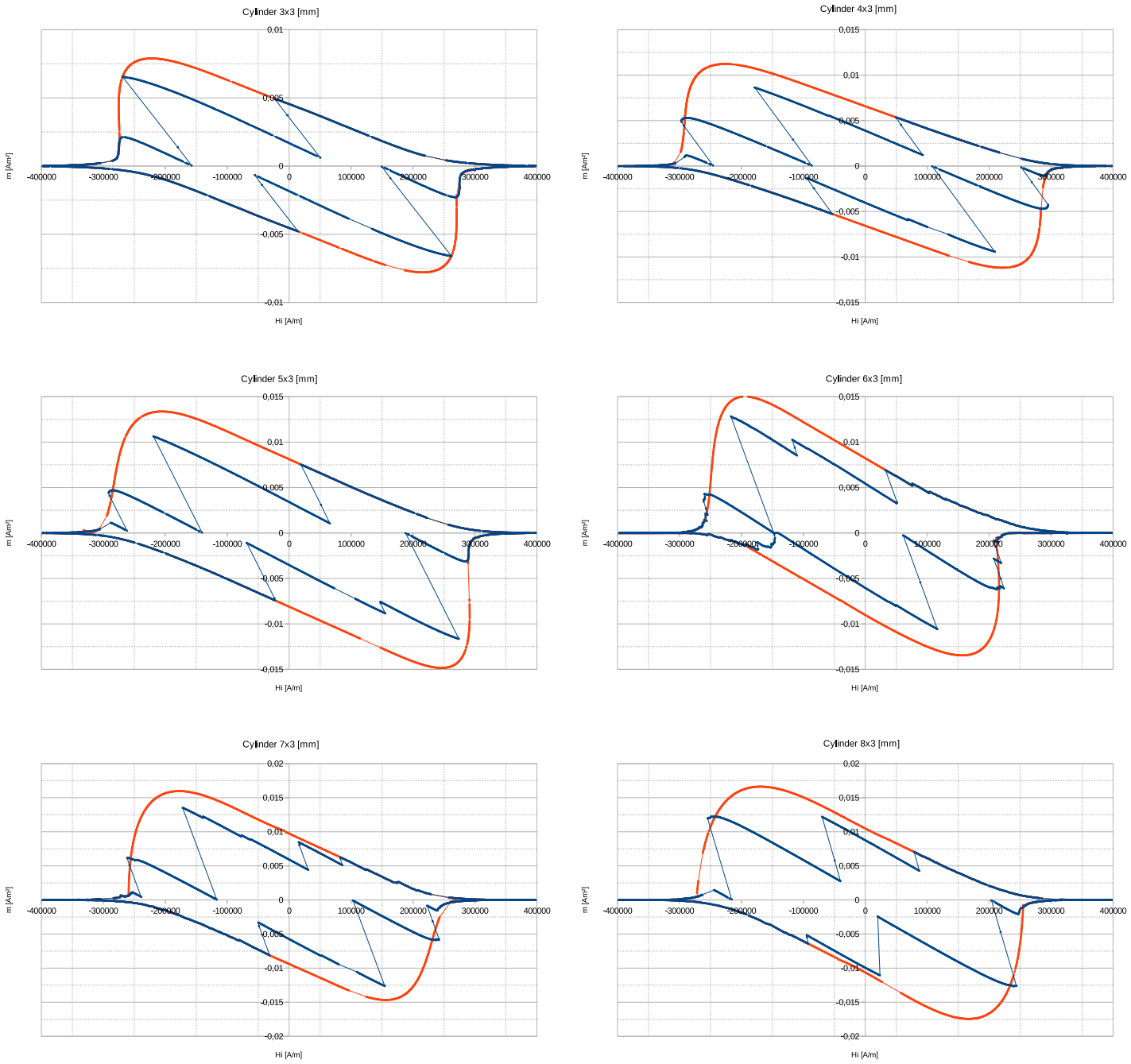

Figure B.9.: Hysteresis curves of cylinders with different geometries with their main axes parallel to the magnetic field, plotted against internal field. The first digit of every label indicates the length of the dimension parallel to the main axis.

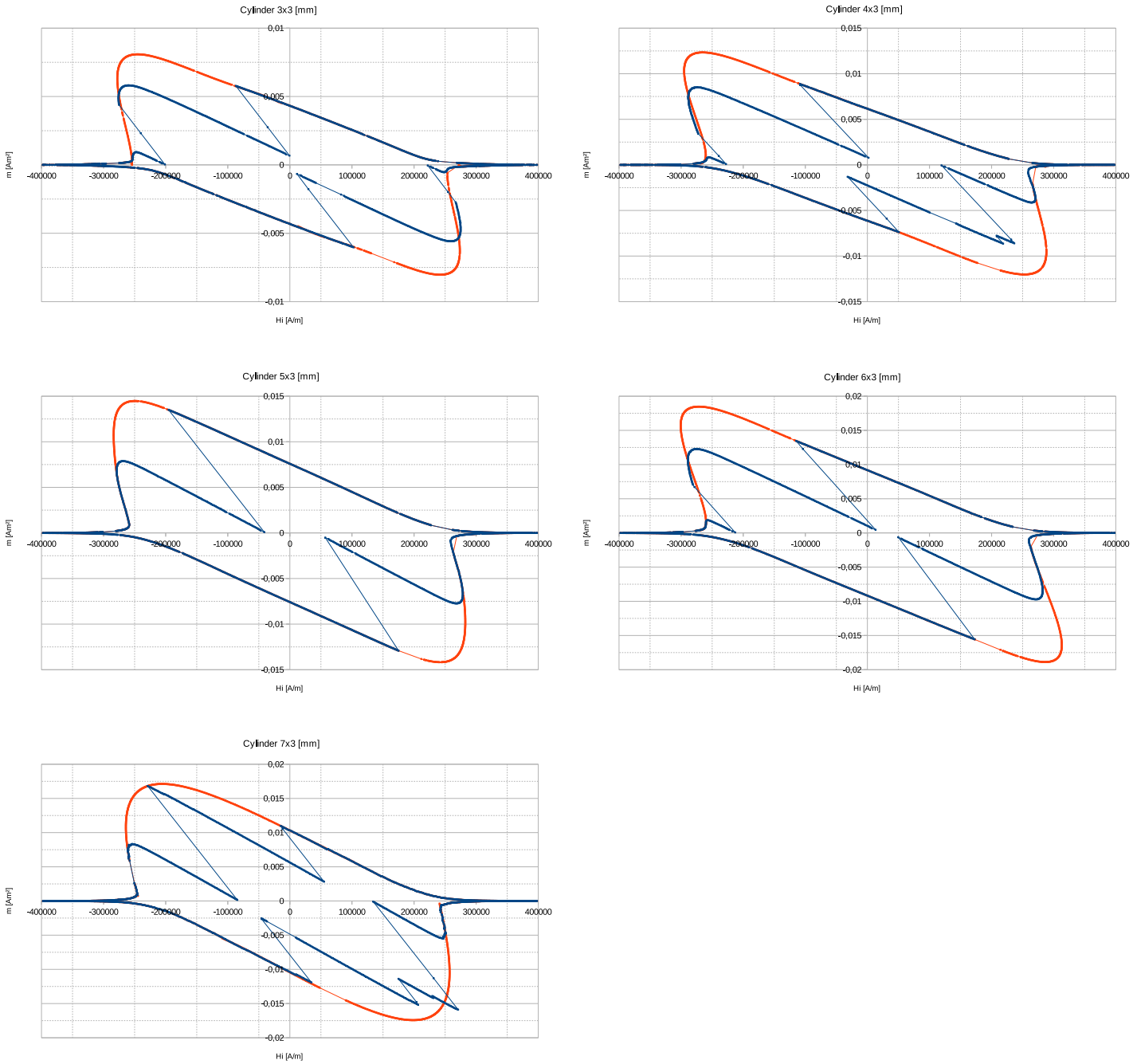

Figure B.10.: Hysteresis curves of cylinders with different geometries with their main axes perpendicular to the magnetic field, plotted against internal field. The first digit of every label indicates the length of the dimension parallel to the main axis.

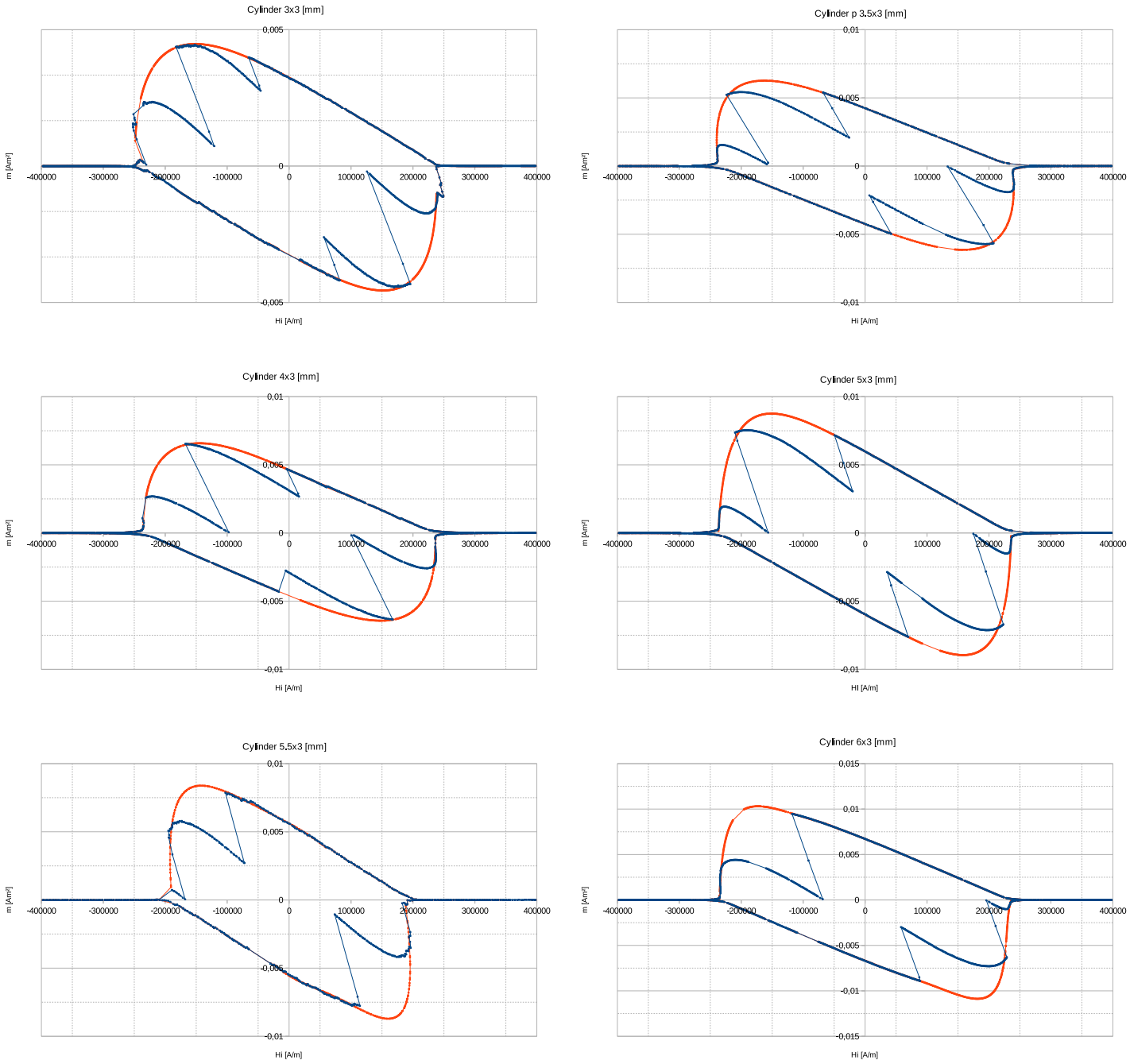

Figure B.11.: Hysteresis curves of degased cylinders with different geometries with their main axes parallel to the magnetic field, plotted against internal field. The first digit of every label indicates the length of the dimension parallel to the main axis.

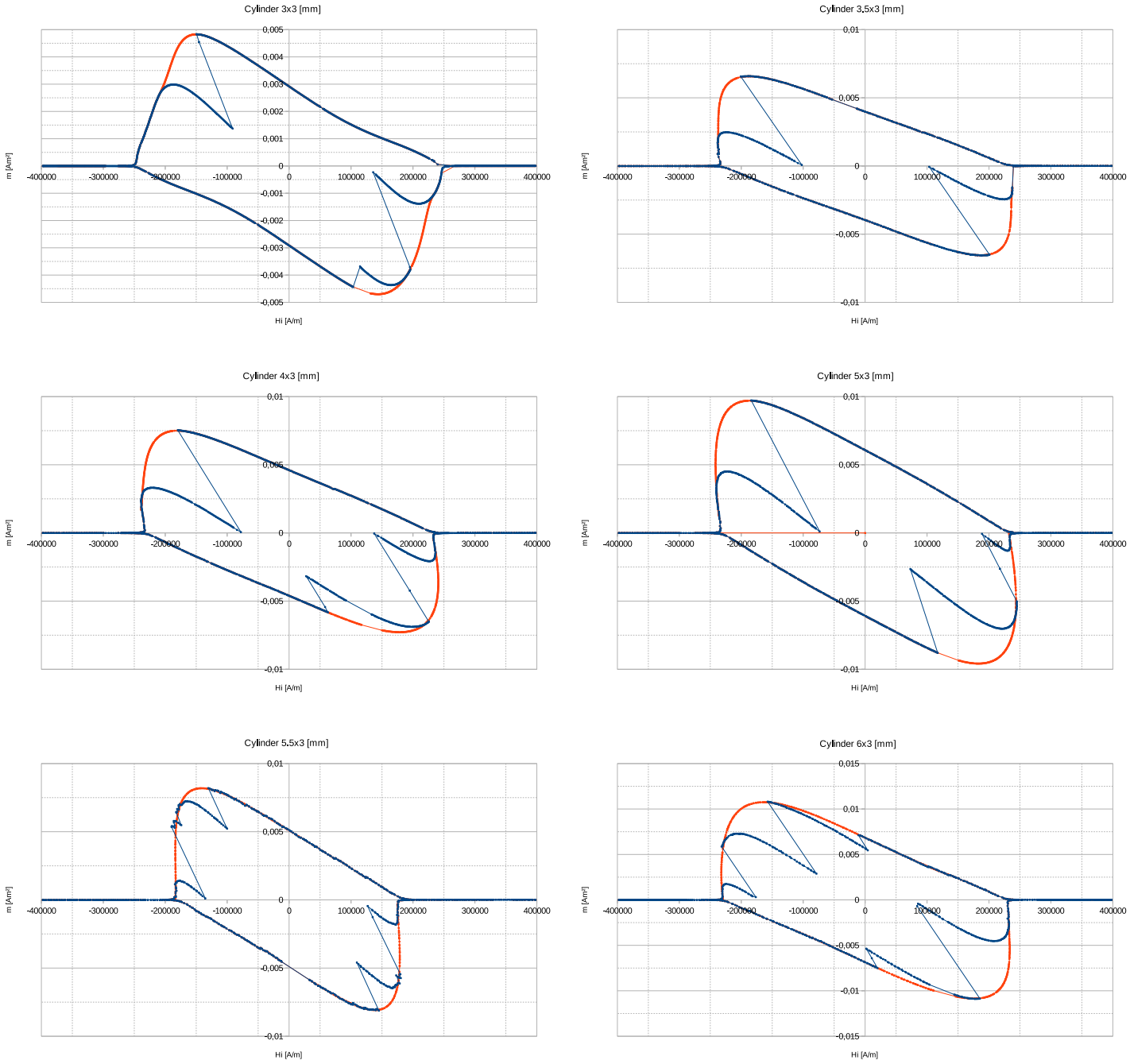

Figure B.12.: Hysteresis curves of degased cylinders with different geometries with their main axes perpendicular to the magnetic field, plotted against internal field. The first digit of every label indicates the length of the dimension parallel to the main axis.

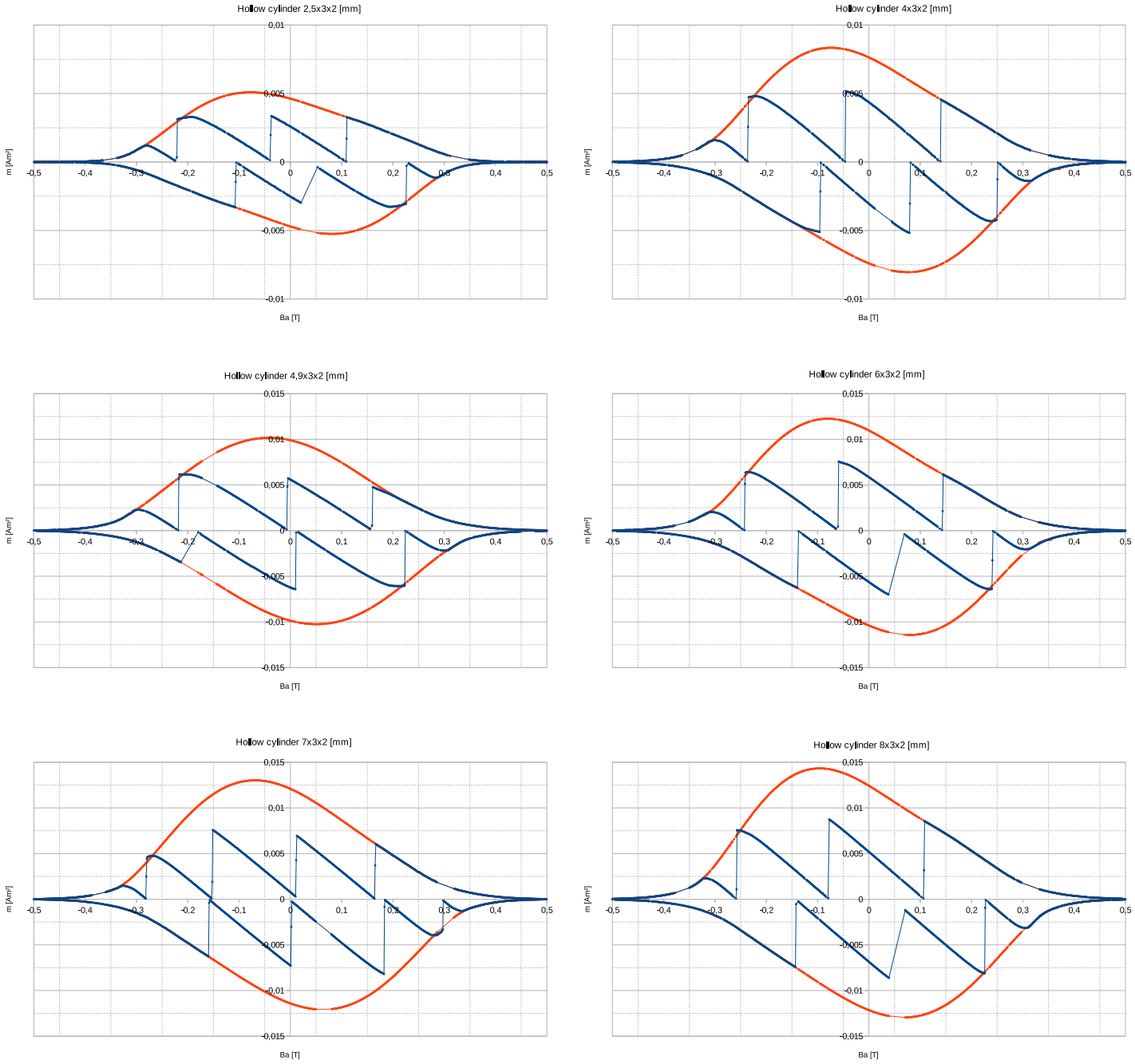

Figure B.13.: Hysteresis curves of hollow cylinders with different geometries with their main axes parallel to the magnetic field, plotted against applied field. The first digit of every label indicates the length of the dimension parallel to the main axis.

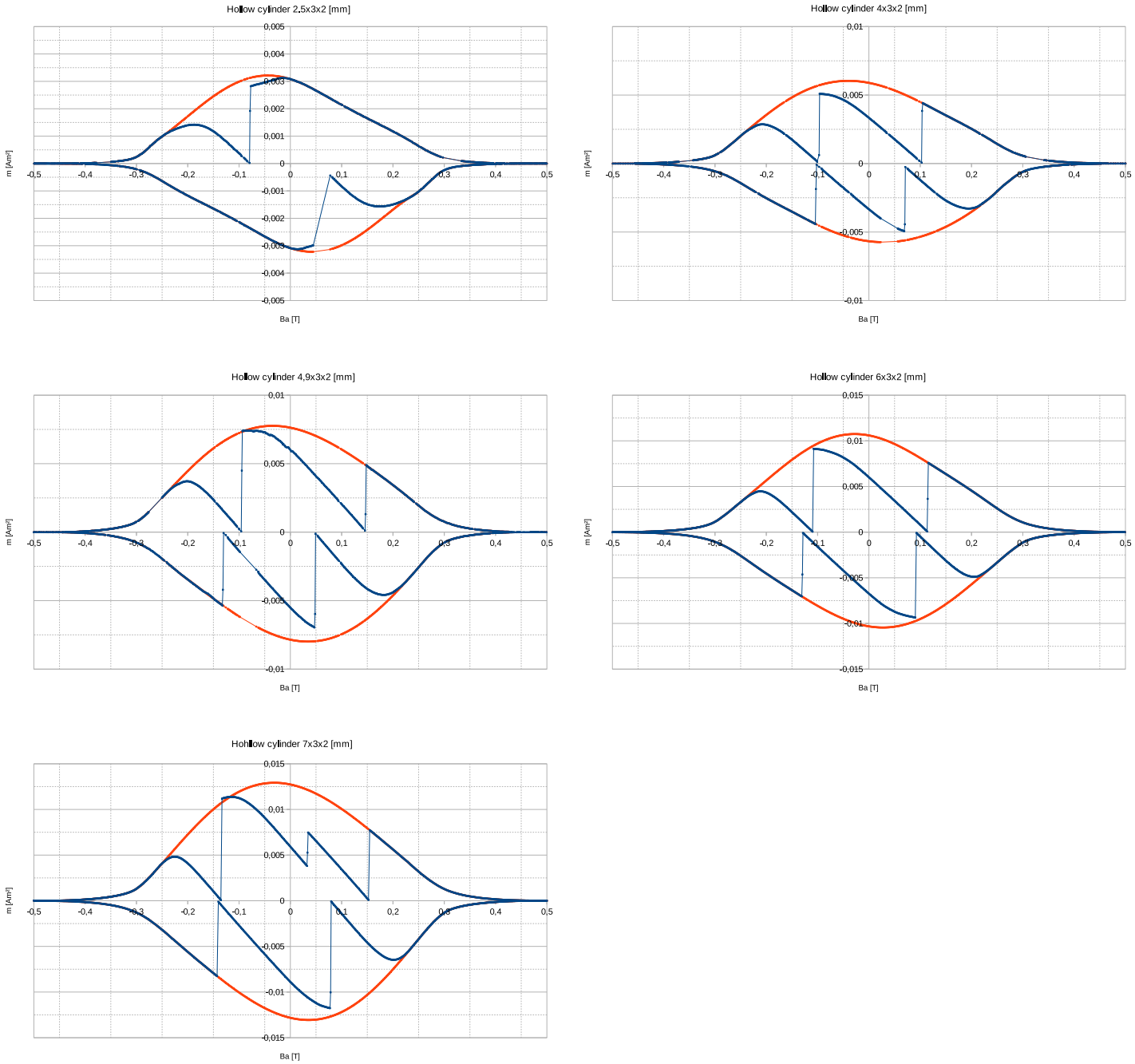

Figure B.14.: Hysteresis curves of hollow cylinders with different geometries with their main axes perpendicular to the magnetic field, plotted against applied field. The first digit of every label indicates the length of the dimension parallel to the main axis.

C. Virgin magnetic moment curves

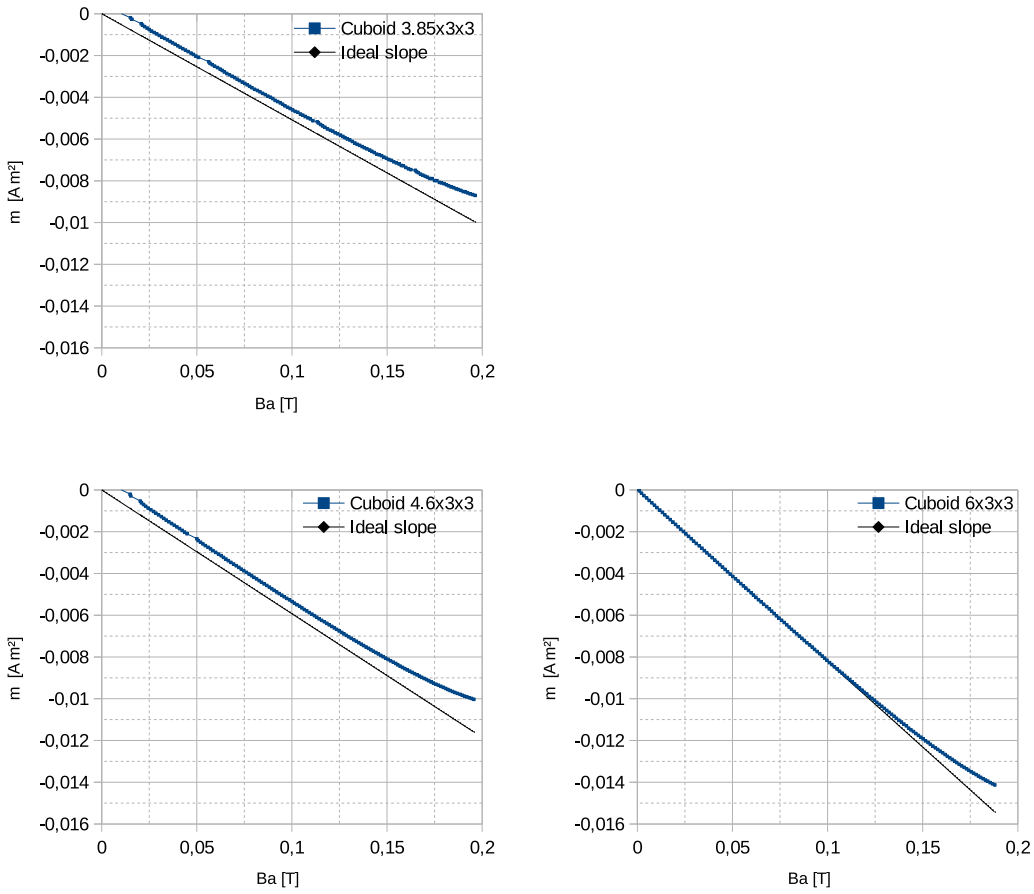

Figure C.1.: Virgin curves of the magnetic moment of cuboids with their longest side perpendicular to the magnetic field. The first digit of every label indicates the length of the dimension perpendicular to the field.

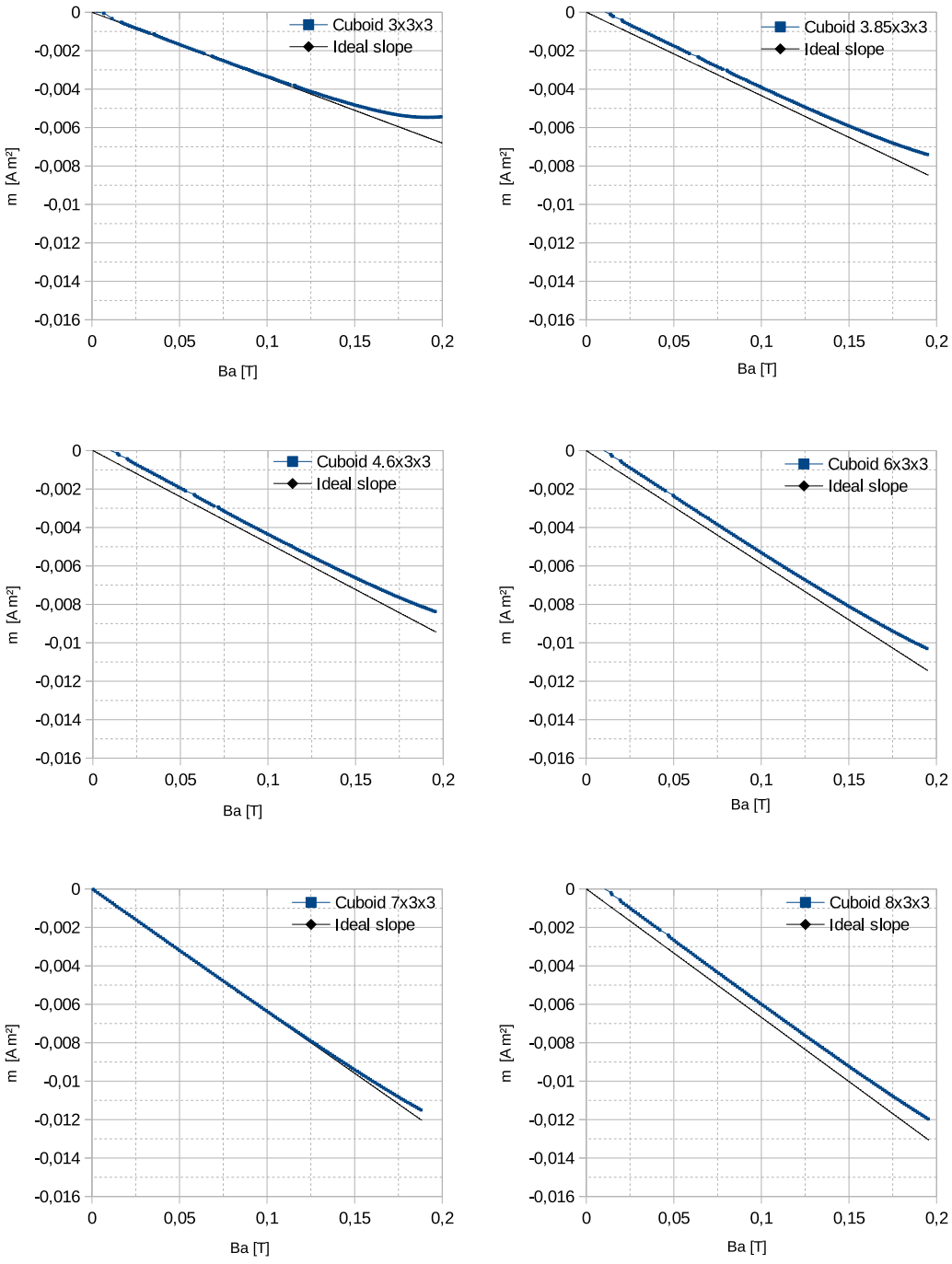

Figure C.2.: Virgin curves of the magnetic moment of cuboids with their longest side parallel to the magnetic field. The first digit of every label indicates the length of the dimension parallel to the field.

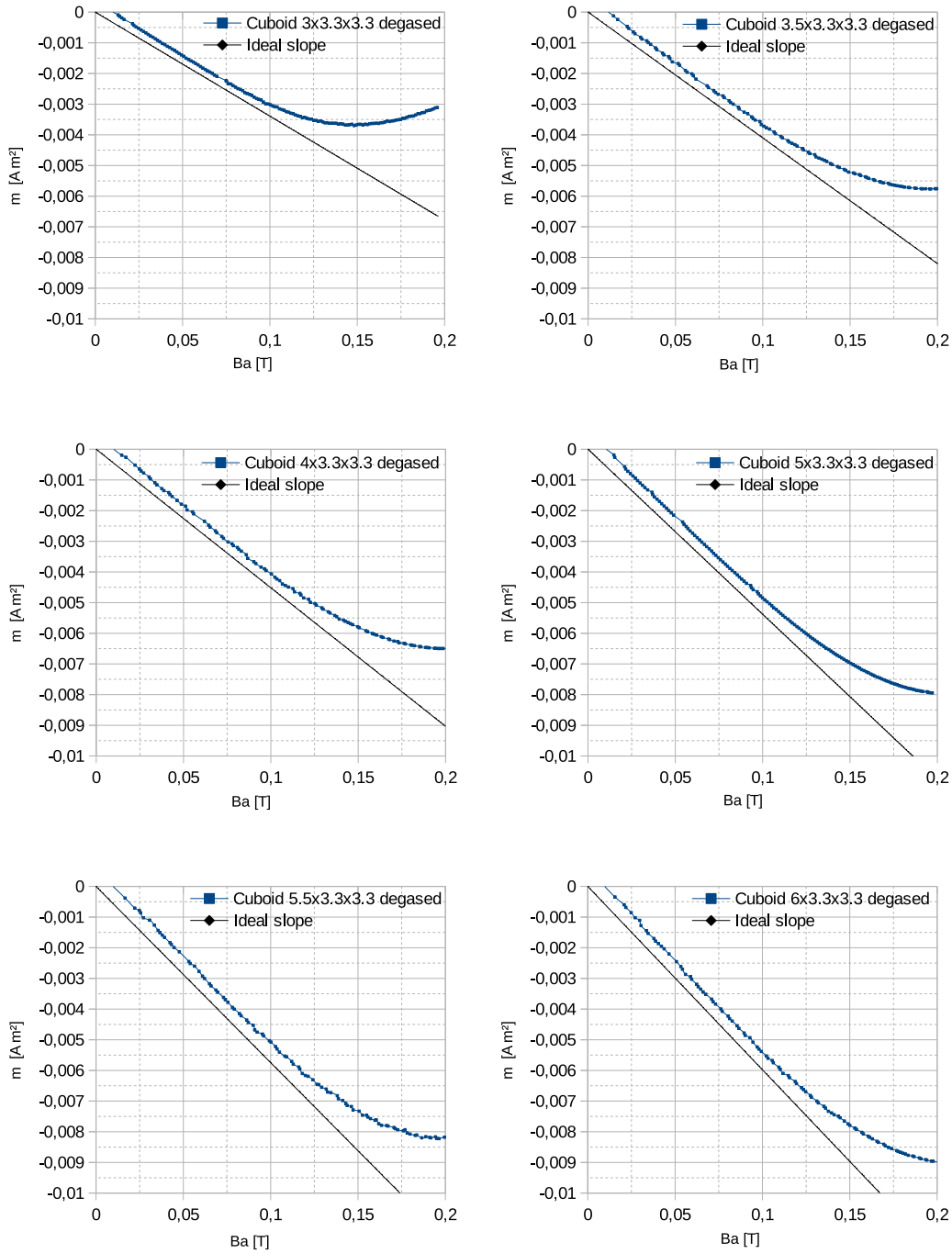

Figure C.3.: Virgin curves of the magnetic moment of degased cuboids with their longest side parallel to the magnetic field. The first digit of every label indicates the length of the dimension parallel to the field.

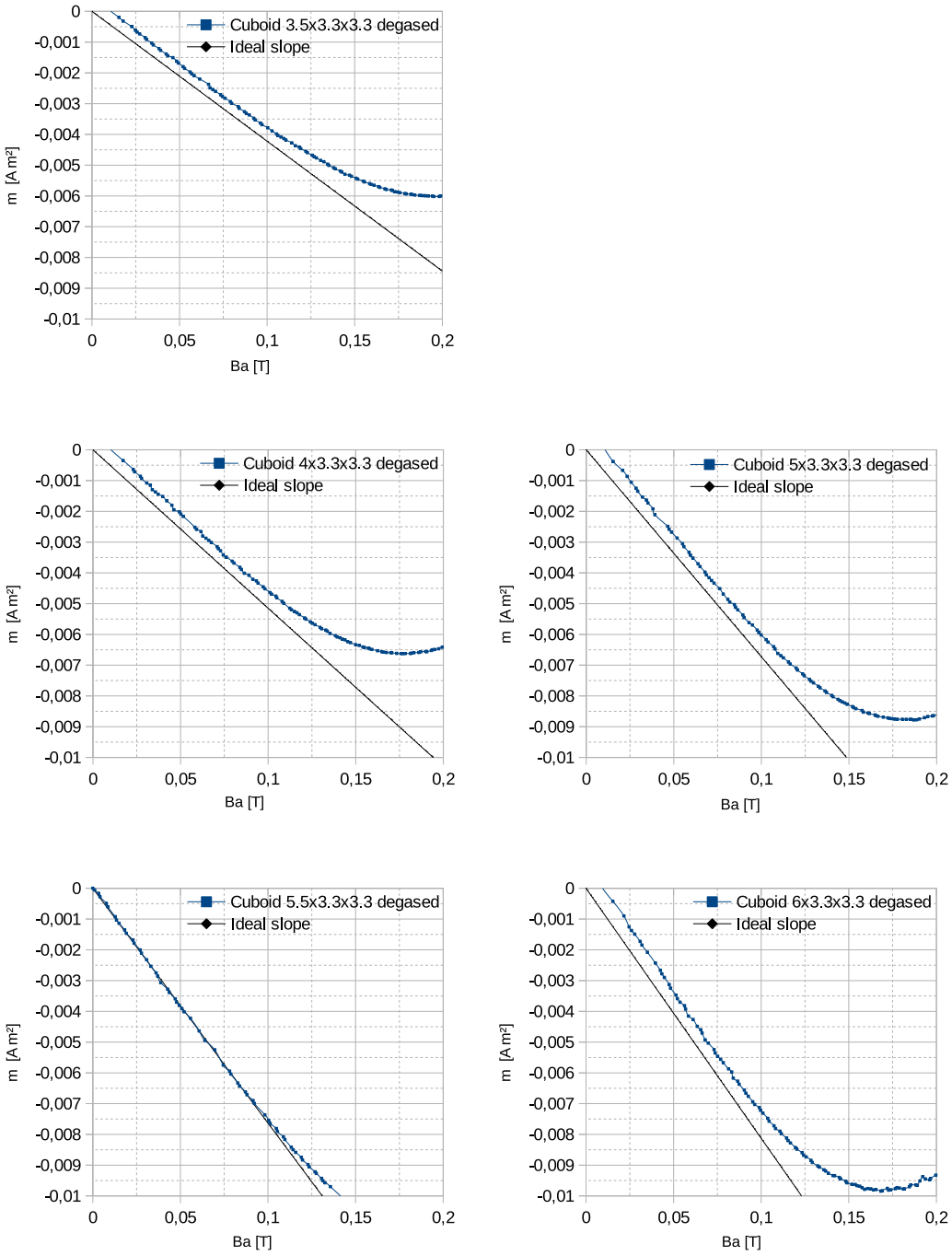

Figure C.4.: Virgin curves of the magnetic moment of degased cuboids perpendicular to the magnetic field. The first digit of every label indicates the length of the dimension perpendicular to the field.

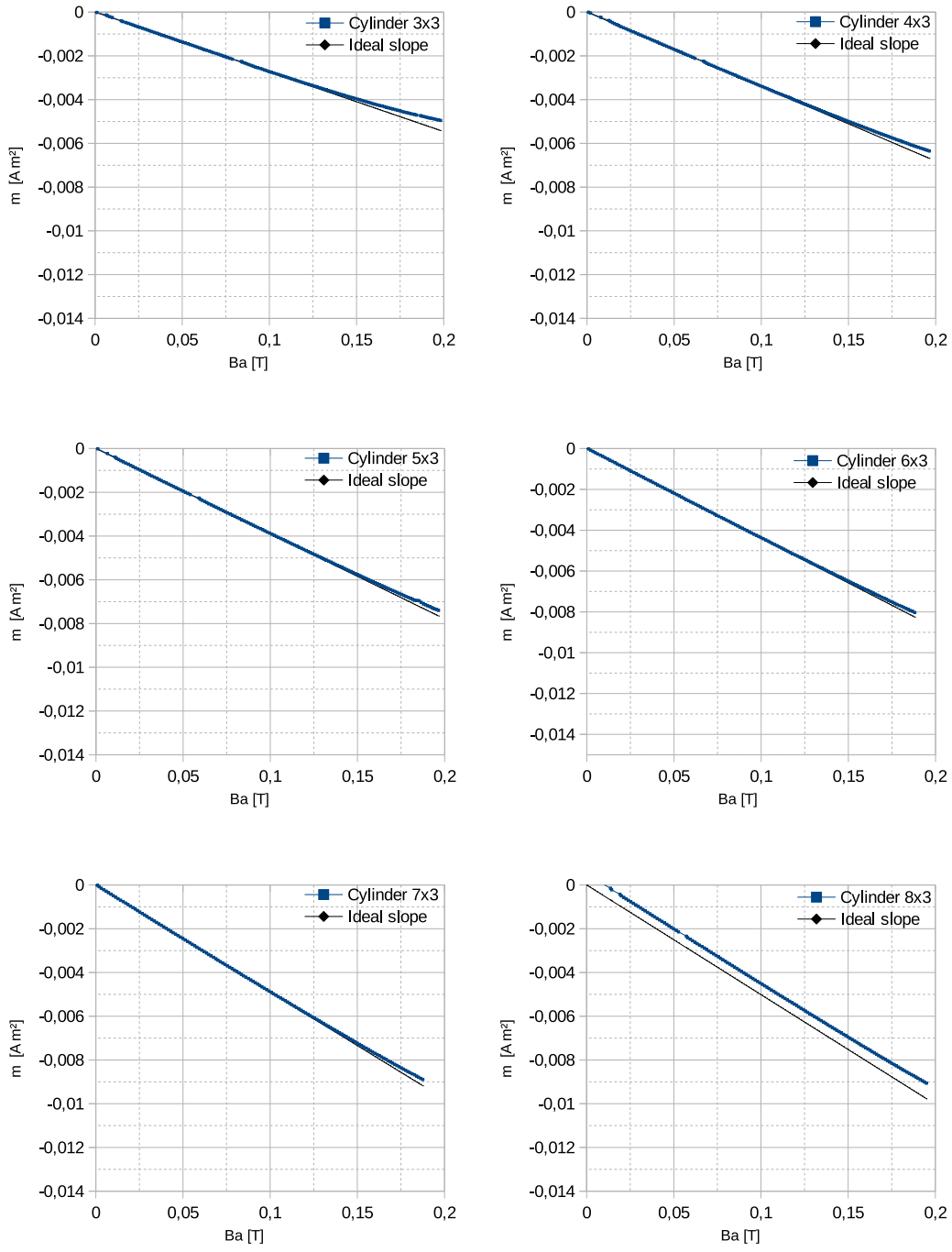

Figure C.5.: Virgin curves of the magnetic moment of cylinders with their main axes parallel to the magnetic field. The first digit of every label indicates the length of the dimension parallel to the main axis.

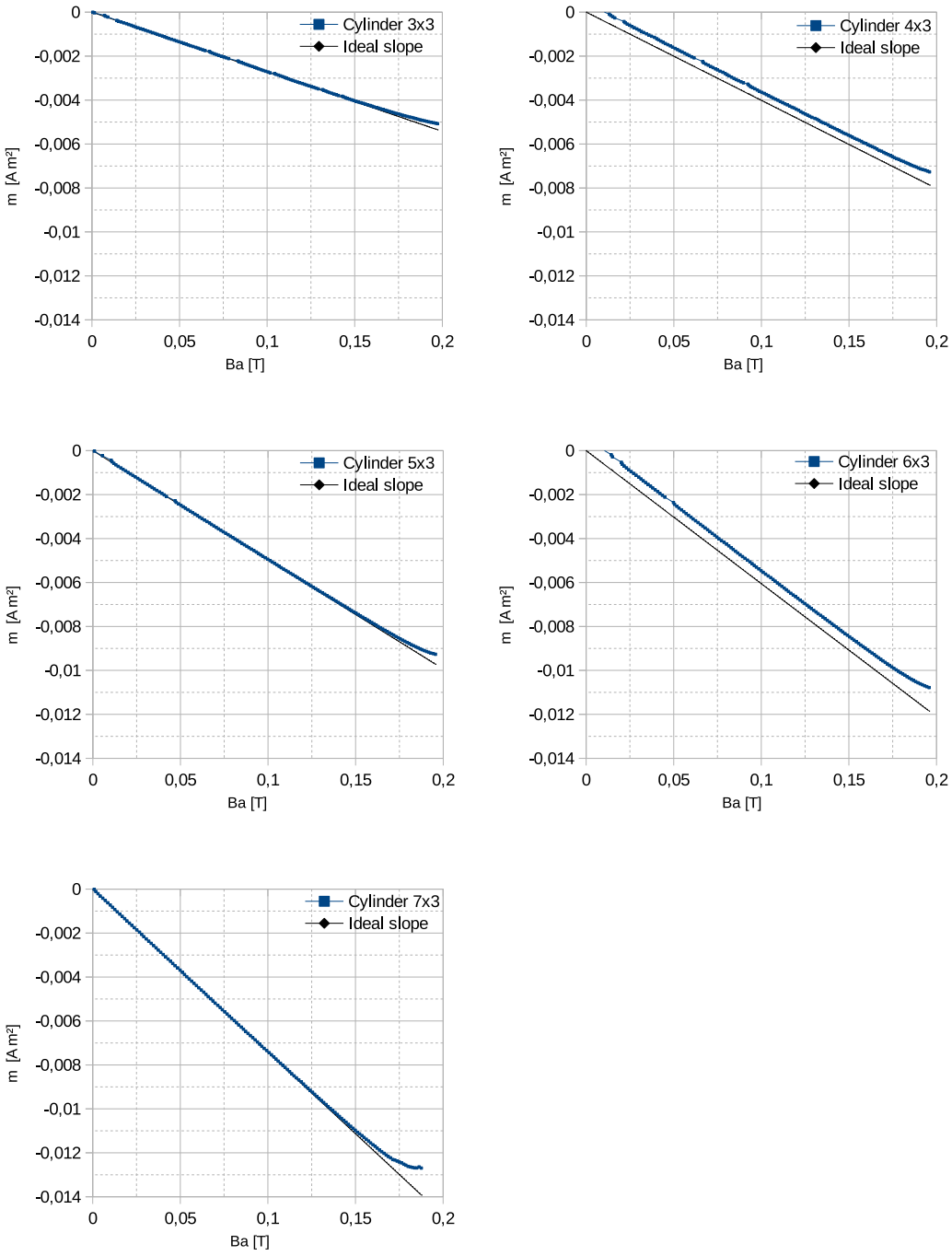

Figure C.6.: Virgin curves of the magnetic moment of cylinders with their main axes perpendicular to the magnetic field. The first digit of every label indicates the length of the dimension parallel to the main axis.

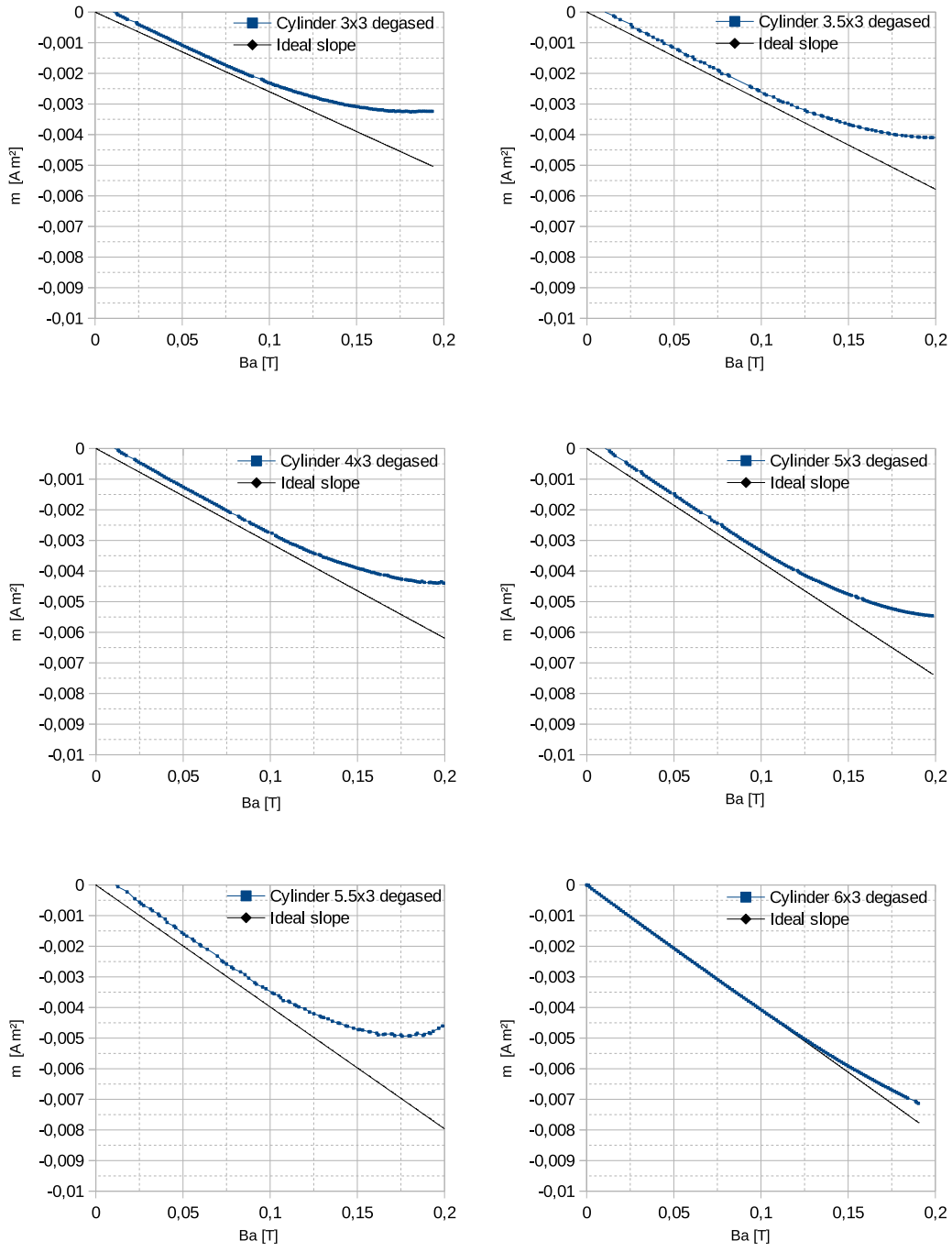

Figure C.7.: Virgin curves of the magnetic moment of degased cylinders with their main axes parallel to the magnetic field. The first digit of every label indicates the length of the dimension parallel to the main axis.

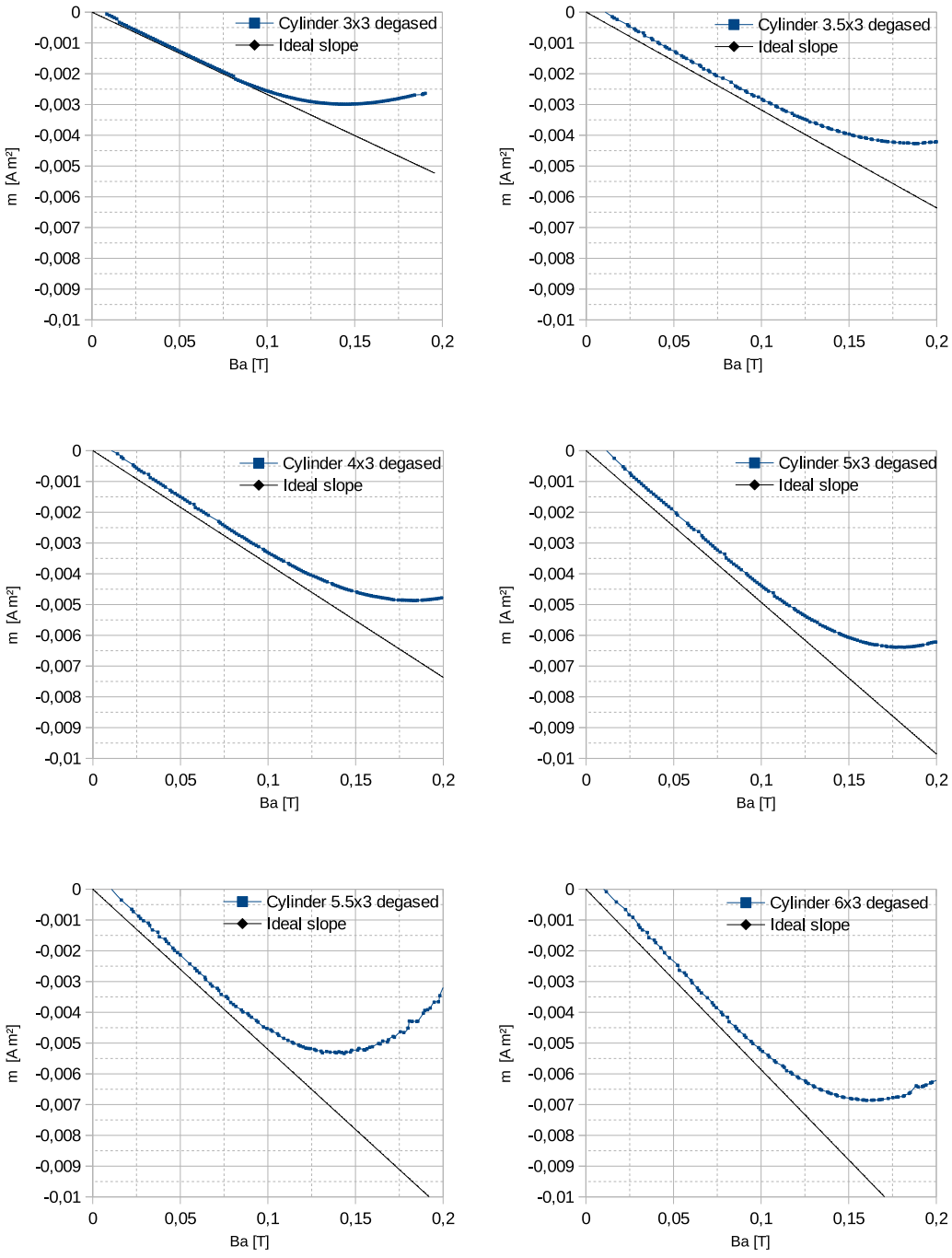

Figure C.8.: Virgin curves of the magnetic moment of degased cylinders with their main axes perpendicular to the magnetic field. The first digit of every label indicates the length of the dimension parallel to the main axis.

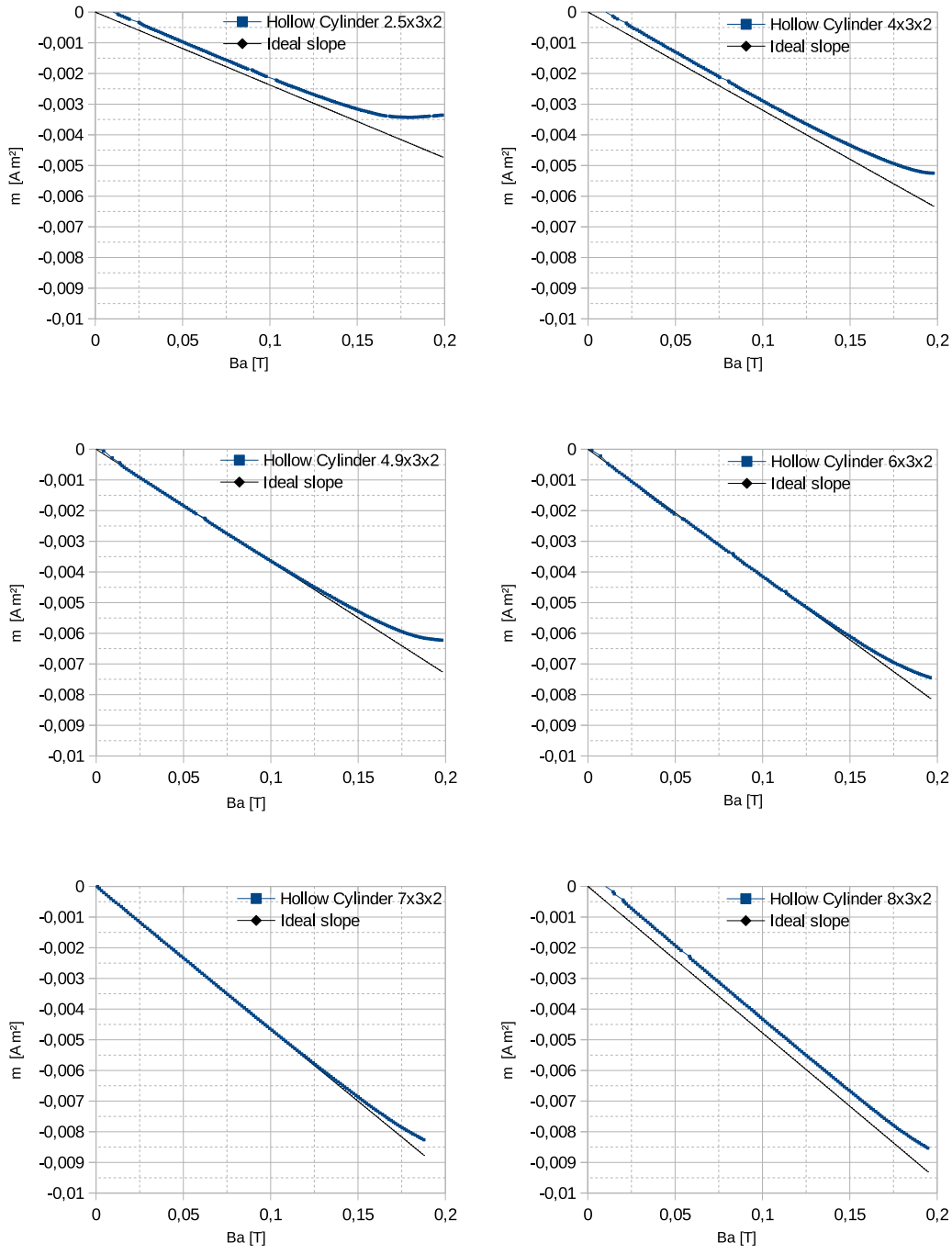

Figure C.9.: Virgin curves of the magnetic moment of hollow cylinders with their main axes parallel to the magnetic field. The first digit of every label indicates the length of the dimension parallel to the main axis.

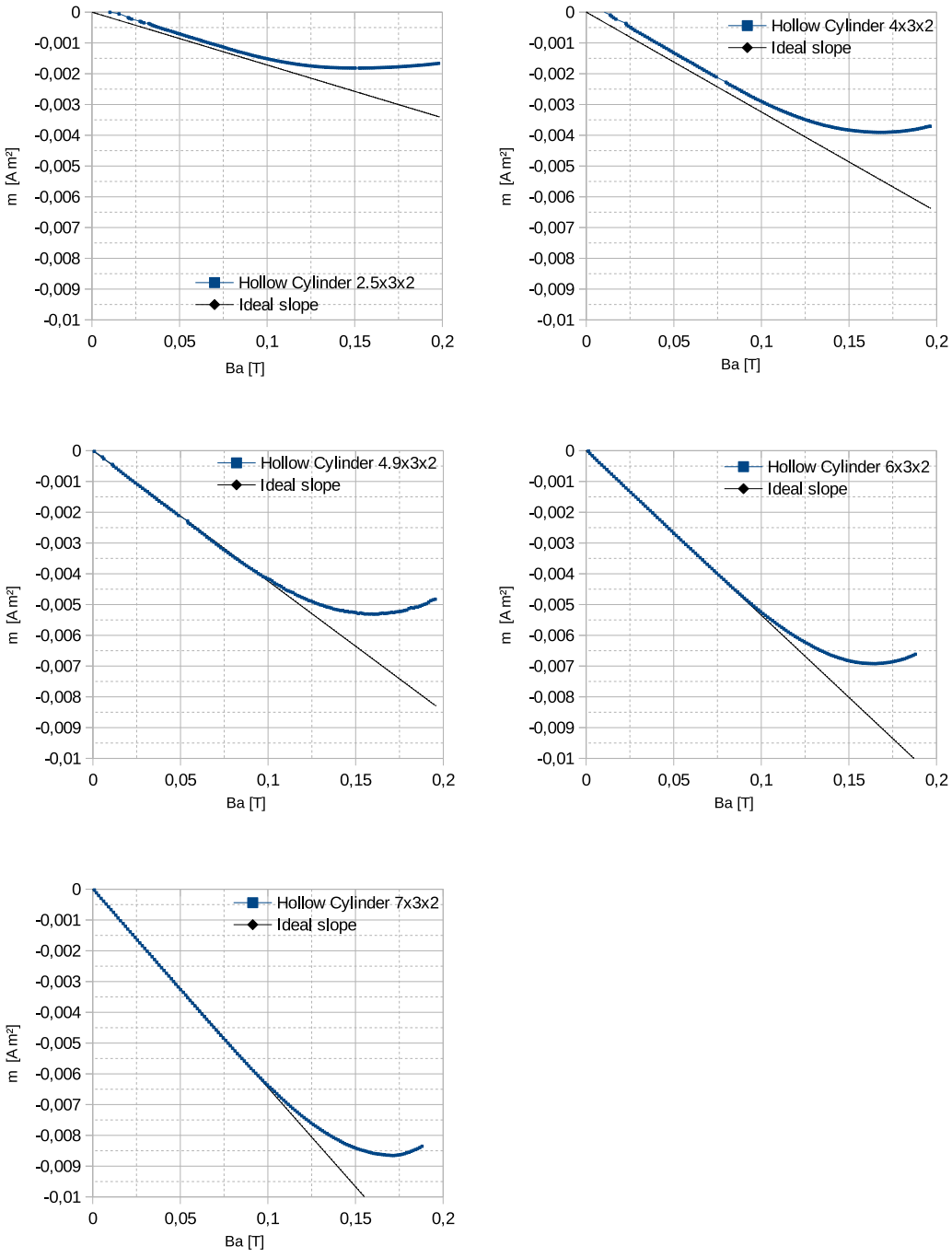

Figure C.10.: Virgin curves of the magnetic moment of hollow cylinders with their main axes perpendicular to the magnetic field. The first digit of every label indicates the length of the dimension parallel to the main axis.

D. Magnetization curves

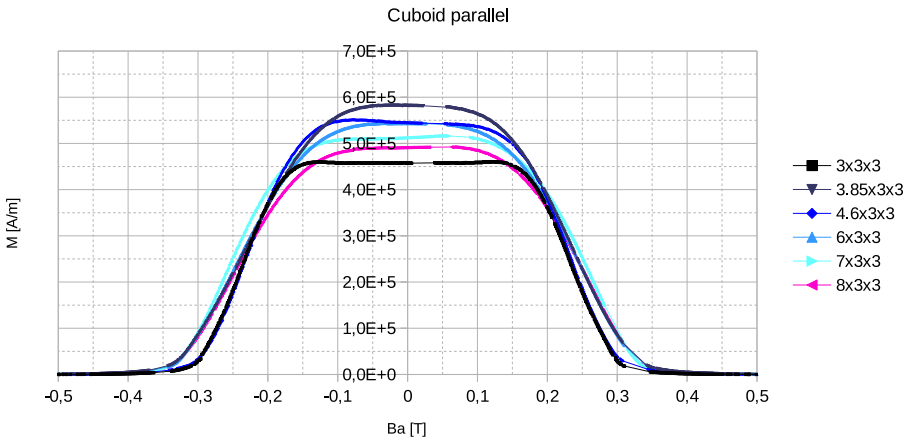

Figure D.1.: Magnetization curves versus applied field of the cuboids of the first test series with their main axes parallel to the magnetic field. The first digit of every label indicates the length of the dimension parallel to the field.

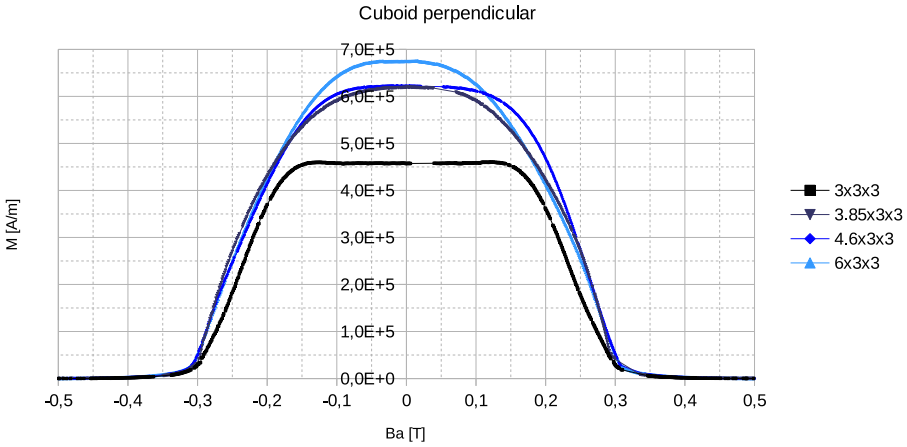

Figure D.2.: Magnetization curves versus applied field of the cuboids of the first test series with their main axes perpendicular to the magnetic field. The first digit of every label indicates the length of the dimension perpendicular to the main axis.

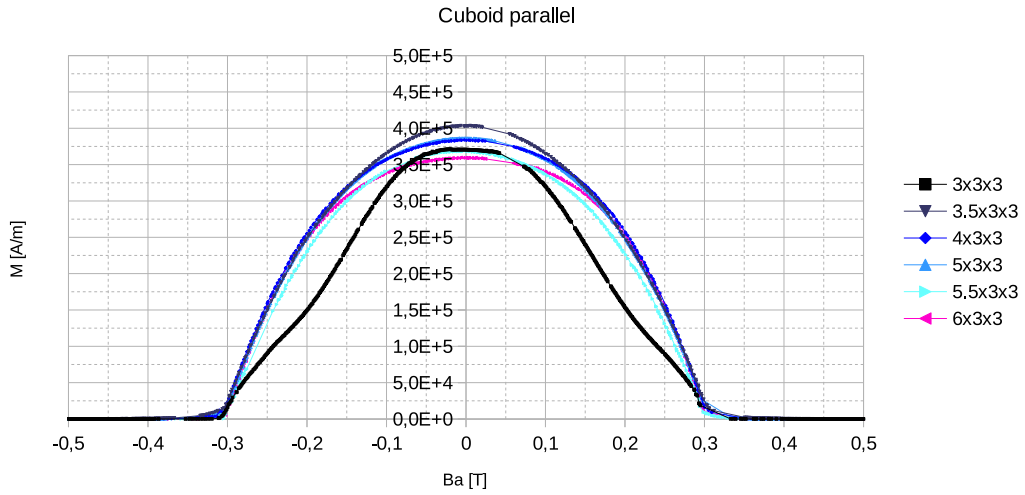

Figure D.3.: Magnetization curves versus applied field of the cuboids of the second test series with their main axes parallel to the magnetic field. The first digit of every label indicates the length of the dimension parallel to the main axis.

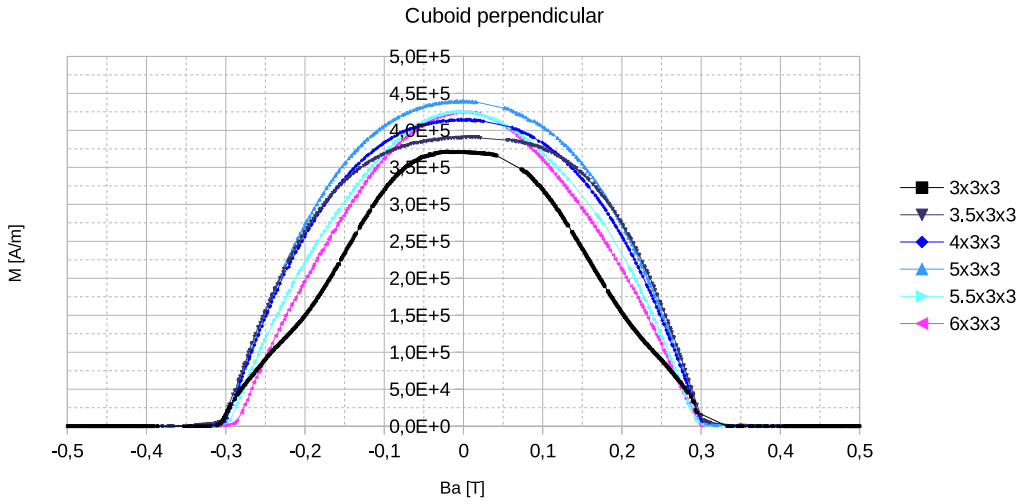

Figure D.4.: Magnetization curves versus applied field of the cuboids of the second test series with their main axes perpendicular to the magnetic field. The first digit of every label indicates the length of the dimension perpendicular to the field.

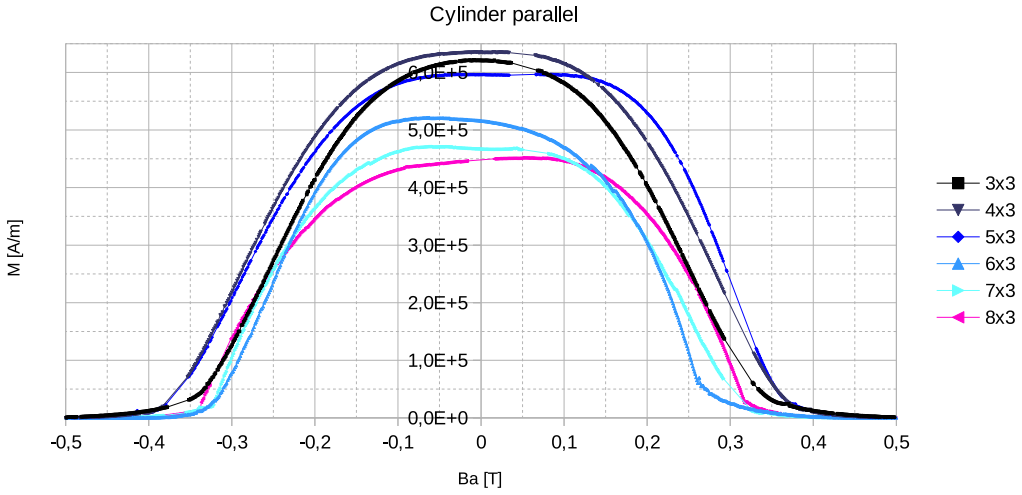

Figure D.5.: Magnetization curves versus applied field of the cylinders of the first test series with their main axes parallel to the magnetic field. The first digit of every label indicates the length of the dimension parallel to the main axis.

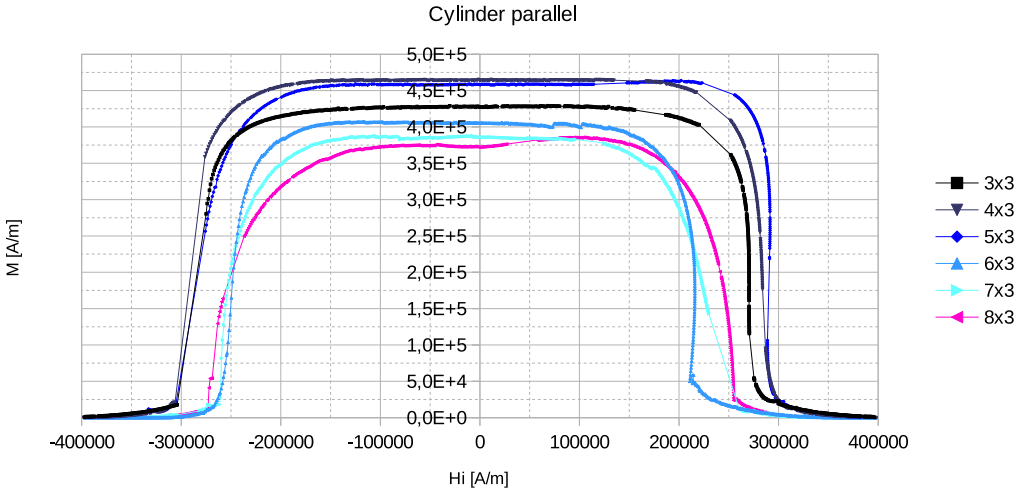

Figure D.6.: Magnetization curves versus internal field of the cylinders of the first test series with their main axes parallel to the magnetic field. Demagnetizing effects have been considered. The first digit of every label indicates the length of the dimension parallel to the main axis.

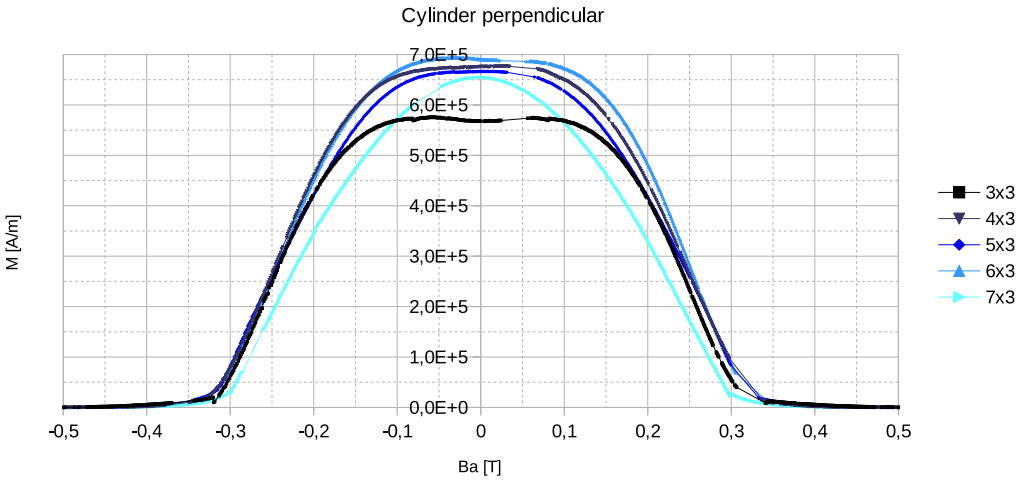

Figure D.7.: Magnetization curves versus applied field of the cylinders of the first test series with their main axes perpendicular to the magnetic field. The first digit of every label indicates the length of the dimension parallel to the main axis.

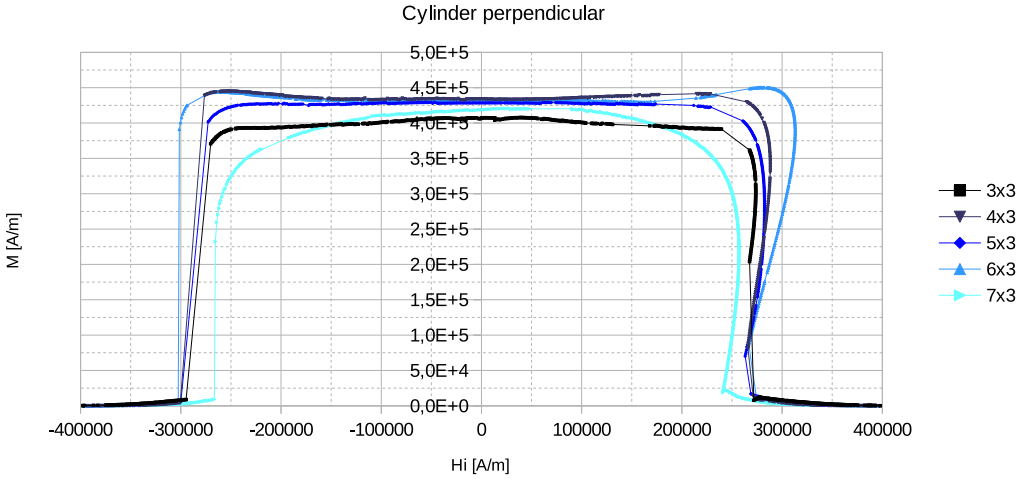

Figure D.8.: Magnetization curves versus internal field of the cylinders of the first test series with their main axes perpendicular to the magnetic field. Demagnetizing effects have been considered. The first digit of every label indicates the length of the dimension parallel to the main axis.

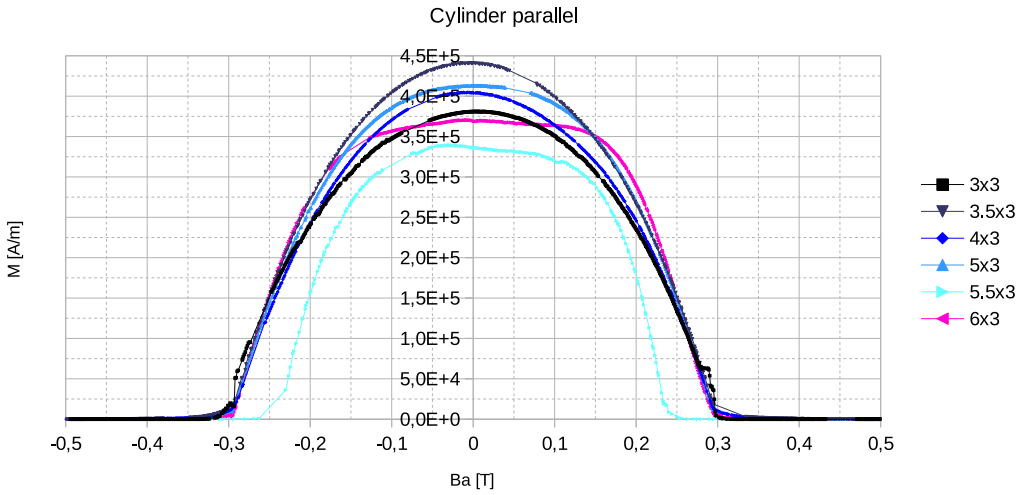

Figure D.9.: Magnetization curves versus applied field of the cylinders of the second test series with their main axes parallel to the magnetic field. The first digit of every label indicates the length of the dimension parallel to the main axis.

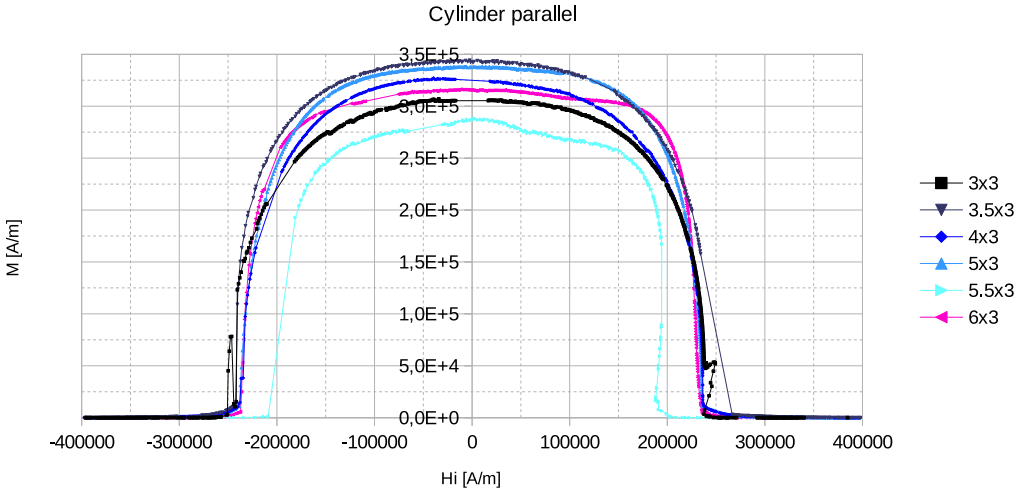

Figure D.10.: Magnetization curves versus internal field of the cylinders of the second test series with their main axes parallel to the magnetic field. Demagnetizing effects have been considered. The first digit of every label indicates the length of the dimension parallel to the main axis.

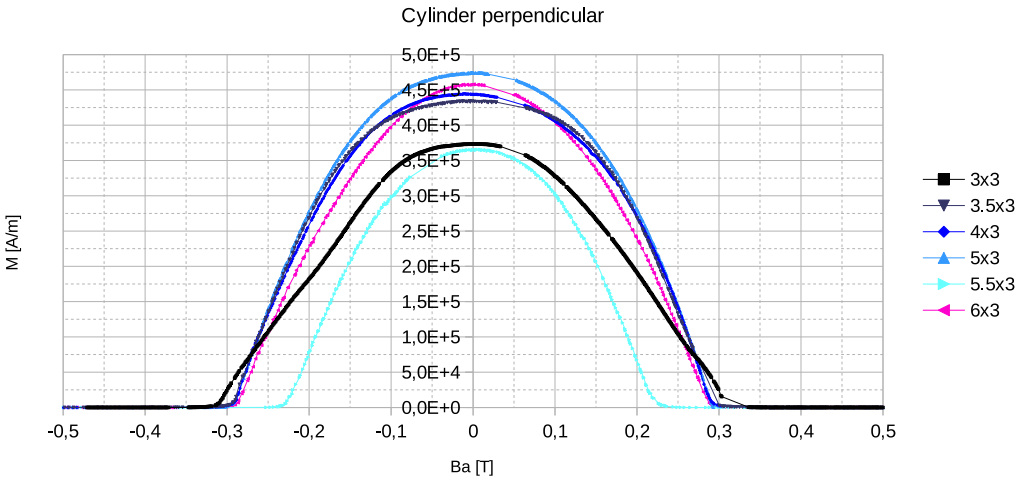

Figure D.11.: Magnetization curves versus applied field of the cylinders of the second test series with their main axes perpendicular to the magnetic field. The first digit of every label indicates the length of the dimension parallel to the main axis.

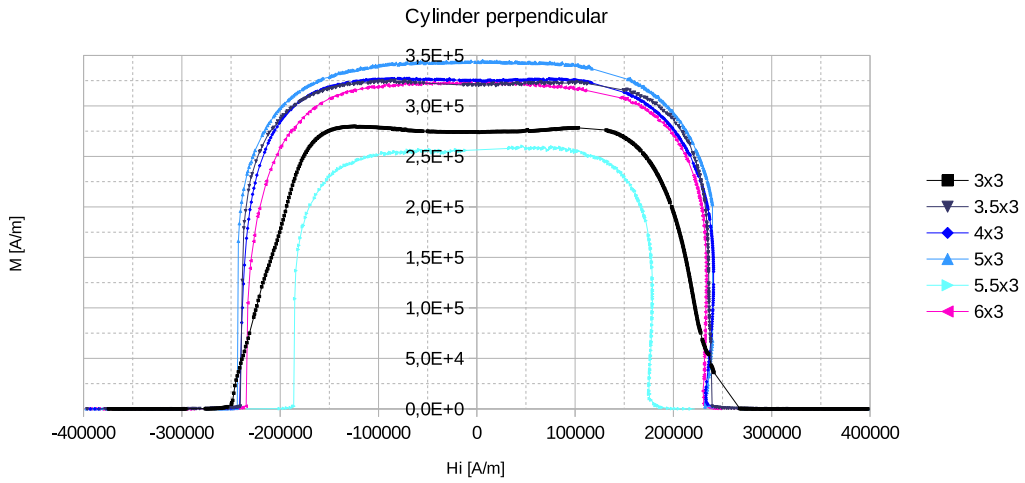

Figure D.12.: Magnetization curves versus internal field of the cylinders of the second test series with their main axes perpendicular to the magnetic field. Demagnetizing effects have been considered. The first digit of every label indicates the length of the dimension parallel to the main axis.

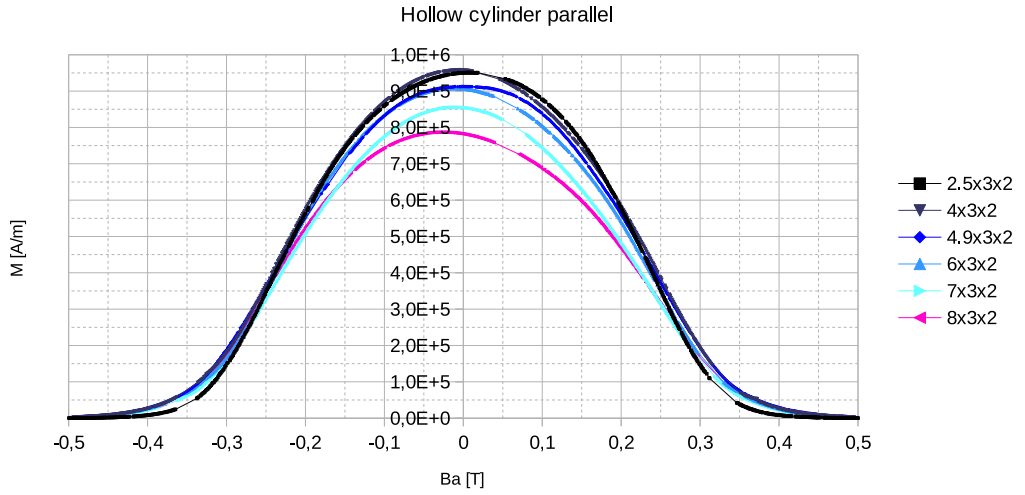

Figure D.13.: Magnetization curves versus applied field of the hollow cylinders of the first test series with their main axes parallel to the magnetic field. The first digit of every label indicates the length of the dimension parallel to the main axis.

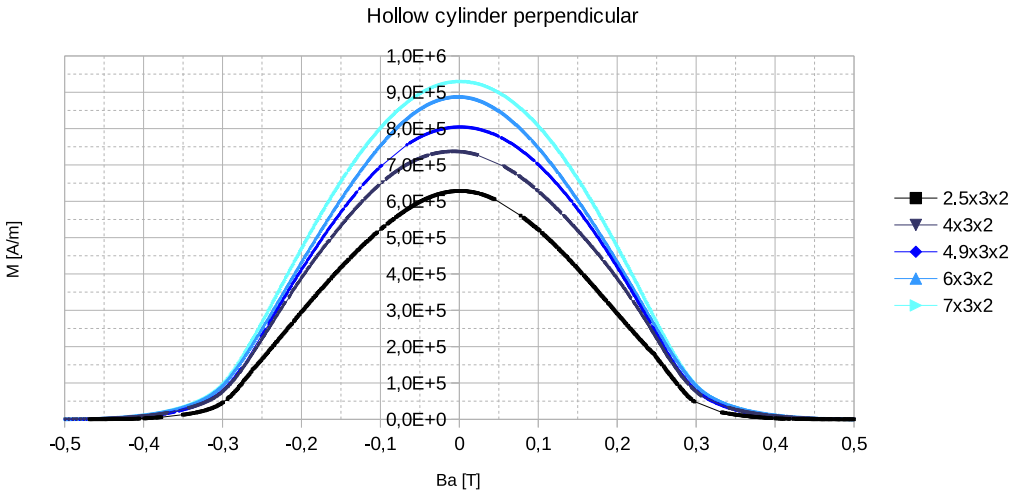

Figure D.14.: Magnetization curves versus applied field of the hollow cylinders of the first test series with their main axes perpendicular to the magnetic field. The first digit of every label indicates the length of the dimension parallel to the main axis.

E. Critical current density curves

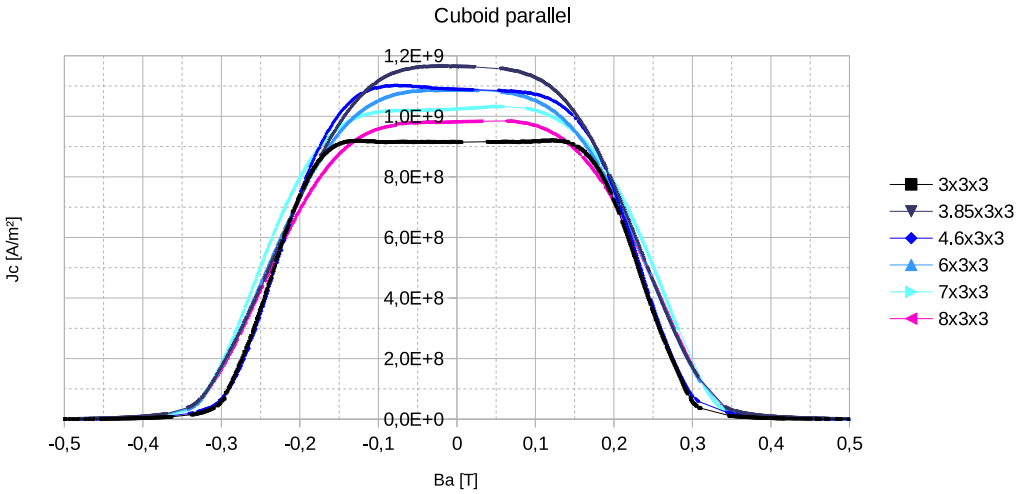

Figure E.1.: Critical current density curves versus applied field of the cuboids of the first test series with their main axes parallel to the magnetic field. The first digit of every label indicates the length of the dimension parallel to the field.

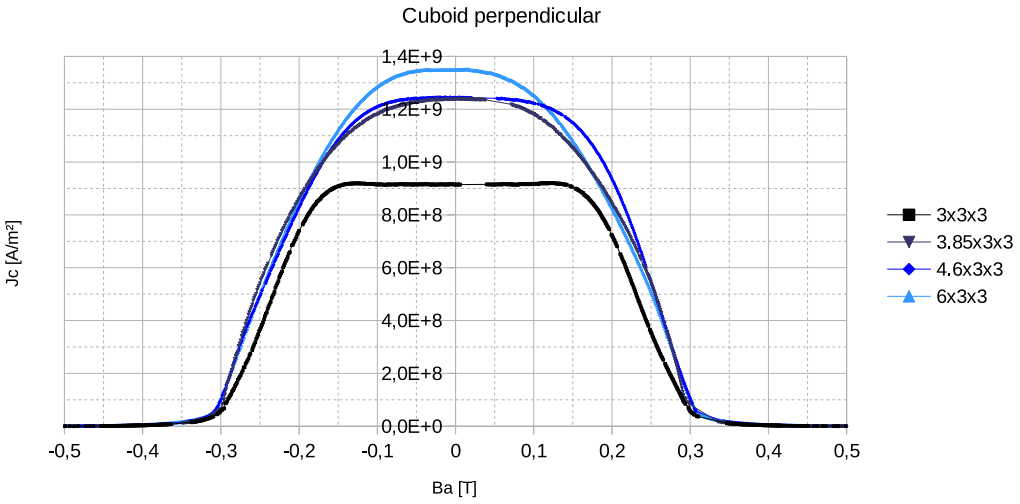

Figure E.2.: Critical current density curves versus applied field of the cuboids of the first test series with their main axes perpendicular to the magnetic field. The first digit of every label indicates the length of the dimension perpendicular to the field.

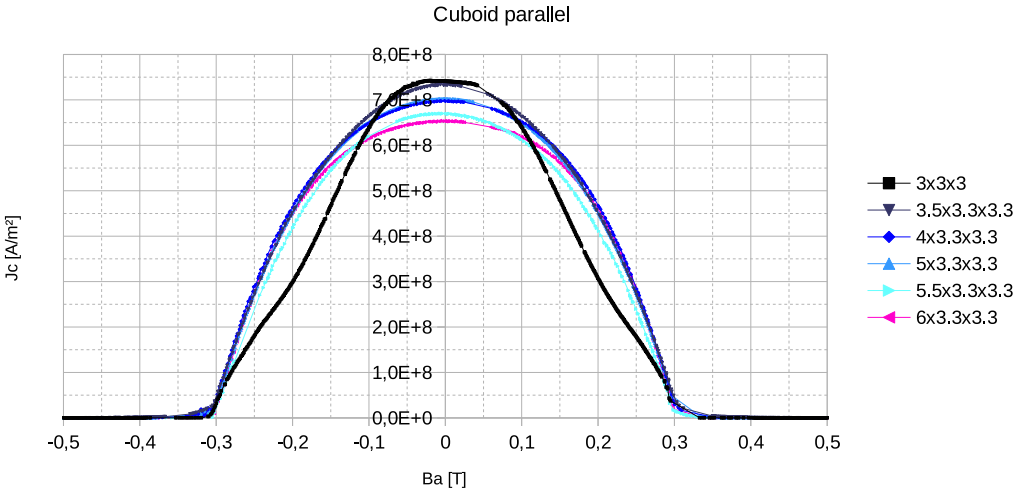

Figure E.3.: Critical current density curves versus applied field of the cuboids of the second test series with their main axes parallel to the magnetic field. The first digit of every label indicates the length of the dimension parallel to the field.

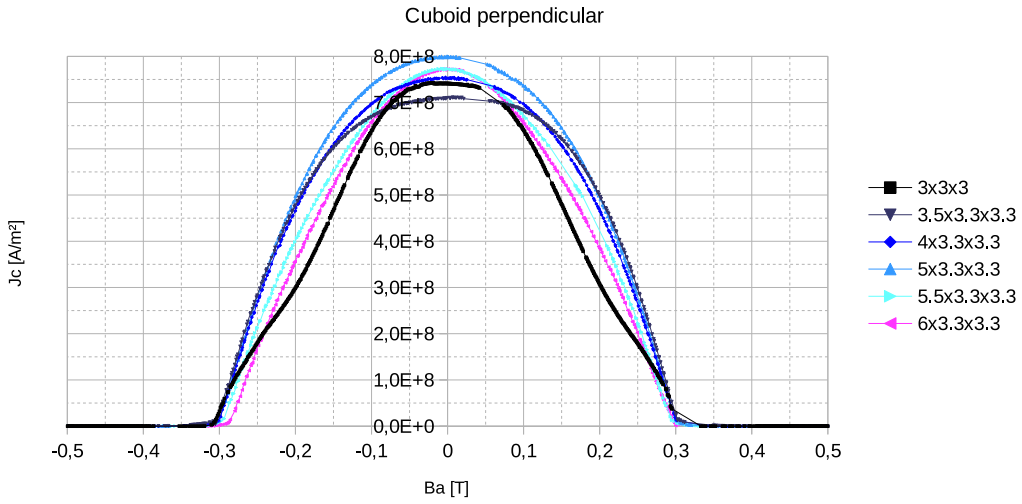

Figure E.4.: Critical current density curves versus applied field of the cuboids of the second test series with their main axes perpendicular to the magnetic field. The first digit of every label indicates the length of the dimension perpendicular to the field.

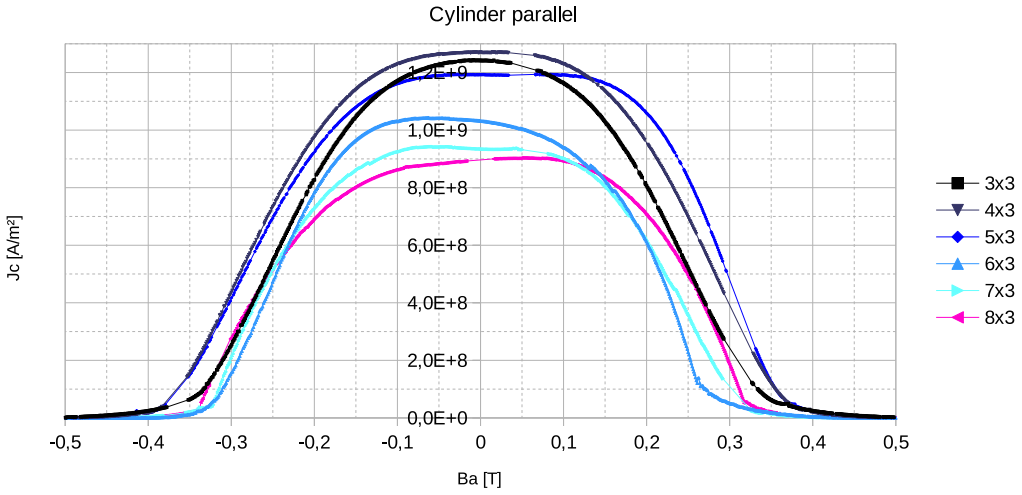

Figure E.5.: Critical current density curves versus applied field of the cylinders of the first test series with their main axes parallel to the magnetic field. The first digit of every label indicates the length of the dimension parallel to the main axis.

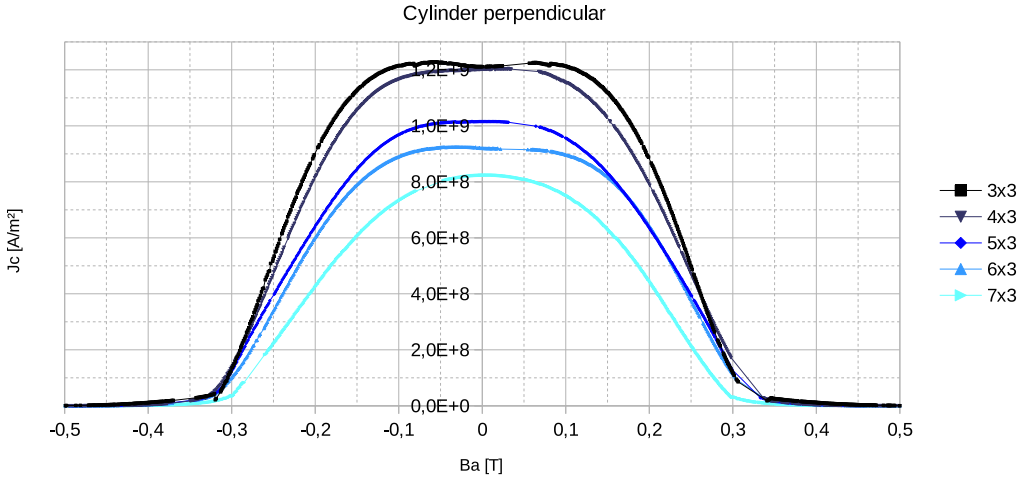

Figure E.6.: Critical current density curves versus applied field of the cylinders of the first test series with their main axes perpendicular to the magnetic field. The first digit of every label indicates the length of the dimension parallel to the main axis.

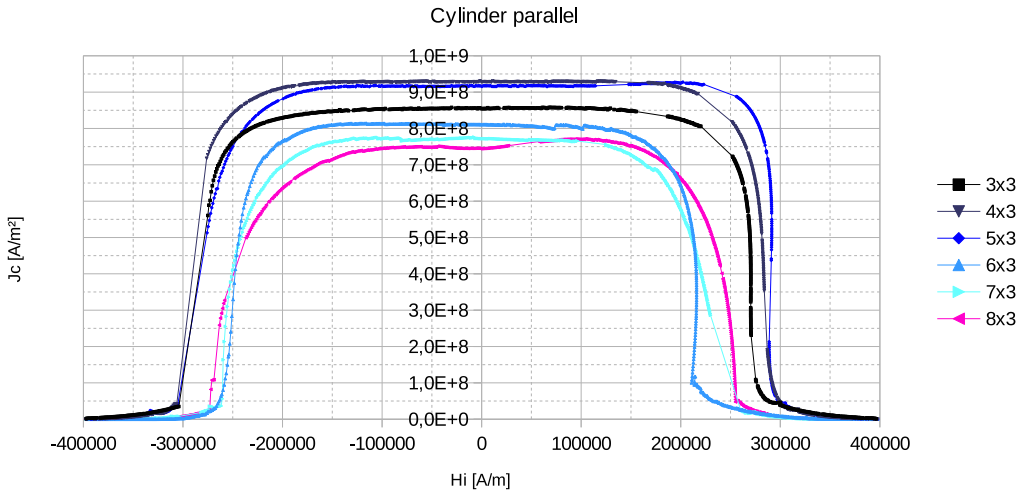

Figure E.7.: Critical current density curves versus internal field of the cylinders of the first test series with their main axes parallel to the magnetic field. Demagnetizing effects have been considered. The first digit of every label indicates the length of the dimension parallel to the main axis.

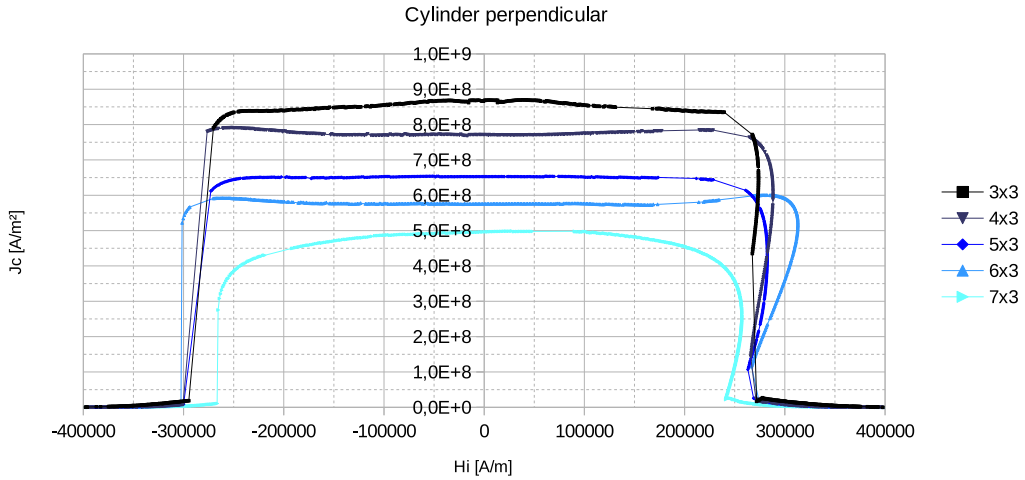

Figure E.8.: Critical current density curves versus internal field of the cylinders of the first test series with their main axes perpendicular to the magnetic field. Demagnetizing effects have been considered. The first digit of every label indicates the length of the dimension parallel to the main axis.

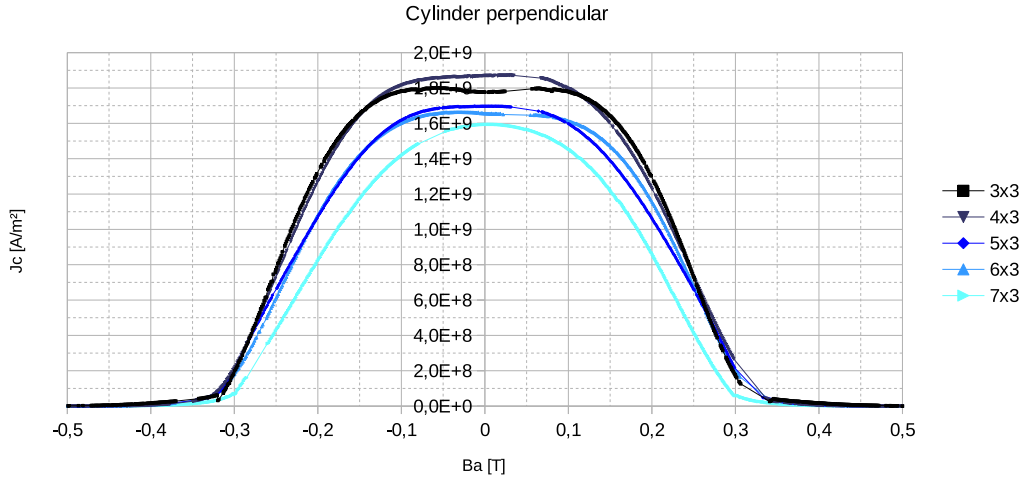

Figure E.9.: Adjusted critical current density curves versus applied field of the cylinders of the first test series with their main axes perpendicular to the magnetic field. The current densities were evaluated using the method from section 2.4 instead of formula (2.5). The first digit of every label indicates the length of the dimension parallel to the main axis.

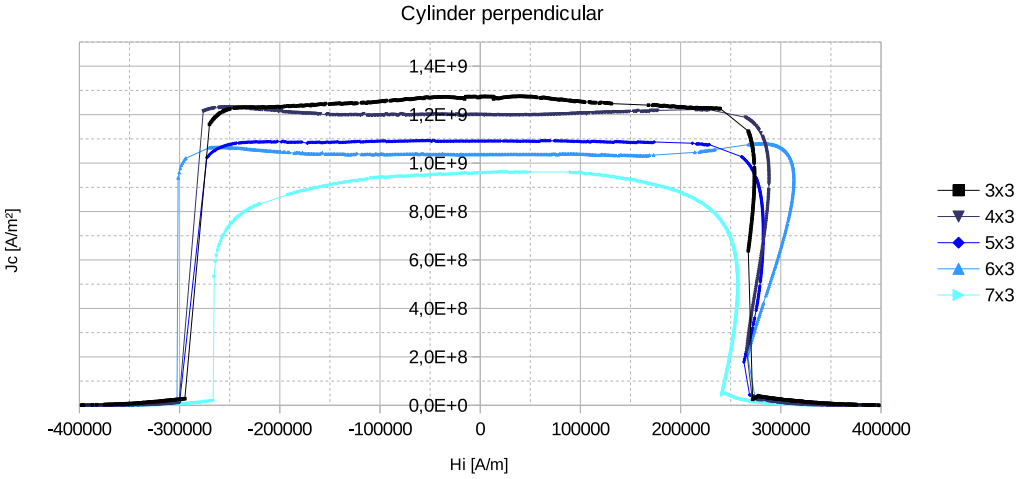

Figure E.10.: Adjusted critical current density curves versus internal field of the cylinders of the first test series with their main axes perpendicular to the magnetic field. The current densities were evaluated using the method from section 2.4 instead of formula (2.5). Demagnetizing effects have been considered. The first digit of every label indicates the length of the dimension parallel to the main axis.

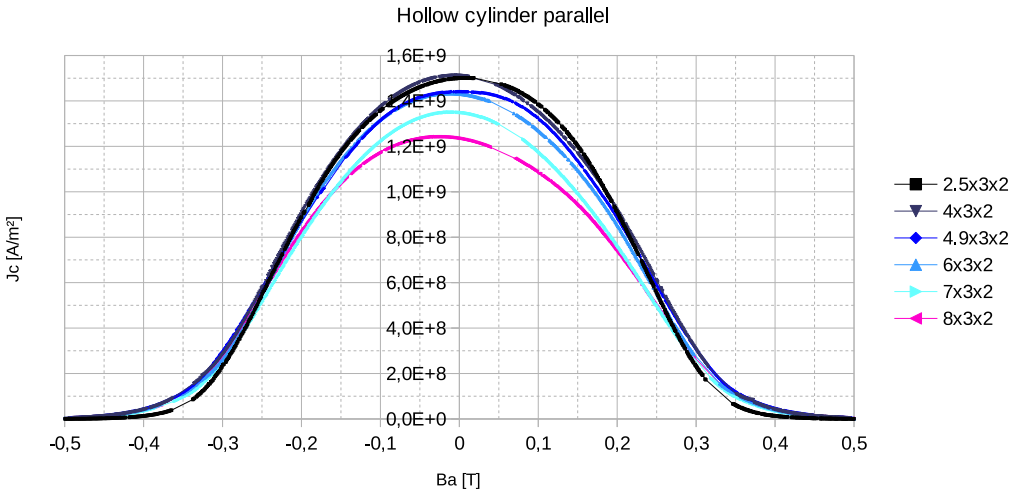

Figure E.11.: Critical current density curves versus applied field of the hollow cylinders of the first test series with their main axes series parallel to the magnetic field. The first digit of every label indicates the length of the dimension parallel to the main axis.

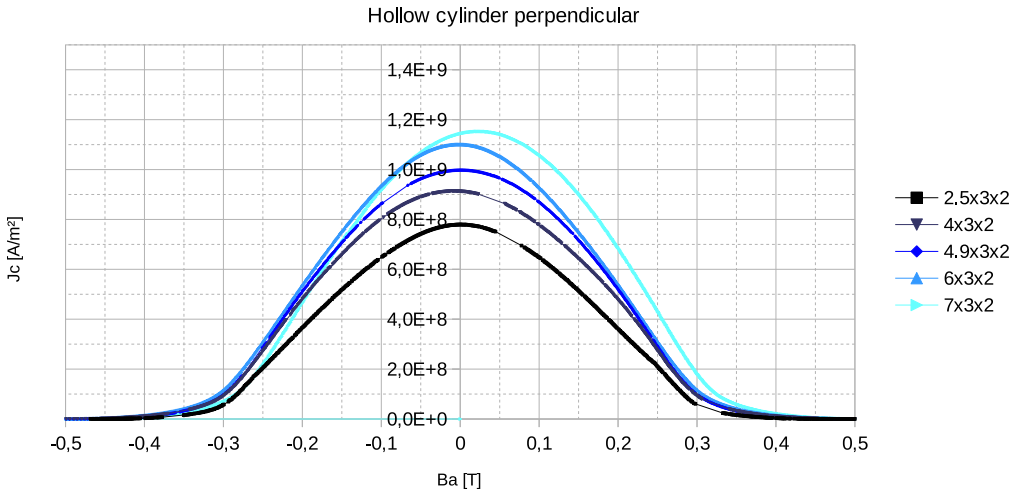

Figure E.12.: Critical current density curves versus applied field of the hollow cylinders of the first test series with their main axes series perpendicular to the magnetic field. The first digit of every label indicates the length of the dimension parallel to the main axis.

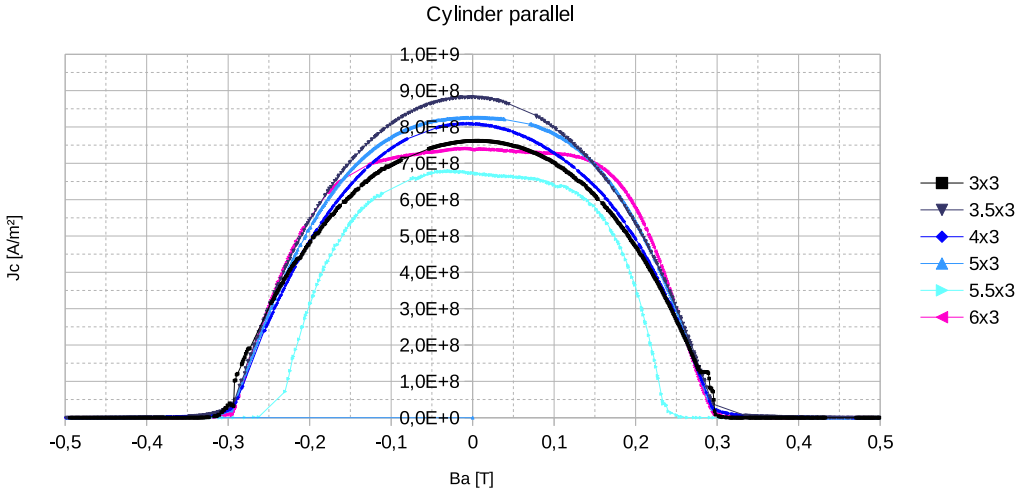

Figure E.13.: Critical current density curves versus applied field of the cylinders of the second test series with their main axes parallel to the magnetic field. The first digit of every label indicates the length of the dimension parallel to the main axis.

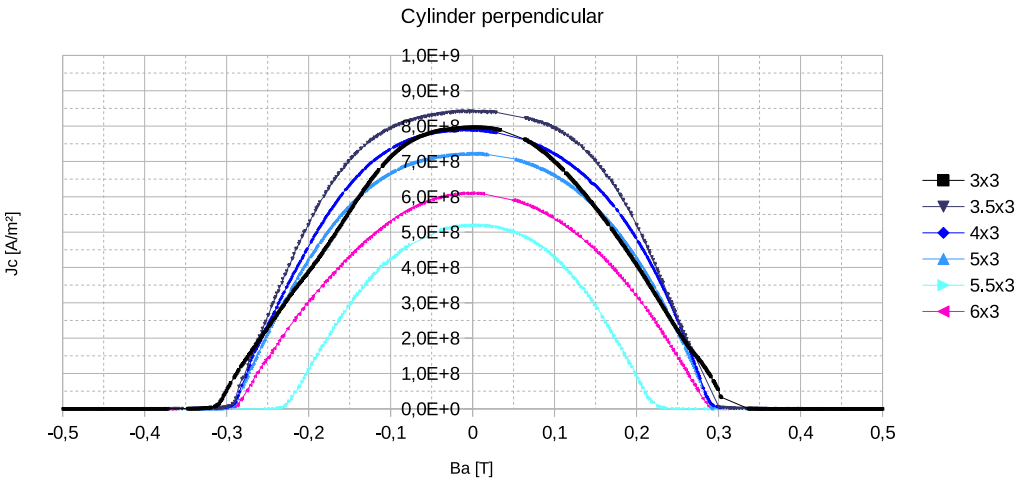

Figure E.14.: Critical current density curves versus applied field of the cylinders of the second test series with their main axes perpendicular to the magnetic field. The first digit of every label indicates the length of the dimension parallel to the main axis.

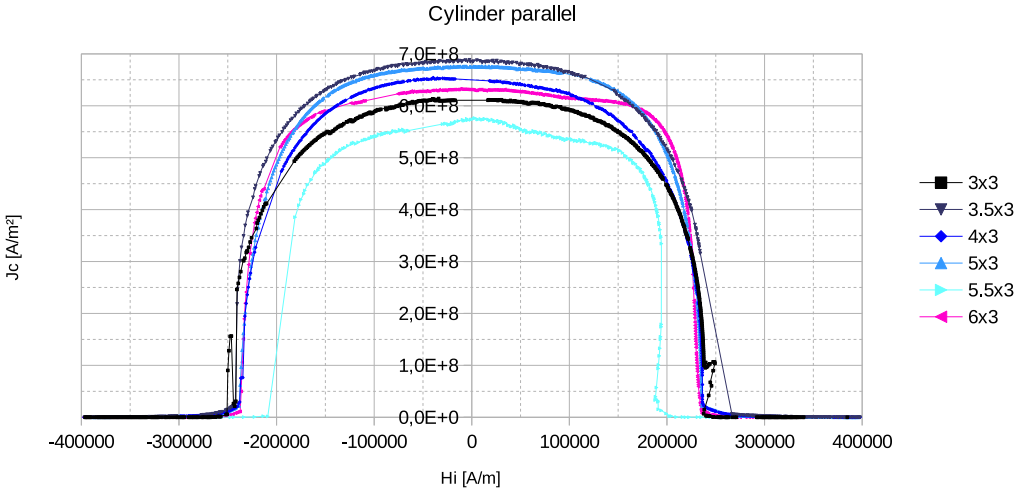

Figure E.15.: Critical current density curves versus internal field of the cylinders of the second test series with their main axes parallel to the magnetic field. Demagnetizing effects have been considered. The first digit of every label indicates the length of the dimension parallel to the main axis.

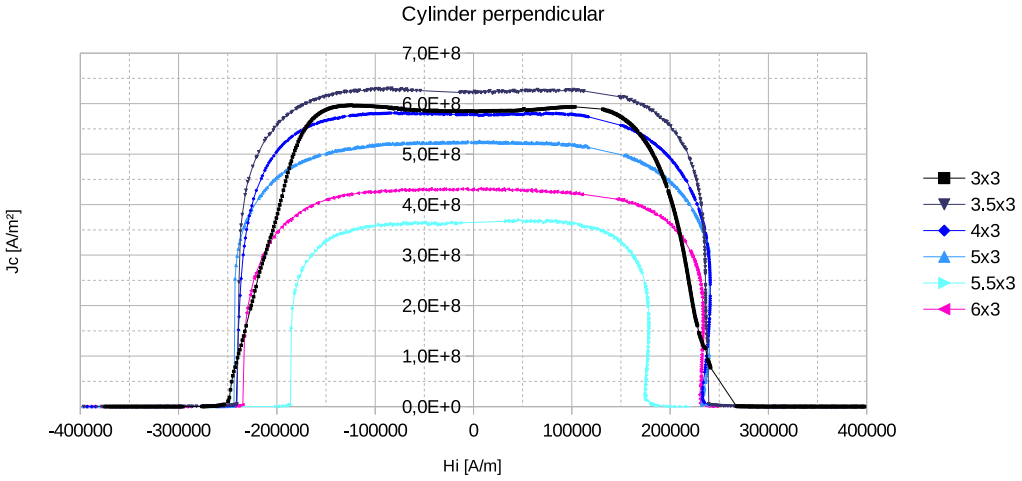

Figure E.16.: Critical current density curves versus internal field of the cylinders of the second test series with their main axes perpendicular to the magnetic field. Demagnetizing effects have been considered. The first digit of every label indicates the length of the dimension parallel to the main axis.

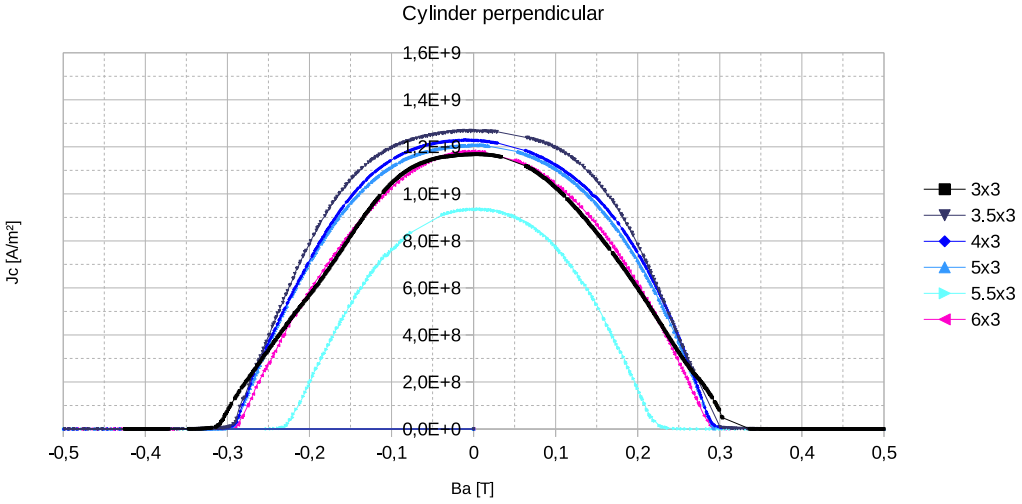

Figure E.17.: Adjusted critical current density curves versus applied field of the cylinders of the second test series with their main axes series perpendicular to the magnetic field. The current densities were evaluated using the method from section 2.4 instead of formula (2.5). The first digit of every label indicates the length of the dimension parallel to the main axis.

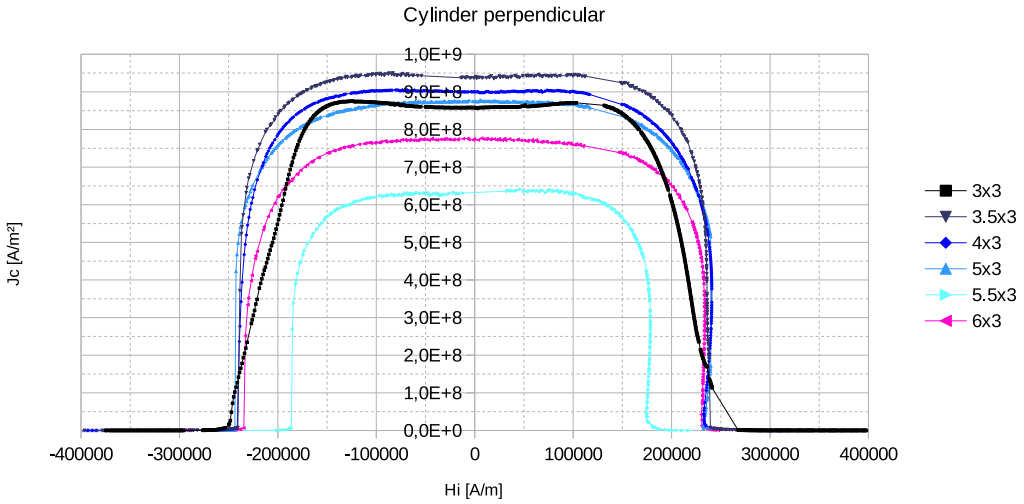

Figure E.18.: Adjusted critical current density curves versus internal field of the cylinders of the second test series with their main axes series perpendicular to the magnetic field. Demagnetizing effects have been considered. The current densities were evaluated using the method from section 2.4 instead of formula (2.5). The first digit of every label indicates the length of the dimension parallel to the main axis.

List of Figures

List of Tables

Bibliography

[1] Ronald B. Goldfarb, Du-Xing Chen, and James A. Brug. Demagnetizing factors for cylinders. *IEEE Transactions on Magnetics*, 27:3601, 1991.

[2] T. T. Taylor. Electric polarizability of a short right circular conducting cylinder. *J. of Res. of the Nat. Bur. of Stand. - B. Math. and Math. Phys.*, 64B,3:135–143, 1960.

[3] T. T. Taylor. Magnetic polarizability of a short right circular conducting cylinder. *J. of Res. of the Nat. Bur. of Stand. - B. Math. and Math. Phys.*, 64B,4:199–210, 1960.

[4] D.-X. Chen, C. Prados, E. Pardo, A. Sanchez, and A. Hernando. Transverse demagnetizing factors of long rectangular bars: I. analytical expressions for extreme values of susceptibility. *J. of Applied Physics*, 91,8:5254–5259, 2002.

[5] Du-Xing Chen, Enric Pardo, and Alvaro Sanchez. Demagnetizing factors for square bars. *IEEE Transactions on Magnetics*, 40,3:1491–1498, 2004.

[6] Alvaro Sanchez and Carles Navau. Magnetic properties of finite superconducting cylinders. i. uniform applied field. *Physical Review B*, 64:1–10, 2001.

[7] Leonid Prigozhin. The bean model in superconductivity: Variational formulation and numerical solution. *Journal of Computational Physics*, 129:190–210, 1996.

[8] A. Badía, J. F. Cariñena, and C. López. Geometric treatment of electromagnetic phenomena in conducting materials: variational principles. *J. Phys. A: Math. Gen*, pages 1–33, 2006.

[9] A. Badía, C. López, and J. L. Giordano. Optimal control model for the critical state in superconductors. *Physical Review B*, 58,14:9440–9449, 1998.

[10] Michael Tinkham. *Introduction to superconductivity.* McGraw-Hill, 2nd edition, 1996.

[11] C. P. Bean. Magnetization of high-field superconductors. *Rev. Mod. Phys.*, 36:31–33, 1964.

[12] Gerard L. Pollack and Daniel R. Stump. *Electromagnetism.* Addison Wesley, 2002.

[13] B. D. Cullity and C. D. Graham. *Introduction to magnetic materials.* IEEE Press, 2 edition, 2009.

[14] Mike McElfresh. *Fundamentals of Magnetism and Magnetic Measurements.* Purdue University and Quantum Design, 1994.

[15] James R. Bunch and John Hopcroft. Triangular factorization and inversion by fast matrix multiplication. *Mathematics of Computation*, 28:231–236, 1974.

[16] Univ. of Tennessee, Berkeley Univ. of California, Univ. of Colorado Denver, and NAG Ltd. http://www.netlib.org/lapack/, 2015.

[17] Shanjie Zhang and Jianming Jin. *Computation of Special Functions.* Wiley-Interscience, 1996.

[18] T. T. Taylor. Electric polarizability of a short right circular conducting cylinder. *J. of Res. of the Nat. Bur. of Stand. - B. Math. and Math. Phys.*, 64B,3:138, 1960.

[19] Ronald B. Goldfarb, Du-Xing Chen, and James A. Brug. Demagnetizing factors for cylinders. *IEEE Transactions on Magnetics*, 27:3611, 1991.

[20] D.-X. Chen, C. Prados, E. Pardo, A. Sanchez, and A. Hernando. Transverse demagnetizing factors of long rectangular bars. ii. numerical calculations for arbitrary susceptibility. *J. of Applied Physics*, 91,8:5260–5267, 2002.

[21] T. T. Taylor. Electric polarizability of a short right circular conducting cylinder. *J. of Res. of the Nat. Bur. of Stand. - B. Math. and Math. Phys.*, 64B,3:140, 1960.

[22] T. T. Taylor. Magnetic polarizability of a short right circular conducting cylinder. *J. of Res. of the Nat. Bur. of Stand. - B. Math. and Math. Phys.*, 64B,4:206, 1960.

[23] D.-X. Chen, C. Prados, E. Pardo, A. Sanchez, and A. Hernando. Transverse demagnetizing factors of long rectangular bars. ii. numerical calculations for arbitrary susceptibility. *J. of Applied Physics*, 91,8:5264, 2002.

[24] D.-X. Chen, C. Prados, E. Pardo, A. Sanchez, and A. Hernando. Transverse demagnetizing factors of long rectangular bars. ii. numerical calculations for arbitrary susceptibility. *J. of Applied Physics*, 91,8:5263, 2002.

[25] T. F. Stromberg. *The superconducting properties of high purity niobium.* PhD thesis, Iowa State Uni. of Scie. and Tech., 1965.

[26] W. DeSorbo. Effect of dissolved gases on some superconducting properties of niobium. *Phys. Rev.*, 132:107–123, 1963.